# THE PHYSIOLOGICAL FUNCTION OF ENDOTHELIN-2 IN MICE

APPROVED BY SUPERVISORY COMMITTEE

Masashi Yanagisawa, M.D., Ph.D.

Joyce Repa, Ph.D.

Steven Kliewer, Ph.D.

Lora Hooper, Ph.D.

Dedicated to my parents, my wife and my son.

# THE PHYSIOLOGICAL FUNCTION OF ENDOTHELIN-2 IN MICE

by

INIK CHANG

DISSERTATION

Presented to the Faculty of the Graduate School of Biomedical Sciences

The University of Texas Southwestern Medical Center at Dallas

In Partial Fulfillment of the Requirements

For the Degree of

DOCTOR OF PHILOSOPHY

The University of Texas Southwestern Medical Center at Dallas

Dallas, Texas

April, 2009

# ACKNOWLEDGEMENTS

Many great people have shown support and encouragement for me during my graduate study and I am grateful to each of them.

First, I would like to thank my mentor, Dr. Masashi Yanagisawa for giving me an interesting and challenging research project to work on with wonderful people in an extraordinary environment. His never-ending curiosity and enthusiasm for science are deeply impressed upon my mind.

I would further like to thank my dissertation committee members, Dr. Joyce Repa (chairperson), Dr. Steven Kleiwer, and Dr. Lora Hooper for all the scientific guidance and inspiration they provided me during the study.

I would also like to express thanks to all the Yanagisawa lab members: Dr. Toshiyuki Motoike, Dr. Hidetoshi Kumagai, Dr. Yuichi Ikeda, Dr. Ayako Suzuki, Dr. Taizo Matsuki, Abdullah Shaito, Allen Tsai, Stephanie Baldock, Shelley Dixon, Amber Skach, Randal Floyd, Marcus Thornton and Makito Sato. I am especially thankful to my friend, Alex Chang for invaluable advice as well as the many hours he spent with me talking about our school life and future careers. Additionally, I am also grateful to several former Yanagisawa lab members: Dr. Hiromasa Funato, Clay Williams, Donna Kirkland, David Sierra and Dr. Amy Baynash.

Finally, I would like to extend my sincerest gratitude to the many Korean friends I met in Dallas. I am particularly grateful to Kiwoo Kim and Euiseok Kim for their friendship and also to the Korean racquetball players at UTSW - not only for the time we spent playing the game, but also for the invigorating discussions about life and science.

This acknowledgement would not be complete without thanking my parents and my lovely wife for all the support and encouragement I received throughout this time of my life.

# THE PHYSIOLOGICAL FUNCTION OF ENDOTHELIN-2 IN MICE

Inik Chang, Ph.D.

The University of Texas Southwestern Medical Center at Dallas, 2009

Masashi Yanagisawa, M.D., Ph.D.

In order to directly explore the physiological function of ET-2, we generated constitutive, tissue-specific and systemically inducible knockout mice. Global *ET-2* deficient mice exhibited severe growth retardation and juvenile lethality. Despite normal milk intake, they suffered from an apparent internal starvation characterized by hypoglycemia, ketonemia, and increased expression of starvation-induced genes in liver. Based on its abundant expression in the gut, I hypothesized that intestinal function of ET-2 is essential for the growth and survival of mice. However, unexpectedly, the intestine was morphologically and functionally normal in the global mutant mice. Moreover, intestine-

specific *ET-2* deficient mice showed no detectable abnormalities in growth and survival. Instead, I observed that colonic ET-2 has a protective role in epithelial cell injury. Global *ET-2* knockout mice were profoundly hypothermic, even at ambient temperatures. Despite the severe hypothermia, *DIO2* and *UCP-1* failed to increase in brown adipose tissue in *ET-2* knockouts. Housing these mice in a warm environment significantly extended the median life span. As temperature regulation is controlled by the central nervous system (CNS), I examined the phenotype in neuron-specific *ET-2* knockout mice. However, the mutant mice displayed normal core body temperature, suggesting that ET-2 is not playing a role in CNS-regulated body temperature. *ET-2* expression is clearly detected in the lung, with a sharp and transient increase soon after birth. The emphysematous structural change, which is associated with an increase of total lung capacity, resulted in chronic hypoxemia, hypercapnia, and increased erythropoietin synthesis. Finally, to rule out effects of ET-2 during embryonic development, I used the *Cre-loxP* system to delete ET-2 in neonatal and adult mice, and found that these mice fully reproduced the phenotype previously observed in global knockouts. Together, these findings reveal that ET-2 is critical for growth and survival of postnatal mice by playing important roles in energy homeostasis, thermoregulation, and maintenance of lung morphology and function. My studies rule out ET-2 function in the intestine and brain as being responsible for these phenotypes. However, the dramatic effects of the lung are newly discovered as a potential candidate tissue for critical ET-2 action and lung ET-2 function deserves further investigation.

# TABLE OF CONTENTS

# LIST OF PRIOR PUBLICATIONS

**Chang, I.**, Bramall, A., Baynash, A., Rattner, A, Nathans, J., Yanagisawa, M. (2008) "Growth retardation, hypothermia, and lung dysfunction in endothelin-2 deficient mice," *In submission*

Kim, H.S.*, **Chang, I.** *, Kim, J.Y., Cho, K.H., Lee, M.S. (2005) "Caspase-mediated p65 cleavage promotes TRAIL-induced apoptosis," *Cancer Res.* 65(14):6111-6119.

Park, S.Y., Cho, N., **Chang, I.,** Chung, J.H., Min, Y.K., Lee, M.K., Kim, K.W., Kim, S.J., Lee, M.S. (2005) "Effect of PK11195, a peripheral benzodiazepine receptor agonist, on insulinoma cell death and insulin secretion," *Apoptosis* 10(3):533-544.

Lee, M.S., **Chang, I.,** Kim, S. (2004) "Death effectors of beta-cell apoptosis in type 1 diabetes," *Mol Genet Metab.* 83 (1-2):82-92. Review

**Chang, I.**, Cho, N., Kim, S., Kim, J.Y., Kim, E., Woo, J.E., Nam, J.H., Kim, S.J., Lee, M.S. (2004) "Role of Calcium in Pancreatic Islet Cells by IFNγ/TNFα," *J. Immunol.*172 (11):7008-70014.

Park, S.Y., **Chang, I.,** Kim, J.Y., Kang, S.W., Park, S.H., Keshav, S., Lee, M.S. (2004) "Resistance of Mitochondrial DNA-Depleted Cells Against Cell Death: Role of Mitochondrial Superoxide Dismutase," *J.Biol. Chem.* 279 (9): 7512-7520.

**Chang, I.,** Cho N., Koh J.Y., Lee, M.S. (2003) "Pyruvate Inhibits Zinc-Mediated Pancreatic Islet Cell Death and Diabetes," *Diabetologia* 46(9):1220-7.

**Chang, I.,** Kim, S., Kim, J.Y., Cho, N., Kim, Y.H., Kim, H.S., Lee, M.K., Kim, K.W., Lee, M.S. (2003) "Nuclear Factor κB Protects Pancreatic β-Cells from Tumor Necrosis Factor-α-Mediated Apoptosis," *Diabetes* 52(5):1169-75.

Kim, K.A., Kang, K., Chi, Y.I., **Chang, I.,** Lee, M.K., Kim, K.W., Shoelson, S.E., Lee, M.S. (2003) "Identification and Functional Characterization of a Novel Mutation of Hepatocyte Nuclear Factor-1α Gene in a Korean Family with MODY3," *Diabetologia* 46(5): 721-7.

Kim, J.Y., Kim, Y.H., **Chang, I.,** Kim, S., Pak, Y.K., Oh, B.H., Yagita, H., Jung, Y.K., Oh, Y.J., Lee, M.S. (2002) "Resistance of Mitochondrial DNA-Deficient Cells to TRAIL: Role of Bax in TRAIL-Induced Apoptosis," *Oncogene* 21(20):3139-48.

Kim, K.A., Kim, S., **Chang, I.,** Kim, G..S., Min, Y.K., Lee, M.K., Kim, K.W., Lee, M.S. (2002) "IFNγ/TNFα Synergism in MHC Class II Induction: Effect of Nicotinamide on MHC Class II Expression but not on Islet-Cell Apoptosis," *Diabetologia* 45(3): 385-93.

Suk, K., Kim, Y.H., **Chang, I.,** Kim, J.Y., Choi, Y.H., Lee, K.Y., Lee, M.S. (2001) "IFNγ Sensitizes ME-180 Human Cervical Cancer Cells to TNFα-Induced Apoptosis by Inhibiting Cytoprotective NF-κB Activation," *FEBS Lett.* 495(1-2): 66-70.

Suk, K.*, **Chang, I.*,** Kim, Y.H., Kim, S., Kim, J.Y., Kim, H., Lee, M.S. (2001) "Interferon γ (IFNγ) and Tumor Necrosis Factor α Synergism in ME-180 Cervical Cancer Cell Apoptosis and Necrosis. IFNγ Inhibits Cytoprotective NF-κB Through STAT1/IRF-1 Pathways," *J. Biol. Chem.* 276(16): 13153-9.

Suk, K., Kim, S., Kim, Y.H., Kim, K.A., **Chang, I.,** Yagita, H., Shong, M., Lee, M.S. (2001) "IFN-γ/TNF-α Synergism as the Final Effector in Autoimmune Diabetes: a Key Role for STAT1/IFNγ Regulatory Factor-1 Pathway in Pancreatic Beta Cell Death," *J. Immunol.* 166(7): 4481-9.

Choi, W.S., Yoon, S.Y., **Chang, I.I.,** Choi, E.J., Rhim, H., Jin, B.K., Oh, T.H., Krajewski, S., Reed, J.C., Oh, Y.J. (2000) "Correlation Between Structure of Bcl-2 and Its Inhibitory Function of JNK and Caspase Activity in Dopaminergic Neuronal Apoptosis,"
*J. Neurochem.* 74(4):1621-6.

Kim, J.E., Oh, J.H., Choi, W.S., **Chang, I.I.,** Sohn, S., Krajewski, S., Reed, J.C., O'Malley, K.L., Oh, Y.J. (1999) "Sequential Cleavage of Poly (ADP- ribose) Polymerase and Appearance of a Small Bax-Immunoreactive Protein are Blocked by Bcl-$X_L$ and Caspase Inhibitors During Staurosporine- Induced Dopaminergic Neuronal Apoptosis," *J. Neurochem.* 72(6): 2456-63.

Kim, H.J., Yoon, H.R., Washington, S., **Chang, I.I.,** Oh, Y.J., Surh, Y.J. (1997) "DNA Strand Scission and PC12 Cell Death Induced by Salsolinol and Copper,"
*Neurosci. Lett.* 238(3):95-8.

* Equal contribution to the work

# LIST OF FIGURES

# LIST OF TABLES

# LIST OF APPENDICES

# LIST OF DEFINITIONS

| | |
|---|---|
| big-ETs | big-endothelins |
| BrdU | 5’-bromo-2’ deoxyurdine |
| BUN | blood urea nitrogen |
| CCSP | Clara cell secretory protein |
| CD | Crohn’s disease |
| cDNA | complementary DNA |
| CIRBP | cold-inducible RNA-binding protein |
| CLP | colipse |
| CTP | cytidine triphosphate |
| DIO2 | type 2 iodothyrosine deiodinase |
| DSS | dextran sulfate sodium |
| E | embryonic day |
| ECE-1,-2 | endothelin converting enzyme-1,-2 |
| EDCF | endothelium derived contracturant factor |
| EDRF | endothelium derived relaxing factor |
| Epo | erythropoietin |
| ES cell | embryonic stem cells |
| ET-1,-2,-3 | endothelin-1,-2,-3 |
| $ET_{A/B}$ | endothelin receptor type A/B |
| FGF21 | fibroblast growth factor 21 |
| FIAU | fialuridine |

| | |
|---|---|
| G418 | geneticin 418 |
| HMGCS2 | hydroxymethylglutaryl-CoA synthase 2 |
| IBD | inflammatory bowel disease |
| ICV | intracerebroventricular |
| KO | knockout |
| LIF | leukemia inhibitory factor |
| *ls* | lethal spotting mutation |
| MAPK | mitogen-activated protein kinase |
| mRNA | messenger RNA |
| n.d. | non detectable |
| Neo | neomycin |
| NEP | neutral endopeptidase |
| n.s. | non-significant |
| NMR | nuclear magnetic resonance |
| P | postnatal day |
| PBS | phosphate buffered saline |
| PCNA | proliferating cell nuclear antigen |
| $pCO_2$ | partial pressure of carbon dioxide |
| PDK4 | pyruvate dehydrogenase kinase isozyme 4 |
| PEPCK | phosphoenolpyruvate carboxykinase |
| PI-3K | phosphatidylinositol- 3-kinase |
| PNLIP | pancreatic lipase |

| | |
|---|---|
| PNLIRP2 | pancreatic lipase-related protein2 |
| Prm | protamine |
| rRNA | ribosomal RNA |
| RT-PCR | reverse transcripton- polymerase chain reaction |
| S phase | synthesis phase |
| SEM | standard error of the mean |
| *sl* | piebald lethal mutation |
| SP-C | surfactant protein- C |
| $SpO_2$ | percent oxygen saturation of arterial hemoglobin |
| SRTX S6 | Sarafotoxin S6 |
| TAM | tamoxifen |
| TK | thymidine kinase |
| TNBS | 2,4,6-trinitrobenzene sulfonic acid |
| TPN | total parenteral nutrition |
| UC | ulcerative colitis |
| UCP-1 | uncoupling protein-1 |
| UTP | uridine triphosphate |
| VIC | vasoactive intestinal constrictor |
| WT | wild type |

# Chapter 1

## Introduction to the endothelin system

### Historical background

In the last 30 years, various discoveries have suggested that the vascular endothelium is not a simple barrier between blood stream and vascular wall, but rather it is a multifunctional tissue in the regulation of vascular function by producing substances of vasodilatation and vasoconstriction. The first vasoactive substance from endothelial cells was prostacyclin which acts as a vasodilator and an inhibitor of platelet aggregation (Moncada et al., 1976). In 1980, it was observed that the presence of endothelium is essential for the vasodilator response to acetylcholine. Activation of muscarinic receptors by acetylcholine in the endothelial cells stimulated the release of a substance which acted on the smooth muscle and thereby activated relaxing mechanisms. This unidentified vasodilator substance was termed Endothelium Derived Relaxing Factor (EDRF) (Furchgott and Zawadzki, 1980). As a result of considerable efforts by numerous investigators, nitric oxide was discovered as EDRF (Palmer et al., 1987).

Shortly after the discovery of EDRF, the presence of endothelium was observed to cause the opposite effect, i.e. vascular constriction under certain conditions. In 1981, De Mey and Vanhoutte realized that destruction of the endothelium reduced vascular contractions provoked by potassium (De Mey and Vanhoutte, 1981). Later, it was demonstrated that endothelial cells produced a contractile factor affected by the presence of extracellular calcium and unaffected by the blockage of the α-adrenergic, cholinergic,

serotonergic, or histaminergic systems (Gillespie et al., 1986; Hickey et al., 1985). Due to the analogy with EDRF, this unidentified vasoconstrictive substance was named Endothelium Derived Contracturant Factor (EDCF).

## Discovery of endothelin system

In 1988, the most potent vasoconstrictive factor was successfully purified from the conditioned medium of cultured porcine endothelial cells. A novel 21-residue peptide was identified and named endothelin (ET). It is known today as endothelin-1 (ET-1) (Yanagisawa et al., 1988). It contains two disulphide bridges joining the cysteines ($Cys^{1}$-$Cys^{15}$ and $Cys^{3}$-$Cys^{11}$) in the N-terminus and a group of hydrophobic amino acid residues at the end of the C-terminus. Within a year of its discovery, human genome studies revealed the presence of two other peptides, endothelin-2 (ET-2) and endothelin-3 (ET-3), with a high structural similarity, but which differ by two and six amino acid residues, respectively (Inoue et al., 1989). Interestingly, the ET exhibits a striking sequence homology with the four members of the Sarafotoxin S6 (SRTX S6) family, vasoconstrictive cardiotoxins isolated from the venom of the Israeli burrowing asp, *Actractaspis egaddensis* (Ambar et al., 1989). The fact that high sequence fidelity, binding site, and functional response have been maintained in fish, amphibians, and reptiles demonstrates that endothelin has been well-conserved during vertebrate evolution (Zigdon-Arad et al., 1992) (Figure 1-1).

Sequence analysis revealed that ET is produced as a ~200-residue precursor, named preproendothelin. After the signal peptide is removed, the preproendothelin is cleaved by a furin-like endopeptidase at the dibasic site ($KR^{52}$-$^{91}RR$) to

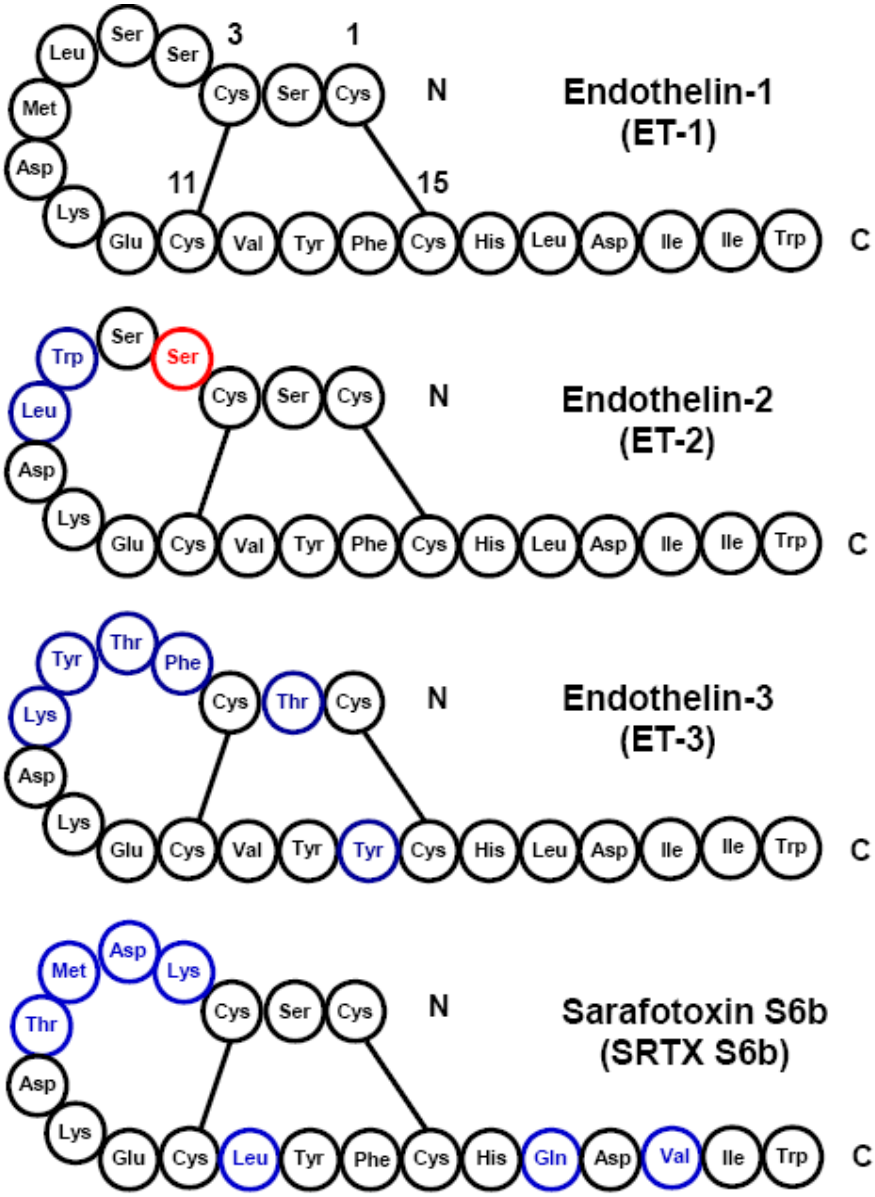


**Figure 1-1 Schematic diagram of the three endothelin isoforms and Sarafotoxin S6b.** The 21 amino acids peptides contains two disulphide bridges joining the cysteines ($Cys^{1}$-$Cys^{15}$ and $Cys^{3}$-$Cys^{11}$) in N-terminal and a group of hydrophobic amino acid residues at the end of C-terminal. ET-2 differs from ET-1 by two amino acids in human and three amino acids in rodents substituting $Ser^{4}$ with $Asn^{4}$. ET-3 differs from ET-1 by six amino acids in both human and rodent. The sequence of one of the members of sarafotoxin S6 family, SRTX S6b, is shown to compare the sequence homology which differs from ET-1 by seven amino acids.

yield biologically inactive intermediates termed big-endothelins (big-ETs). These 37~ 40-amino acid big endothelins are further cleaved at the Trp-Val of ET-1 and ET-2 or at the Trp-Ile of ET-3 by specific metalloproteases called endothelin-converting enzymes (ECEs) which generate the active, 21-residue mature form of the endothelins (Emoto and Yanagisawa, 1995; Xu et al., 1994). ECE-1 and ECE-2 are two ECE isoforms involved in big-ET processing. Their sequences are highly conserved and very similar to two other metalloproteases, the neutral endopeptidase 24.11 (NEP) and the human Kell blood group protein. ECE-1 is found in a variety of cells including endothelial cells and cleaves both intracellular and extracellular big-ETs at neutral pH (Xu et al., 1994). ECE-2 is also located in diverse cell types including neurons but only processes intracellular big ETs at pH 5.8 (Emoto and Yanagisawa, 1995). *In vitro* cleavage analysis showed that ECEs cleave big ET-1 much more efficiently than big ET-2 and big ET-3. Since *ECE-1* and *ECE-2* double mutant mice still contain significant amount of mature ET peptides, the presence of another unidentified ECE isoform(s) is predicted (Yanagisawa et al., 2000) (Figure 1-2).

Each member of the endothelin family is encoded by a separate gene. *ET-1* is found on human chromosome 6, and mouse chromosome 13, *ET-2* is located on human chromosome 1, and mouse chromosome 5 and *ET-3* is assigned on human chromosome 20, and mouse chromosome 2 (Bloch et al., 1989). Although originally isolated and purified from the endothelial cells, ET isopeptides are produced in a variety of tissues and cell types. Endothelial cells, regardless of origin, appear to express *ET-1* mRNA. *ET-2* and *ET-3* are not expressed in either vascular endothelium or smooth muscle. *ET-1* gene expression was also found in epithelial cells in the breast, and lung. Keratinocytes,

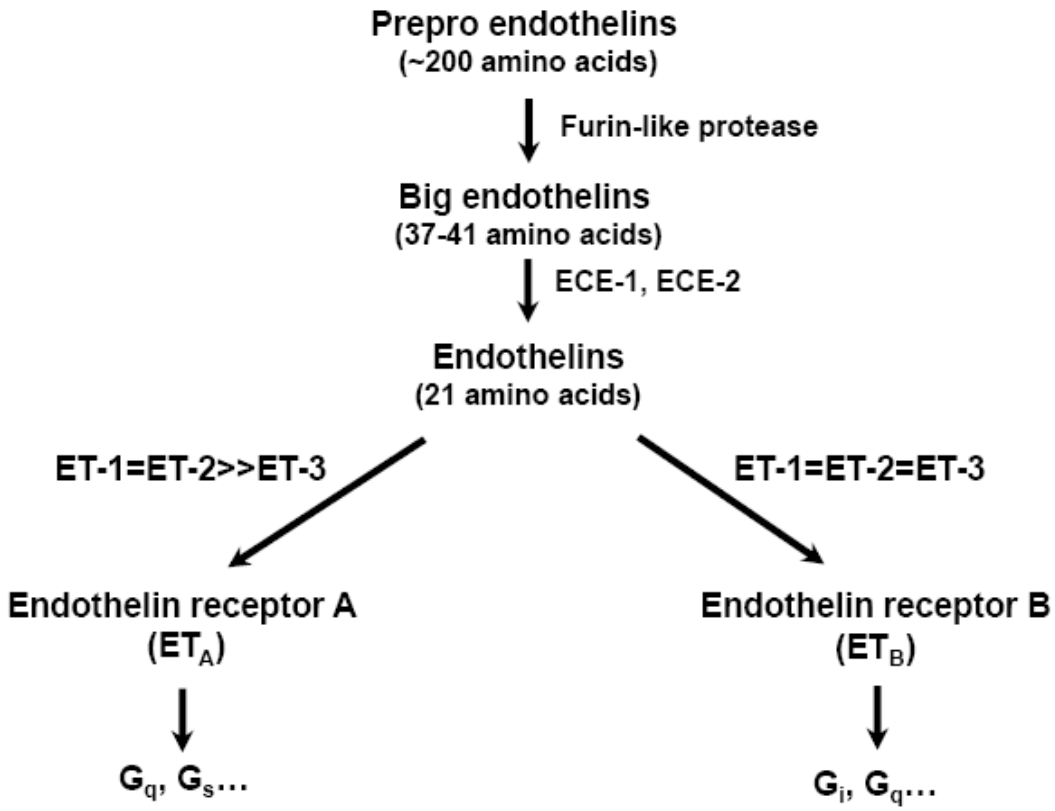


**Figure 1-2 The molecular components and pathway of endothelin.** Preproendothelins are processed by furin-like proteases to form big endothelins. These inactive intermediates are further cleaved to three physiologically active endothelin peptides by endothelin-converting enzymes. The peptides interact with a pharmacologically selective $ET_A$ receptor and nonselective $ET_B$ receptor. These receptors coupled to various G proteins to produce a variety of different physiological responses. ET-1/ECE-1/$ET_A$ pathway is essential for the development of pharyngeal arch-derived, craniofacial and cardiac tissues. ET-3/ECE-1/$ET_B$ pathway is important for the development of the enteric nervous system and skin melanocytes.

fibroblasts, macrophages, cardiomyocytes, neurons of brain and spinal cord, astrocytes, bone marrow and mast cells are all positive for *ET-1* mRNA. *ET-3* is expressed by brain neurons, renal tubular and intestinal epithelial cells (Rubanyi and Polokoff, 1994). At the tissue level, *ET-1* expression was observed in vascular epithelium, in the lung, brain,

uterus, stomach, heart, adrenal gland, liver, spleen, placenta, skeletal muscle and kidney (Sakurai et al., 1991). *ET-3* expression was present in the eye ball, submandibular gland, brain, kidney, intestine, stomach, and spleen (Shiba et al., 1992). The expression of *ET-2* mRNA is much more limited than *ET-1* and *ET-3* and it is discussed in the section below.

Endothelins act on two pharmacologically and molecularly distinct receptors called $ET_A$ and $ET_B$ (Arai et al., 1990; Sakurai et al., 1990). Both receptors belong to the G-protein coupled heptahelical family of receptors and are expressed in a wide range of cell types with distinct, but partially overlapping tissue distribution. Vascular smooth muscle cells express $ET_A$ and $ET_B$, both of which can mediate the direct vasoconstrictor action of endothelins. On the other hand, endothelial cells express $ET_B$ that mediates endothelin-induced activation of nitric oxide synthetase which counteracts vasoconstriction. $ET_A$ is found on vascular endothelial cells, airway smooth muscle cells, cardiomyocytes, liver stellate cells and hepatocytes, brain neurons, osteoblasts, melanocytes, keratinocytes, adipocytes, and various cells in the reproductive tract. $ET_B$ exists on liver hepatocytes and Ito cells, renal collecting duct epithelial cells, airway smooth muscle cells, osteoblasts, neurons of the central and peripheral nervous system, and various cells of the reproductive tract. The two receptors have highly distinct isopeptide selectivity. Although $ET_A$ receptor exhibits different affinities for each ligand with a potency rank order of ET-1≥ET-2>>ET-3, the $ET_B$ subtype recognizes all three ET peptides equally (Kedzierski and Yanagisawa, 2001).

On binding of endothelins, both $ET_A$ and $ET_B$ receptors trigger a similar set of intracellular signaling pathways via the activation of heterotrimeric G proteins, including phospholipase C and D, $Ca^{2+}$ ions, activation of the Ras, mitogen-activated protein kinase

(MAPK) and phosphatidylinositol-3-kinase (PI-3K). This leads to a variety of cellular actions depending on the target cell types, e.g. on contraction of vascular smooth muscle cells, hypertrophy of cardiac myocytes, and proliferation and cell survival of ovarian carcinoma cells, which is mediated by the ET-1/$ET_A$ pathway (Clerk and Sugden, 1997; Kawanabe and Nauli, 2005; Pollock et al., 1995; Yamboliev et al., 1998).

The production of endothelins is tightly regulated at the level of mRNA transcription because many endothelin-producing cells do not have storage vesicles or regulated secretory pathways. It is thought that endothelins act as autocrine and paracrine factors at multiple sites in the body rather than as circulating hormones because (1) the receptor expressing target cells and ligand producing cells are always juxtaposed within the same tissue; (2) the circulating plasma concentration is much lower than the pharmacological threshold; and (3) circulating endothelins are rapidly cleared by the lung, kidney, and other organs (Yanagisawa, 1994).

### *In vivo* roles of the endothelins

Endothelins exert a number of physiological functions and are involved in pathological conditions. ET-1 is the only endothelin produced by vascular endothelial cells. ET-1 interacts with $ET_A$ expressed on vascular smooth muscle cells as well as $ET_B$ on endothelial cells and on some smooth muscle cells. Activation of the vascular endothelin system has a basal vasoconstricting role and contributes to the development of vascular disease in hypertension and atherosclerosis. In the heart, endothelin system leads to myocardial contractility, chronotropy, and arrhythmogenesis, as well as to myocardial remodeling after congestive heart failure. In the lung, it regulates bronchial tone and the

proliferation of pulmonary airway blood vessels. It promotes the development of pulmonary hypertension. In the kidney, endothelin system controls water and sodium excretion and acid–base balance under physiologic conditions. It accelerates the development of glomerulosclerosis. In the brain, the endothelin system modulates cardiorespiratory centers and the release of hormones and contributes to growth guidance of developing sympathetic neurons. In addition, endothelin components participate in the physiology and pathophysiology of the immune system, liver, muscle, bone, skin, prostate, adipose tissue and reproductive tract (Barton and Yanagisawa, 2008; Rubanyi and Polokoff, 1994) (Figure 1-3).

## Elucidating the Endothelin Signaling System by Evaluating Knockout Mice

A) Endothelin knockout mice

The developmental roles of the endothelin system components have been extensively studied using gene targeted mice. The ET-1/$ET_A$ pathway is essential for the development of pharyngeal arch-derived, craniofacial and cardiac tissues. *ET-1* and $ET_A$ deficient mice die at birth from mechanical asphyxia due to critical malformation of neural crest-derived facial and throat structures. *ET-1* and $ET_A$ knockout mice commonly display craniofacial malformations including a cleft palate, underdeveloped mandible, abnormal fusion of the hyoid bone at the base of skull, and abnormal middle ear structures. These mice also have arterial defects including the absence of the right subclavian artery, the interruption of the aorta, the presence of a right-sided aortic arch, and ventricular septal defects (Clouthier et al., 1998; Kurihara et al., 1994) (Figure 1-4).

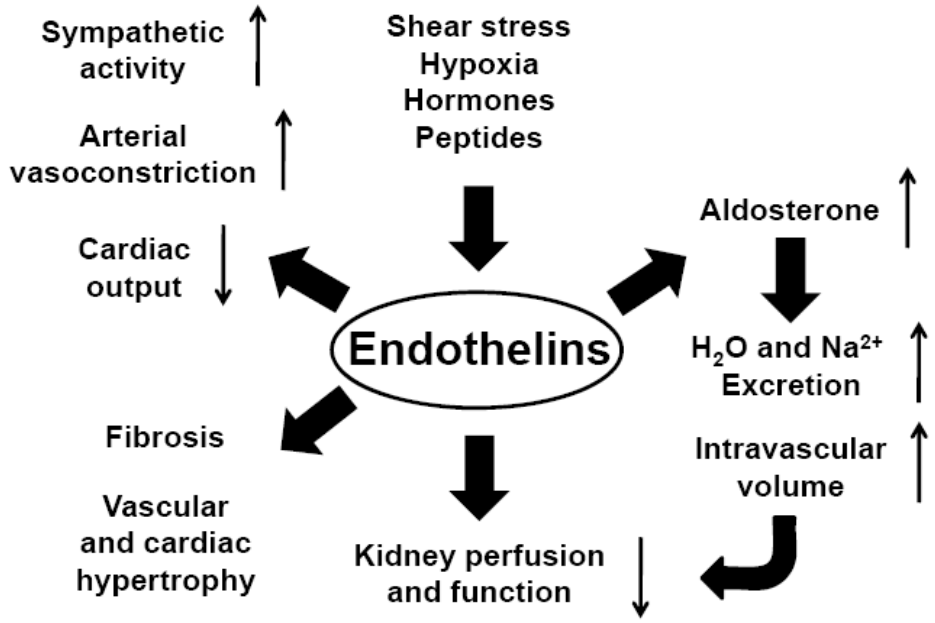


**Figure 1-3 Dysfunction of endothelin impacts multiple organs and systems.** (Adapted from http://www.endothelinscience.com/endopath.dfm)

The ET-3/$ET_B$ pathway is essential for the development of the enteric nervous system and skin melanocytes. *ET-3* and $ET_B$ knockout mice are viable at birth, but fail to thrive and die at about 2 to 8 weeks of age. The distal colon of *ET-3* and $ET_B$ deficient mice is narrowed and functionally obstructed due to the absence of enteric neurons. This leads to dilation of the proximal colon, intestinal dysfunction and eventually death. The natural recessive mouse or rat mutations, piebald lethal (*sl*) and lethal spotting (*ls*), also exhibit distal colonic-aganglinosis and the loss of epidermal melanocytes. Further, it was found that mutations of ET-3 and $ET_B$. *ET-3* and $ET_B$ knockout mice also exhibit deficient epidermal melanocytes which result in white- spotted hair and skin color but normal retinal melanin pigmentation. In humans, mutations in *ET-3* and $ET_B$ result in congenital Hirschsprung's disease, found in 1/10,000 births and it causes gradual bloating of the

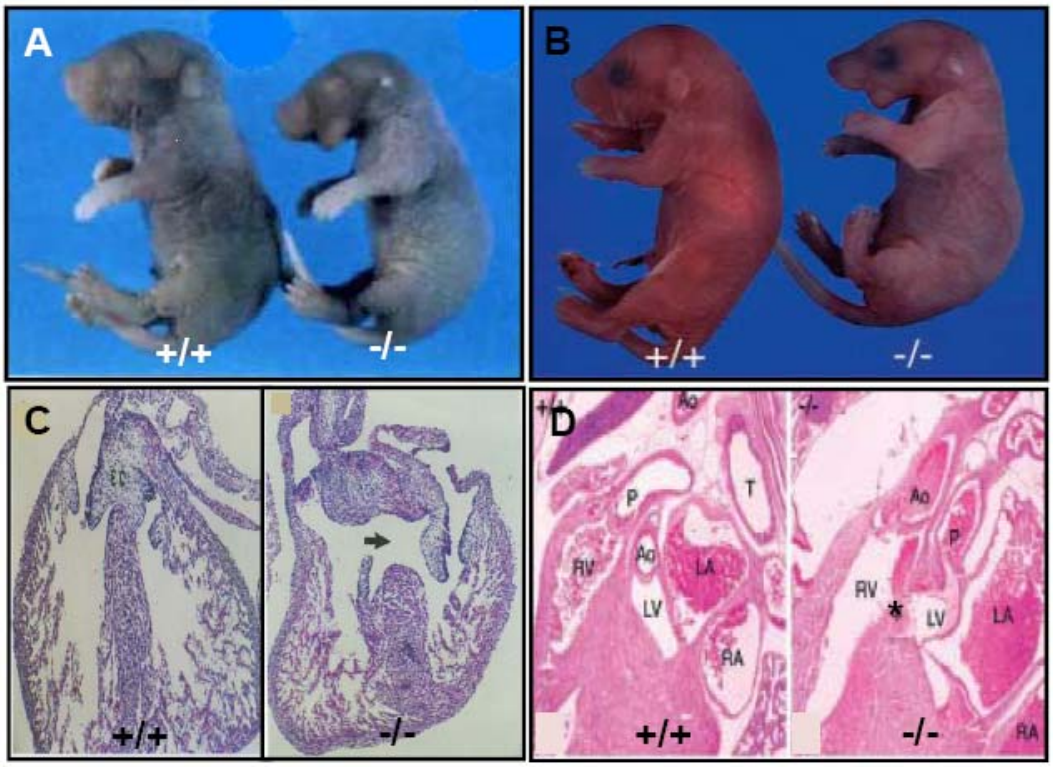


**Figure 1-4 Defects in the development of craniofacial and cardiac structures in *ET-1* and $ET_A$ deficient mice.** (A and B) Gross appearance of *ET-1* (A) and $ET_A$ (B) knockout pups and their wild type controls. Mutant pups have a shortened mandible, hypoplastic pinnae and appear cyanotic. (C and D) Histological analysis of the heart in *ET-1* (C) and $ET_A$ (D) null mice. Hematoxylin and eosin staining of parasagittal sections through the interventricular septum. The ventricular septal defect in the mutant is marked by arrow and asterisk, respectively. (Adapted from Kurihara, 1994, 1995; Clouthier, 1998)

abdomen, onset of vomiting and fever. (Baynash et al., 1994; Hosoda et al., 1994) (Figure1-5).

B) ECEs knockout mice

A majority of *ECE-1* null embryos die in utero. The *ECE-1* deficient mice display a phenotype that exhibits combined features of animals lacking ET-1/$ET_A$ and ET-3/$ET_B$ pathways revealing the critical importance of this enzyme in producing both ET-1 and

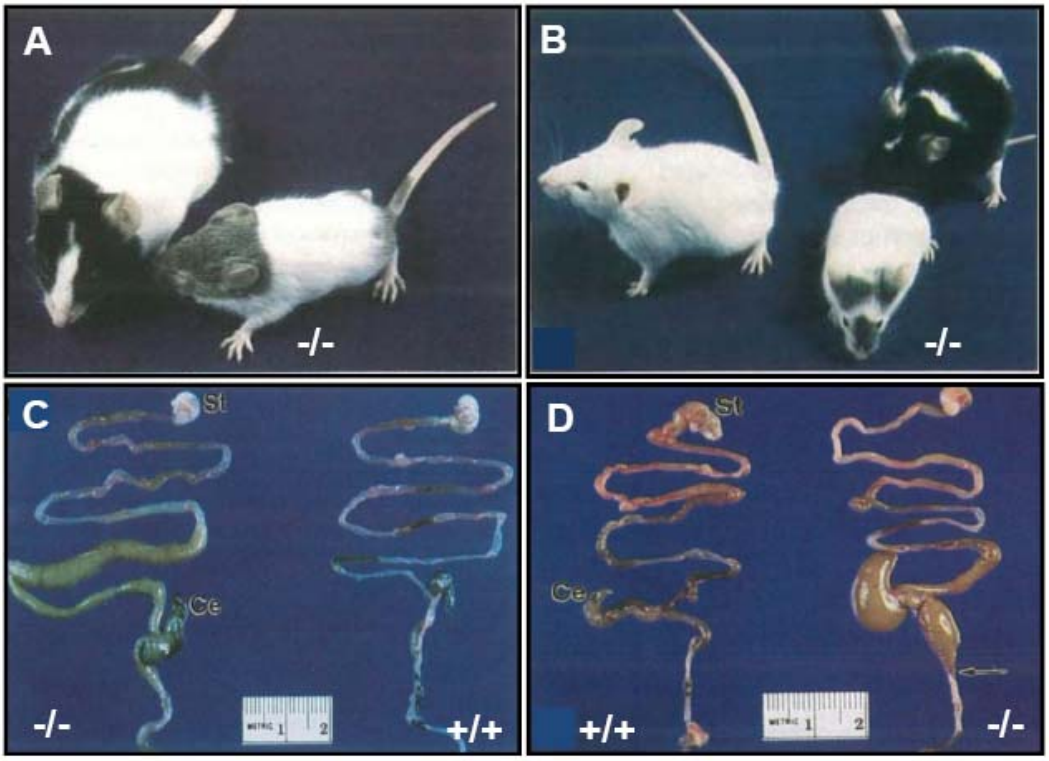


**Figure 1-5 Abnormalities in the development of epidermal melanocytes and enteric nervous system in *ET-3* and $ET_B$ knockout mice.** (A) Coat color spotting in *ET-3* deficient mouse (right) and an *ls/ls* mouse (left). Note the large continuous pigmented patches in the head and hip regions of these mice. (B) White-spotted coat color of $ET_B$ knockout mouse (middle). A $s^l/s^l$ mouse (left) almost completely white. A *s/s* mouse (right) exhibits less extensive spotting. (C and D) Dissection of the entire gastrointestinal tract from *ET-3* (C) and $ET_B$ (D) null mouse with their wild type controls. St, stomach; Ce, cecum. Distension of the ileum and cecum is evident in the *ET-3* knockout mouse. Distension of the distal ileum, cecum, and proximal colon is evident in the $ET_B$ deficient mouse. An arrow indicates the transitional zone between the proximal distended and distal narrow (aganglionic) segments of the colon. (Adapted from Baynash, 1994; Hosoda, 1994)

ET-3 (Yanagisawa et al., 1998) (Figure1-6). Although ECE-2 null mice revealed no marked abnormalities, ECE-1/ECE-2 double mutants exhibited more severe cardiac abnormalities including endocardial cushion defects (Yanagisawa et al., 2000).

C) Selective deletions using the *Cre-loxP* system

Tissue specific roles of the endothelin system have been investigated in mice using *Cre/loxP* technology. Cardiomyocyte-specific deletion of *ET-1* (Kedzierski et al., 2003; Shohet et al., 2004) and $ET_A$ (Kedzierski et al., 2003) confined their roles in cardiac hypertrophy. Collecting duct-specific inactivation of *ET-1* (Ahn et al., 2004), $ET_A$ (Ge et al., 2005), $ET_B$ (Ge et al., 2006), and both $ET_A$ and $ET_B$ (Ge et al., 2008) revealed their functions in blood pressure and sodium excretion.

## ET-2: The last member

Murine ET-2 was initially discovered by genomic library screening using human ET-1 as a probe. The ET-2 peptide was found to have a strong intestinal contractile activity. Because its expression seemed to be confined to the intestine, it was called the Vasoactive Intestinal Constrictor (VIC) despite the fact that VIC is the mouse and rat orthologous peptide of human ET-2 (Bloch et al., 1991; Inoue et al., 1989; Saida et al., 1989). Sequence analysis of a full-length *ET-2* gene revealed that the mouse *ET-2* is encoded by five exons, interrupted by four introns spanning 5912 bp of genomic DNA. The first exon represents the 5'- sequences encoding the first 19 residues of prepro *ET-2*, which includes the putative signal peptide. The second exon consists of 53 residues of prepro *ET-2* encoding the mature *ET-2* and the first 5 residues of the 17-residue tail portion of big *ET-2*. The third exon consists of 42 residues of prepro *ET-2*, which encode the rest of big *ET-2*. The fourth exon encodes 34 residues of prepro *ET-2*. The fifth exon encodes the 31 carboxyl-terminal residues of prepro *ET-2* and the whole 3'-untranslated region (Deng, 1997; Saida et al., 2000; Sharma et al., 1998).

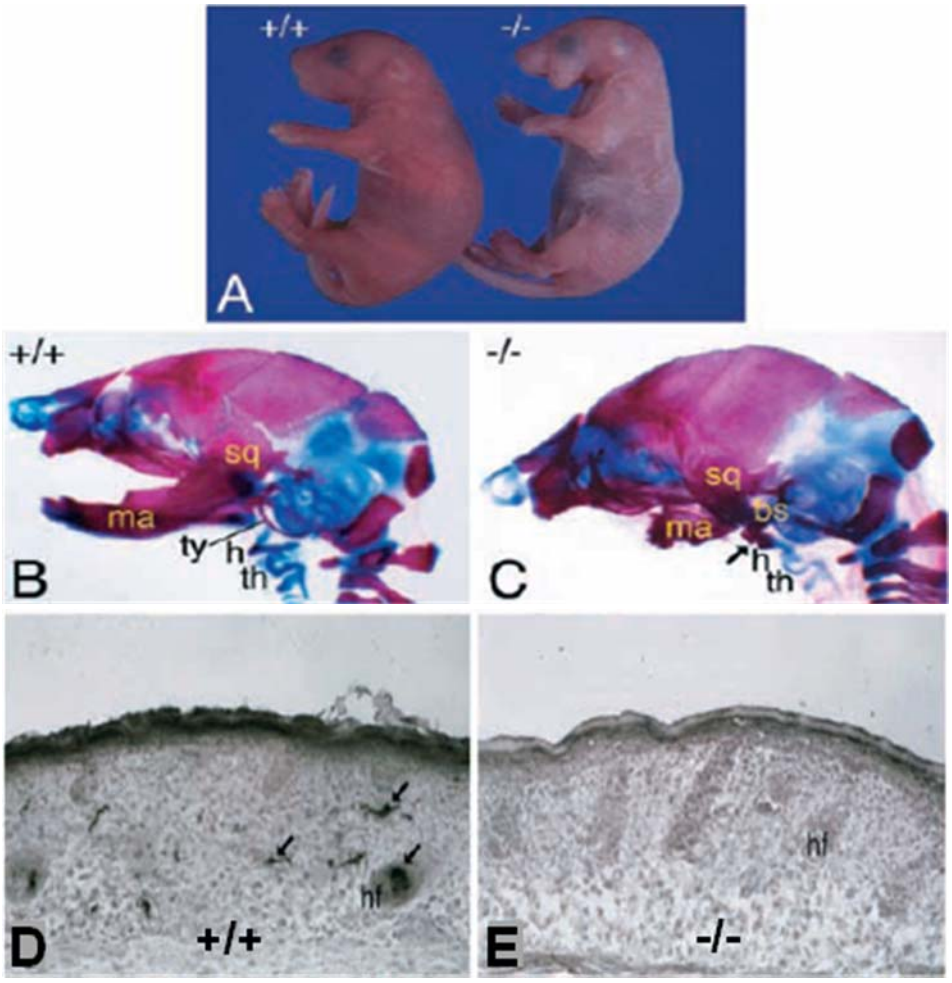


**Figure 1-6 Combined phenotype of animals lacking ET-1/$ET_A$ and ET-3/$ET_B$ pathways in *ECE-1* deficient mice.** (A,B and C) Craniofacial defects in *ECE-1* knockout mice. (A) Gross appearance of P0 wild-type and *ECE-1* knockout mice. Mutant mouse (right) is cyanotic and shows hypoplastic jaw and pinna. (B and C) Skeletal preparations with alizarin red and alcian blue. Note hypoplastic mandible (ma) and abnormal fusion (arrow) of the hyoid (h) with basisphenoid bone (bs) and thyroid cartilage (th) in the mutant (C). (D and E) L-DOPA histochemistry on frozen sections of dorsal skin. Interfollicular melanocytes (arrows) are absent in *ECE-1* deficient embryo (E). hf, hair follicle (Adapted from Yanagiswa, 1998)

ET-2 has been relatively ignored in the endothelin research field because (1) it is pharmacologically and immunologically indistinguishable from ET-1; (2) it is expressed at much lower levels in comparison to *ET-1* and to *ET-3*; and (3) the tissue distribution of ET-2 is highly limited; *ET-2* is most abundantly expressed in the intestine. Therefore, a specific role for ET-2 in the gastrointestinal tract has been speculated.

Quantitative analysis of tissue distribution has demonstrated that *ET-2* is expressed in a variety of tissues including brain, testis, ovary, uterus, and lungs, as well as most highly in intestine as previously described (Uchide et al., 1999). During the developmental period, low expression was observed in the brain, heart, lungs, and kidney, remaining almost constant throughout the period examined. Interestingly, in the intestine, *ET-2* showed a gradual increase at later embryonic stages and then it remained constant throught adulthood. In lung tissue, *ET-2* displayed a sharp increase soon after birth (Uchide et al., 2002). In brain tissue, *ET-2* gene expression was observed at high levels in the pituitary gland and medulla oblongata, and moderate to low levels of expression were observed in other brain regions containing the cortex, septum, striatum, hypothalamus and midbrain (Masuo et al., 2003). These results indicate that ET-2 may play other physiological roles outside the gastrointestinal tract.

In an attempt to define the role of ET-2 in physiology and pathophysiology, transgenic rats expressing the human *ET-2* gene was generated (Liefeldt et al., 1995; Liefeldt et al., 1999). The *ET-2* transgene expression was detected in the brain, lung, and adrenal glands, as well as predominantly in the kidney and gastrointestinal tract. Although peptide levels were increased, blood pressure was not elevated. The litter size of the *ET-2* transgenic animals did not differ from that of nontransgenic controls. Twelve-

month-old transgenic animals exhibited glomerular sclerosis, interstitial fibrosis, and diffused vascular changes (Liefeldt et al., 1999).

Recently, several potential roles of ET-2 have been proposed: *ET-2* mRNA is strongly induced in photoreceptor cells in retinal diseases and injury, which may function as a stress signal to Muller cells through $ET_B$ (Rattner and Nathans, 2005). During the ovulatory process, ET-2 is transiently produced in granulosa cells of preovulatory follicles and induces follicular rupture through $ET_A$ (Ko et al., 2006). In the field of tumor biology, ET-2 may serve as a marker for uveal melanoma (Zuidervaart et al., 2003), and is highly induced by hypoxia in squamous carcinoma cell lines derived from both pharynx and cervix (Koong et al., 2000). ET-2 may act as a chemoattractant for macrophages in tumors (Grimshaw et al., 2002b), and as an inducer of metastatic invasion (Grimshaw et al., 2004) as well as being a survival factor for breast tumor cells (Grimshaw et al., 2002a). However, despite these reports, very little was known about the biological function of endogenous ET-2 until now.

In this dissertation, I will describe my studies using constitutive and conditional knockout mouse models to investigate the physiological role of endogenous endothelin-2. Chapter Two will present data to confirm initial findings and describe for constitutive *ET-2* deficient mice and the reproduction of this phenotype in mice with a systemic deletion of *ET-2* in young and adulthood. Chapter Three will present the evidence that ET-2 is important for energy homeostasis. Chapter Four will present finding to suggest that ET-2 is essential for thermoregulation. Chapter Five will report data demonstrating that ET-2 is critical for lung morphology and function. Chapter Six will describe the protective role of intestinal ET-2 in inflammatory bowel disease. Chapter Seven will

discuss possible physiological models to define the role of ET-2 underlying these phenotypes, present a hypothesis to identify the physiologically relevant receptor for the ET-2 ligand, and suggest future directions for better understanding of ET-2 function *in vivo*.

# Chapter 2

## Initial Characterization of Endothelin-2 Knockout Mice

### Introduction

In order to determine the precise role of ET-2 in the *in vivo* system, our lab genetically inactivated the *ET-2* gene in mice. *ET-2* deficient mice are born severely growth retarded and die within the first four weeks of life. These phenotypes were equivalently displayed in four different clonal lines of mixed 129 SvEv/C57B1/6 or pure 129 SvEv background (Baynash, 2006).

Because of the relatively high expression of *ET-2* in the small intestine and colon, initial analyses were mainly focused on examining intestinal structure and function. General histology was performed to evaluate intestinal neurons and all four cell types in the small intestine were examined. *In vitro* contractile activity and barium transit assays showed that the intestine from the mutant mice appears to function normally. Upon necropsy, *ET-2* knockout mice are observed to have distended abdomens and their lower intestines are filled with abnormal quantities of gas. Gnotobiotic rederivations of these animals did not alleviate the anomaly, indicating that intestinal bacteria are not responsible for the gas accumulation. Although milk was often present in their stomachs, blood chemistry indicated a severe hypoglycemia in the face of normal insulin levels. Glucose tolerance tests demonstrated that *ET-2* knockout mice are impaired in their ability to reduce blood glucose level after an intraperitoneal glucose challenge. *In vivo* glucose absorption experiments revealed a decrease of glucose uptake in the intestine of

*ET-2* deficient mice. Taken together, these early studies supported a physiological role of ET-2 in glucose homeostasis (Baynash, 2006).

The hypothesis that ET-2 deficiency impairs glucose utilization and homeostasis and, therefore, leads to growth retardation and early death was proposed (Baynash, 2006). However, additional molecular and hormonal studies would be required to elucidate the mechanism leading to the low blood glucose levels observed in the *ET-2* deficient mice. The diminutive size and early lethality of *ET-2* mutant mice limited many essential experiments and was one of the most difficult aspects of pursuing this project.

To clarify the unique and essential function of ET-2, I revisited its gene expression pattern using a comprehensive set of tissues throughout mouse development. In order to find additional functional roles of ET-2 outside the intestine, I also reexamined overall phenotypes of *ET-2* deficient mice. To overcome the limitation presented by the small size restriction for many of the experiments and to determine when ET-2 action is important, I established inducible *ET-2* knockout mice and analyzed the phenotypes. I found that postnatal inactivation of the *ET-2* gene reproduces the phenotype of constitutive *ET-2* deficient mice, and concluded that ET-2 has a critical role in the growth regulation and survival of postnatal mice, but has little impact on embryonic development.

## Results

### Tissue distribution of *ET-2* mRNA

To identify sites of ET-2 action, *ET-2* expression was examined by quantitative RT-PCR with a variety of mouse tissues. As previously reported (Uchide et al., 1999), I confirmed

*ET-2* mRNA is abundantly expressed in the upper and lower gastrointestinal tract (Figure 2-1A). Albeit at lower levels, ET-2 was also detected in a number of additional tissues including the brain, lung, pancreas, testis, and ovary (Figure 2-1A). During the embryonic period, *ET-2* expression is markedly increased from embryonic day (E) 15 and remains roughly constant until birth (Figure 2-1B).

**Generation of constitutive *ET-2* knockout mice**

The *ET-2* constitutive knockout mouse was generated by complete deletion of exon 2, which encodes the mature ET-2 peptide (Figure 2-2A; Baynash, 2006). Because ET-2 is immunologically indistinguishable from ET-1, I confirmed that the absence of ET-2, by demonstrating *ET-2* mRNA was not evident in the stomach, small intestine, and colon of knockout mice by quantitative RT-PCR (Figure 2-2B). To assure that this targeting strategy had no effect on neighboring genes, I measured *human immunodeficiency virus type 1 enhancer-binding protein 3 (HIVEP3)* and *Foxo6* which are located at 26kb and 99kb apart from 5' and 3' end of *ET-2* on chromosome 4, respectively and found unaltered mRNA levels in the brain, heart, and small intestine of *ET-2* knockout mice (data not shown).

**Growth retardation and juvenile lethality of *ET-2* knockout mice**

Constitutive *ET-2* knockout mice were born healthy with the expected frequencies. Out of 154 pups examined, there were 40 (26.0%) $ET\text{-}2^{+/+}$, 72 (52.6%) $ET\text{-}2^{+/-}$, and 42 (27.2%) $ET\text{-}2^{-/-}$ mice. At postnatal day (P) 3, the appearance and size of the pups were

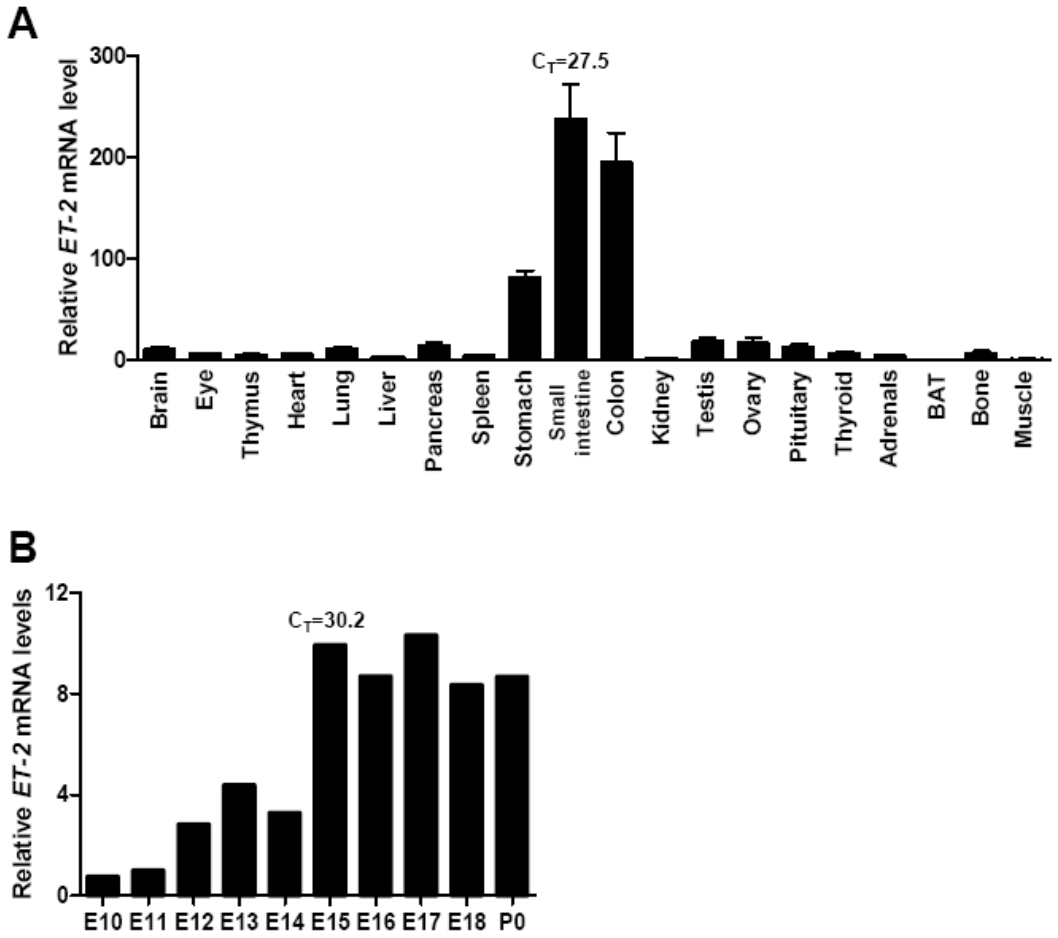


**Figure 2-1 Expression profile of *ET-2* mRNA.** (A) Quantitative RT-PCR analysis of *ET-2* mRNA expression in individual tissues (n=3). (B) Time course of *ET-2* mRNA expression in whole embryo at the designated ages by quantitative RT-PCR (E, embryonic day; P, postnatal day). Values were normalized by *18s rRNA* expression. Error bars indicate ± SEM.

similar to their littermates. Although they were frequently observed being nursed and a normal amount of milk was detected in the stomach (Figure 3-2A), by P5, *ET-2* null mice failed to thrive (Figure 2-3A) and displayed severe growth retardation. The mutant mice eventually die by 3-4 weeks of age (Figure 2-3B).

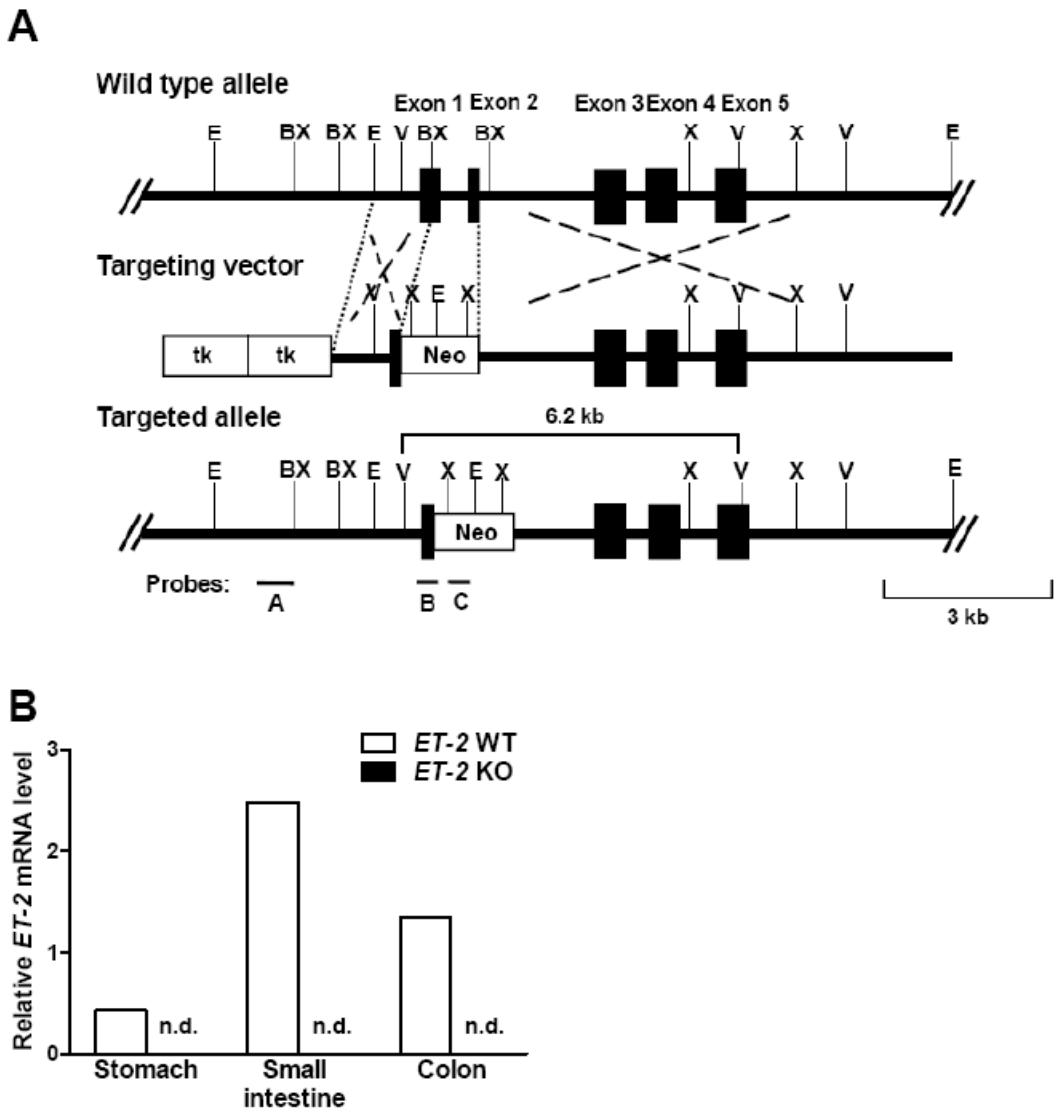


**Figure 2-2 Generation of mouse with a constitutive *ET-2* mutation.** (A) Schematic representation of the mouse *ET-2* locus and the targeting strategy. Dashed lines show site specific recombination events. Positions of probes for Southern blot analysis are shown as probe A, B, and C. Probe A and B correspond to a probe in the 5' short arm and 3' long arm, respectively. Probe C is a 5' fragment of the Neo gene used to confirm single insertion. tk, thymidine kinase; Neo, neomycin resistance cassette; E, EcoR I; BX, BstX I; V, EcoRV; X, Xba I (Baynash , 2006). (B) Quantitative RT-PCR analysis demonstrating absence of *ET-2* mRNA in individual tissues. (C) Quantitative RT-PCR analysis of *HIVEP3* and *FoxO6* mRNA in indicated tissues. Values were normalized by *18s rRNA* expression. n.d., non detectable

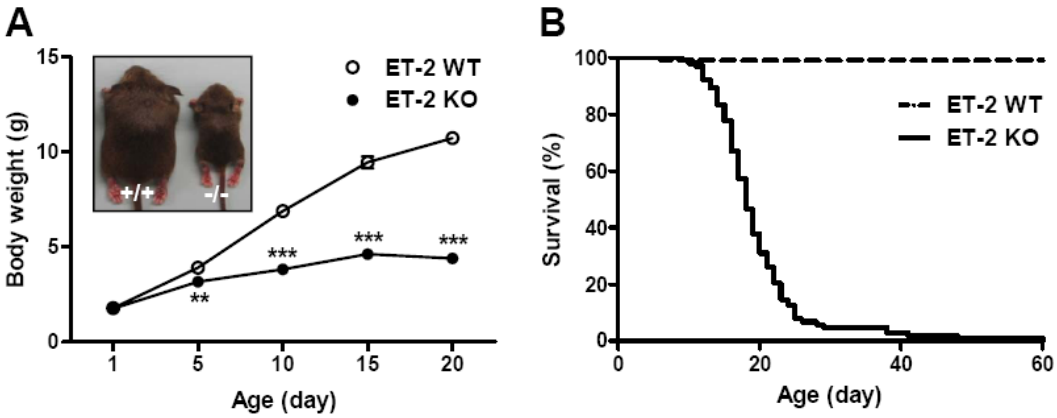


**Figure 2-3 Growth retardation and juvenile lethality of constitutive *ET-2* knockout mice.** (A) Body weight during pre-weaning period of constitutive *ET-2* knockout mice and wild type controls (n=15 per group). Inset: Representative photograph of wild type (left) and *ET-2* knockout mice (right) at 2 weeks of age. Error bars indicate ± SEM. $^{**}p<0.01$, $^{***}p<0.001$ (B) Survival ratio of constitutive *ET-2* knockout mice (n=100) and wild type controls (n=102).

**Generation of globally inducible ET-2 knockout mice**

Despite the obvious phenotype at only the postnatal period, increased *ET-2* expression was detected from E15 (Figure 2-1B). Hence, to examine whether the presence of ET-2 is important for growth and survival during embryonic and postnatal development, I generated systemically inducible *ET-2* knockout mice by crossing *ET-2*$^{flox}$ mice and mice harboring tamoxifen-activated *Cre* recombinase transgene (Hayashi and McMahon, 2002). The ET-2 mutant allele contains two loxP sites flanking exon 2 (Figure 2-4A and B). Before establishing the transgenic lines, I confirmed the reliability of floxed *ET-2* transgene by crossing with mice expressing Cre recombinase driven by *protamine 1* promoter that globally excises the loxP-flanked genomic region in the germline (O'Gorman et al., 1997). *ET-2*$^{flox/flox}$*; Prm-Cre* mice showed growth retardation and

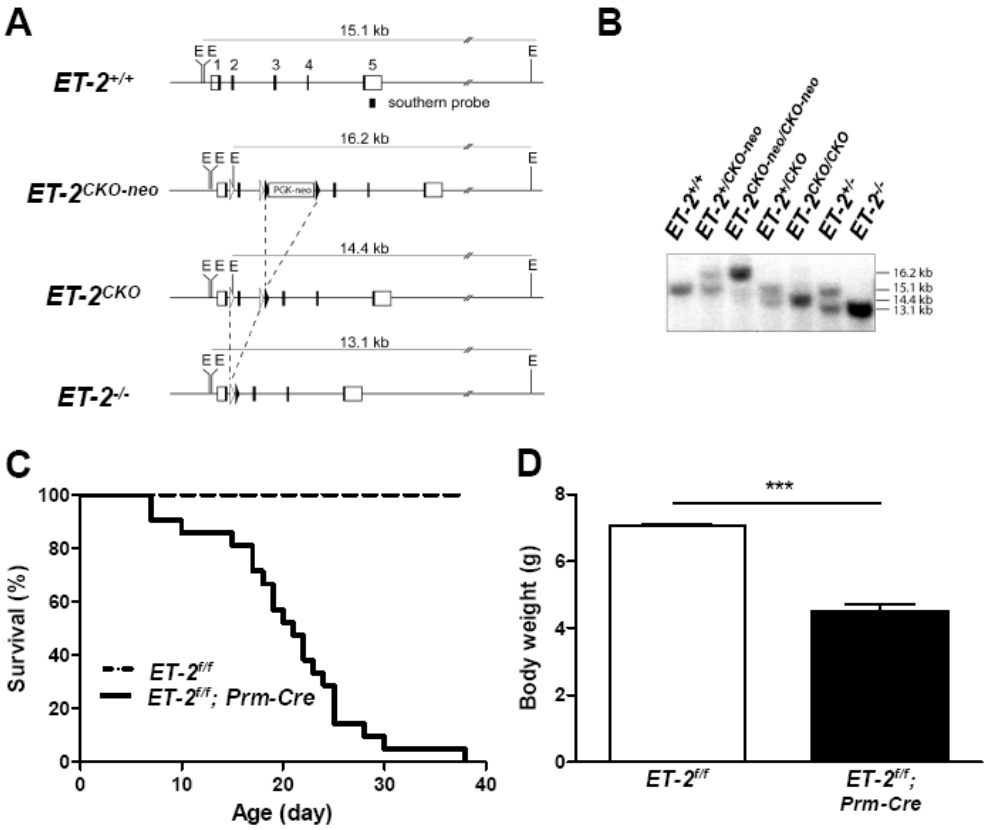


**Figure 2-4 Conditional knockout allele for *ET-2*.** (A) Top to bottom: genomic structure of the *ET-2* gene: exons are represented by boxes with the coding region filled and exon numbers marked above, and the Southern blot probe is below; the initial gene targeting product in which exon 2 is flanked by loxP sites (open triangles) and is followed by Frt (filled triangles)-flanked PGK-neo ($ET\text{-}2^{CKO\text{-}neo}$); the targeted allele following Frp-mediated excision of the PGK-neo cassette ($ET\text{-}2^{CKO}$); the *ET-2* null allele obtained by Cre-mediated excision of exon 2. Dashed lines show site specific recombination events. The predicted lengths of the EcoRI restriction fragments are shown above each of the alleles. E, EcoR I. (B) Southern blot hybridization of EcoR I digested genomic DNA showing hybridization patterns for the four alleles illustrated in panel A. (Rattner and Nathans, unpublished data) (C) Survival ratio of $ET\text{-}2^{flox/flox}$*; prm-Cre* and wild type controls (n=20). (D) Body weight of $ET\text{-}2^{flox/flox}$*; prm-Cre* and wild type controls (n=10) at 3 weeks of age. Error bars indicate ± SEM. ***$p<0.001$

juvenile lethality, consistent with the phenotypes of constitutive *ET-2* knockout mice

(Figure 2-4C and D). Reduced expression of *ET-2* mRNA by tamoxifen administration to

*ET-2*$^{flox/flox}$; TAM-*Cre* mice at P1 or 6 weeks of age was confirmed by quantitative RT-PCR in individual tissues including the brain, lung, pancreas, stomach, small intestine and colon (Figure 2-5A).

When *ET-2* was inactivated at P1 by gavage feeding tamoxifen to the dam (hereafter referred to as neonate *ET-2*$^{flox/flox}$ mice for wild type controls and neonate *ET-2*$^{flox/flox}$*;* TAM-*Cre* mice for *ET-2* mutant mice), it fully recapitulated the phenotypes of constitutive knockout mice: growth retardation (Figure 2-5B) and early lethality (Figure 2-5C). Even deletion of *ET-2* at 6 weeks of age (henceforth referred to as adult *ET-2*$^{flox/flox}$ mice for wild type controls and adult *ET-2*$^{flox/flox}$*;* TAM-*Cre* mice for *ET-2* mutant mice) led to diminished weight gain (Figure 2-5D and E).

## Discussion

My tissue survey demonstrated that ET-2 is expressed in a variety of tissues, but most highly in the upper and lower gastrointestinal tract. Its expression is markedly increased from embryonic day (E) 15 and remained roughly constant until birth. As initial observation, *ET-2* deficient mice are smaller than their wild type littermates. Furthermore, their growth retardation becomes more obvious with time and finally leads to premature death of the mutant mice. Conditional deletion of *ET-2* using *Prm-Cre* at early development revealed the same defects with the constitutive deficient mice. *ET-2* inactivation from P1 also showed growth retardation and juvenile lethality, revealing the importance of ET-2 at the postnatal stage. Interestingly, loss of body weight was clearly observed in mice inactivating *ET-2* as adults. These data indicate that ET-2 is essential

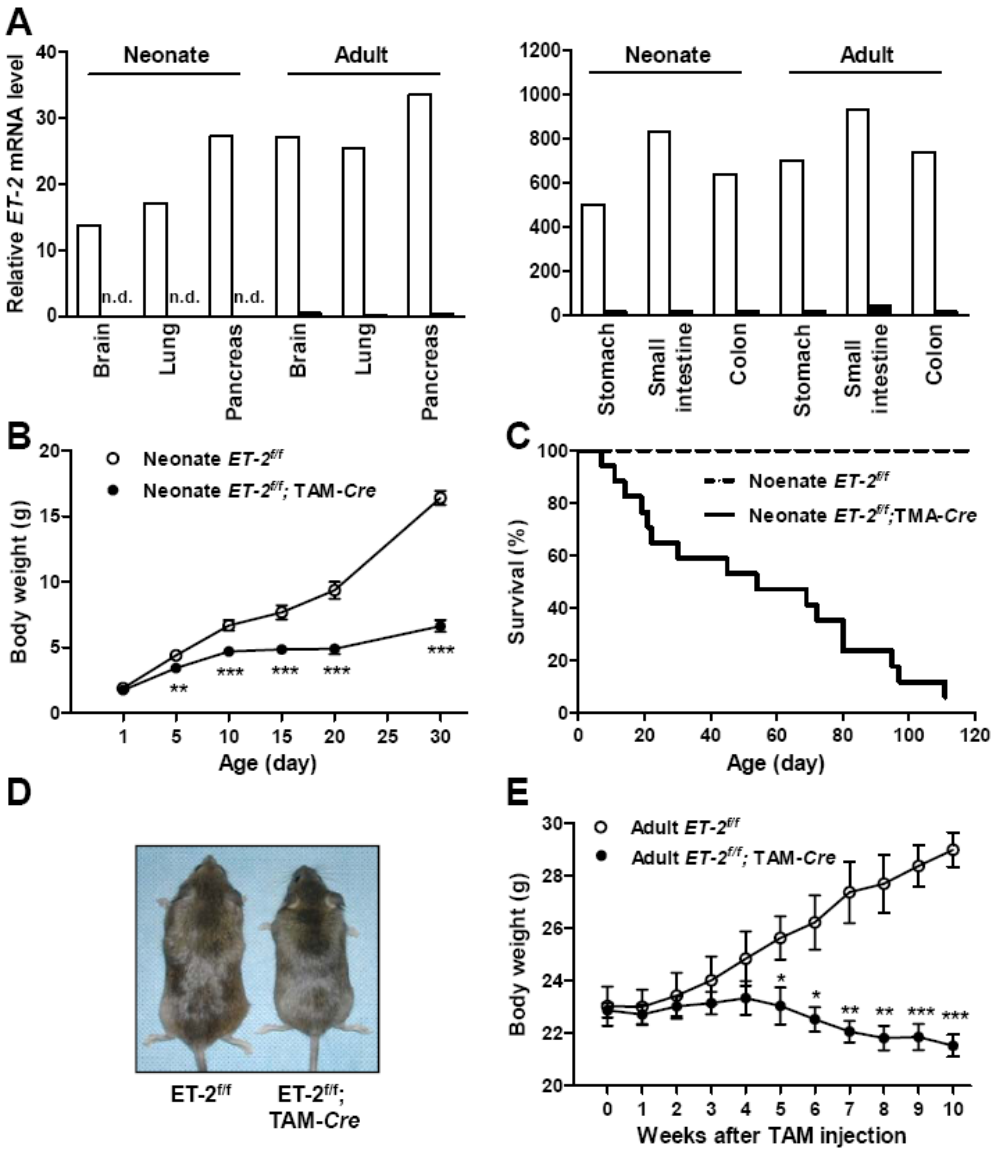


**Figure 2-5 Generation and gross phenotype of systemically inducible *ET-2* knockout mice.** (A) Quantitative RT-PCR of *ET-2* mRNA level in knockout mice systemically inactivated *ET-2* at P1 (neonate) and at 6 week-old (adult), and their wild type littermates, respectively. Values were normalized by *18s rRNA* expression. (B) Body weight of neonate *ET-2$^{f/f}$;* TAM-*Cre* (n=17) and *ET-2$^{f/f}$* (n=9) mice. (C) Survival ratio of neonate *ET-2$^{f/f}$;* TAM-*Cre* (n=17) and *ET-2$^{f/f}$* (n=9) mice. (D) Representative photograph of adult *ET-2$^{f/f}$;* TAM-*Cre* (right) and *ET-2$^{f/f}$* (left) mice after 10 weeks of *ET-2* inactivation. (D) Body weight of adult *ET-2$^{f/f}$;* TAM-*Cre* and *ET-2$^{f/f}$* (n=10) mice. Error bars indicate ± SEM. **p*<0.05, ***p*<0.01, ****p*<0.001

for growth regulation and survival of postnatal mice, and maintenance of energy homeostasis even in adulthood.

In the previous report by Baynash (Baynash, 2006), the role of ET-2 in regulating glucose homeostasis was proposed based on the results from glucose tolerance tests and from *in vivo* glucose absorption assays. However, these experiments were difficult due to the small size of animals, and the large experimental variation observed for both inter- and extra-experimental results. These sources of error could be derived from possible glucose loss by injector leakage or solution loss by evaporation. If these mice are essentially unable to absorb glucose at a normal rate through their intestine, then glucose would be excreted (and thus water with it, through the colon). However, these mutant mice did not appear to have diarrhea, which might be the expected consequence. Since the hypothesis is still feasible despite the afore listed caveats, the next logical studies would evaluate macro- and micronutrition management (Chapter 3).

In summary, I successfully generated systemically inducible *ET-2* knockout mice and determined that these mice recapitulated the phenotype of constitutively deficient animals. These studies suggest that ET-2 plays a minimal role in embryonic development. In addition, the opportunity to use older mice with *ET-2* deletion will now allow me to perform metabolic studies that were technically impossible with the constitutive knockout strain.

## Materials and methods

### Mice

Mice were housed in a temperature-controlled environment with 12 hr light/dark cycles. A rodent diet (Teklad) and water were provided *ad libitum*.

**Generation of constitutive *ET-2* knockout mice**

A Lamda FIX II mouse 129/SV genomic library (Stratagene) was screened with a 0.56 kb fragment of the mouse *ET-2* cDNA. A 17.5 kb genomic clone containing all ET-2 exons and about 4 kb of upstream genomic sequences was isolated, as demonstrated by restriction mapping, oligonucleotide hybridization, and partial sequencing. To construct the targeting vector, a universal neo-TK template plasmid vector that contained a neo and two tandem TK cassettes was used (Ishibashi et al., 1993). A 1.0 kb Bst XI-EcoR1 genomic fragment containing a portion of exon 1 was blunt-end inserted into the unique Xho I site of the plasmid between the neo and TK cassette. A 11.5 kb BstXI-Sal I genomic fragment containing exon 4 and 5 was then blunt-end ligated into the unique BamHI site of the plasmid. This arrangement deletes a portion of exon 1 and all of exon 2 of the ET-2 gene replacing it with the neo cassette. The construct was linearized at its unique Sal I site immediately 3' to the TK cassettes. The SM-1 mouse ES cell line was cultured on irradiated LIF-containing STO feeder layers as described (Ishibashi et al., 1993). ES cell were electroporated with the linearized targeting vector and selected for double resistance to G418 and FIAU as described (Rosahl et al., 1993). Double-resistant ES cell clones were screened by PCR with a 5' neo primer, GAGGATTGGGAAGAC AATAGCAGGCATGC, and 3' primer external to the targeting vector, AGGTGACACAAAATATTCTGTTCAGTCCAC. For deletion of the wild type allele by PCR, a third primer, GCAGTGTTCACCCAGATGATGTCCAGGTG, was added to

PCR reactions performed for 35 cycles with PCR Optimization Kit (Invitrogen) by using buffer J. Microinjection of blastocysts and production of chimeric mice were performed as described (Rosahl et al., 1993).

**Generation of systemically inducible *ET-2* knockout mice**

The *ET-2*$^{flox}$ mice were obtained from Dr. Jeremy Nathans' lab (Johns Hopkins University) and were crossed with a transgenic line expressing Tamoxifen-inducible *Cre* recombinase under the control of the chicken β *actin* promoter/enhancer (B6.Cg-Tg(cre/*Esr1*)5Amc, The Jackson Laboratory). For *ET-2* inactivation at P1, tamoxifen (3mg/40g of body weight; Sigma, St. Louis, MO) in sunflower oil was delivered by gavage feeding to the dam. For *ET-2* inactivation in adult, mice were injected intraperitoneally with tamoxifen (3 mg/40 g of body weight in sunflower oil) into 6~8 week-old mice for 4 consecutive days.

**Measurement of body weight and survival ratio**

Body weight was recorded every 5 days (Figure 2-3B and 2-5B) or weekly (Figure 2-5E). Mice were checked daily for survival studies.

**Quantitative RT-PCR analysis**

Tissues were harvested and weighed before freezing at -80$^{o}$C for RNA extraction. Total RNA was extracted from tissues using RNA STAT 60 (Tel-Test Inc.), treated with RNase-free DNase I (Roche Molecular Biochemicals), and reverse-transcribed into cDNA using random hexamers (Roche Molecular Biochemicals) and SuperScript II First-

Strand Synthesis System (Invitrogen). Real-time PCR reactions contained 25 ng of cDNA, 150 nM of each primer, and 10 µl of SYBR Green PCR Master Mix (Applied Biosystems) in 20 µl of total volume and were performed using ABI Prism 7000 Sequence Detection System. Relative mRNA levels were calculated with $\Delta\Delta C_T$ method normalized to *18s rRNA* level. Primer sequences were designed using Primer Express Software (PerkinElmer Life Sciences) and are provided in Appendix A.

**Statistical Analysis**

Values depict the mean ± SEM. Statistical significance was evaluated using two-tailed unpaired student's *t* tests (GraphPad Prism 5) and considered significantly different $p<0.05$.

**Acknowledgement**

Amy Baynash and Amir Rattner generated the constitutive *ET-2* and *ET-2*$^{flox}$ alleles, respectively.

# CHAPTER 3

## Internal Starvation in Endothelin-2 Deficient Mice

### Introduction

Endothelins function as highly local, paracrine/autocrine mediators. Concentrations of endothelin peptides in circulating plasma are quite low (picomolar levels) and well below the pharmacological threshold for receptor activation (Kedzierski and Yanagisawa, 2001). Endothelin ligands and receptors are usually expressed in adjacent cell types within the same organ. Furthermore, *ET-1* and *ET-3* null mice exhibit developmental phenotypes totally different from each other, indicating that *ET-1* expressed in nearby endothelial cells does not compensate for *ET-3* deficiency and vice versa.

The gastrointestinal tract is a complex organ system composed of the esophagus, stomach, small intestine and colon that performs essential functions of digestion, nutrition absorption and metabolic homeostasis. The small intestine is the organ for initial absorption of energy-rich nutrients (Thomson et al., 2001). Fats, carbohydrates, and proteins are broken down and absorbed by epithelial cells in the villous epithelium. At the base of each villous is a loop-like invagination of cells that form a crypt. Within the lower third of each crypt, stem cells give rise to progenitor cells that undergo three or four cycles of division and differentiate into mature cells that perform the functions associated with nutrient absorption. As they move up the villous, progenitor cells differentiate into the absorptive enterocytes, which comprise the majority of epithelial cells in the small intestine, mucus-producing goblet cells, and peptide hormone-

producing enteroendocrine cells. They eventually undergo apoptosis and are exfoliated from the apical extrusion zone of villi to the intestinal lumen within a 2-5 day period. Paneth cells, which contribute to innate intestinal defense, are also generated from progenitor cells. Unlike the other three cell lineages, they migrate down from the stem cell zone to the crypt base where they are relatively long-lived (20 days) (Hauck et al., 2005). The epithelial cells interact with mesenchymal cells, such as myofibroblasts, and immunologically active macrophages, dendritic cells and lymphocytes, both intraepithelial and in the lamina propria (Walters, 2005). The development of the mouse intestinal epithelium is not fully complete until the second to third week of postnatal life, when the intervillous epithelium is converted into a mature crypt. The number of crypts then increases during the third postnatal week of life (Stappenbeck et al., 1998).

Regional and cellular distribution of *ET-2* expression was first reported for adult rat gastrointestinal tract (de la Monte et al., 1995). *ET-2* mRNA levels increase in a gradual manner the along proximo- to- distal axis of the small intestine. By *in situ* hybridization, specific localization was mainly observed in intestinal lamina propria cells showing an increasing crypt-to-villous gradient (de la Monte et al., 1995). These observations suggested that ET-2 may have autocrine or paracrine stimulatory effects on intestinal epithelial and stromal cell function such as local villous motility, and cell proliferation and maturation.

Contrary to the previous report, mouse ET-2 was determined to be expressed predominantly in epithelial cells of the small intestine and colon, and it exhibited very weak signals in stromal cells of the lamina propria. The expression of the *ET-2* mRNA displayed a gradient pattern along the villous-crypt axis of the small intestine and the

bottom-up axis of the colonic crypt (Takizawa et al., 2005). ET-2 peptide is specifically localized in the vicinity of basement membrane in epithelial cells, proposing that it might be secreted from the epithelial cells into the lamina propria where it could modulate the mucosal immune system. Gradual expression of ET-2 suggests that it might be involved in the differentiation of epithelial cells (Takizawa et al., 2005). Despite the different expression pattern of ET-2 in both mouse and rat, general consensus is that ET-2 modulates intestinal functions in an intracrine/autocirne/paracrine manner.

Intestinal ET-2 expression progressively increased from late embryonic stage (E14) and then remained constant into adulthood in mouse (Uchide et al., 2002). Soon after birth, the gene expression nearly reaches the level of expression observed in the adult suggesting that ET-2 might be involved in intestinal function that is critical after birth- e.g. nutrient absorption or immune responses to contact with foreign pathogens.

Although it has been speculated that ET-2 may play important (patho)physiological roles in the intestine because of its local activity and abundant expression, the detailed role of ET-2 has not yet been defined clearly. This chapter will present data demonstrating that *ET-2* deficient mice appear to be in a severe state of internal starvation, evident by hypoglycemia, ketonemia, increased expression of liver genes involved in adapting to starvation, and reduced metabolism and physical activity. Unexpectedly, functional, histological and genetic analysis revealed that intestinal ET-2 is not essential for the growth and survival of postnatal mice. These data indicate the possibility that there are other undetermined mechanisms through which ET-2 exerts a crucial role in energy homeostasis and growth.

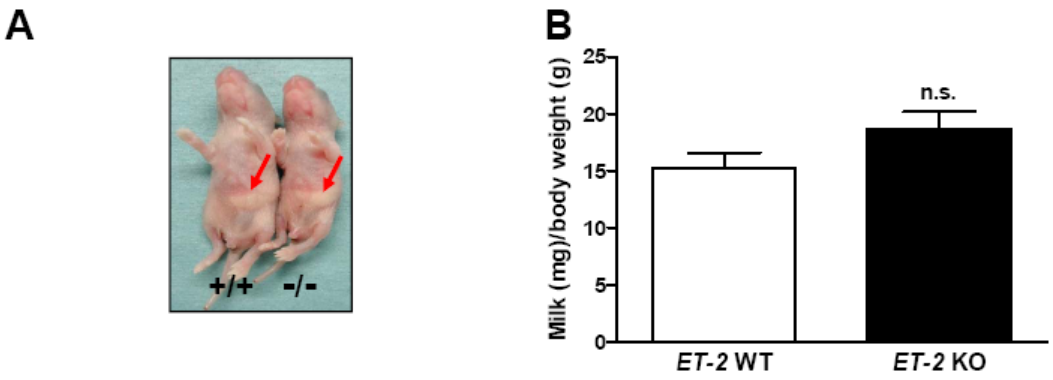


**Figure 3-1 Normal milk intake of constitutive *ET-2* knockout mice.** (A) A representative photograph displaying presence of milk (arrow) in wild type (left) and *ET-2* knockout (right) mice at 3 days of age. (B) Milk intake of *ET-2* knockout mice at 10 days of age. Error bars indicate ± SEM. n.s., non-significant

## Results

### Internally starved state of *ET-2* knockout mice

The striking growth retardation and reduced survival rate of *ET-2* knockout mice led me to investigate whether the mutant mice were consuming enough energy to grow. First, I examined (Figure 3-1A) and measured the amount of milk in the stomach of P3 (data not shown), P10 (Figure 3-1B), and P15 (data not shown) mice at 8 hour intervals for 3 days. The results show that *ET-2* knockout mice had an equal amount of milk in their stomachs compared with wild type controls. I also reduced the litter number to 2~3 knockout mice and wild types per dam in order to limit competition for nursing with the mother. However, this attempt did not contribute to an increase in the body weight or life span of *ET-2* knockout mice (data not shown).

| | *ET-2* WT | *ET-2* KO |
|---|---|---|
| Sodium (mEg/dl) | 136.3±3.2 | 126.8±5.7 |
| Calcium (mEg/dl) | 9.5±0.2 | 9.6±0.2 |
| Phosphorous (mEg/dl) | 7.7±0.8 | 7.4±0.2 |
| Potassium (mEg/dl) | 9.16±0.62 | 8.98±0.33 |
| Magnesium(mEg/dl) | 1.92±0.03 | 1.84±0.04 |
| Chloride (mEg/dl) | 107.8±0.23 | 103.3±0.43 |
| Creatine (mg/dl) | 0.24±0.04 | 0.26±0.02 |
| Glucose (mg/dl) | 147.4±8.6 | 42.6±4.4 *** |
| Uric acid (mg/dl) | 0.84±0.05 | 1.37±0.11 * |
| BUN (mg/dl) | 16.5±1.1 | 32.5±2.4 ** |
| Total protein (mg/dl) | 4.09±0.14 | 3.86±0.09 |
| Albumin (g/dl) | 1.57±0.07 | 1.41±0.09 |
| Cholesterol (mg/dl) | 129.5±4.5 | 179.0±11.0 * |

**Table 3-1 Blood chemistry of constitutive *ET-2* knockout and wild type control mice.** Plasma from each mice was analyzed by Dallas Children's Medical Center, Pathology Laboratory (n=5 mice per group). Error bars indicate ± SEM. *$p$<0.05, **$p$<0.01, ***$p$<0.001

In order to gain insight into the mechanism of this intriguing phenotype, I analyzed blood parameters of constitutive *ET-2* knockout mice (Table 3-1). Overall, there was no significant difference between the genotypes. However, blood glucose levels were strikingly low in *ET-2* knockout mice under the casual condition and this was maintained in all ages. Hypoglycemia was also observed in both neonate and adult *ET-2*$^{flox/flox}$*;* TAM-*Cre* mice (Figure 3-2). Blood urea nitrogen (BUN) and uric acid levels were significantly elevated suggesting the increased catabolic response to the energy deprivation (Table 3-

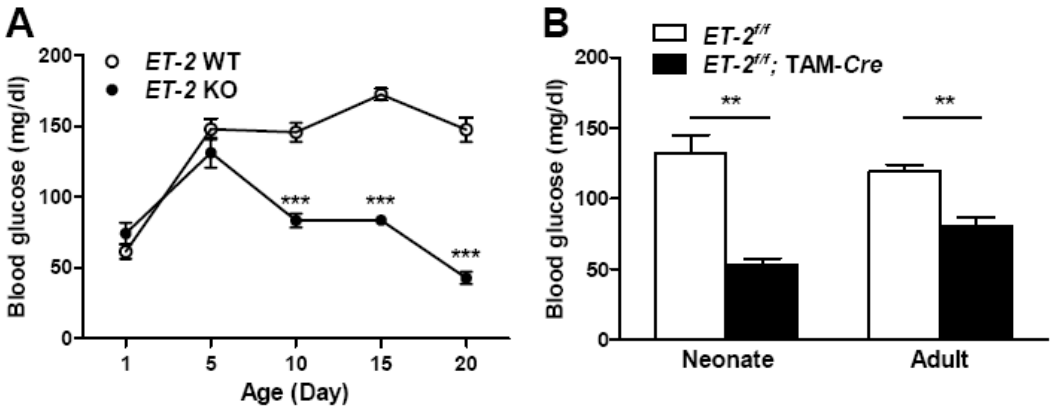


**Figure 3-2 Profound hypoglycemia of constitutive and inducible *ET-2* knockout mice.** (A) Casual blood glucose levels of constitutive *ET-2* null mice and wild type controls (n=10 mice per group). (B) Blood glucose levels of neonate (at 3 weeks of age) and adult *ET-2*$^{flox/flox}$; TAM-*Cre* mice (at 8 weeks after *ET-2* inactivation), and their wild type controls (n=10 mice per group). Error bars indicate ± SEM. ***p*<0.01, ****p*<0.001

1). Despite the low blood glucose concentrations, insulin levels of *ET-2* knockout mice were not significantly different from that of wild type controls and were normally regulated in both casual and fasted conditions (Table 3-2). Unlike normal insulin levels, plasma glucagon concentrations were elevated in *ET-2* knockout mice upon casual sampling, which is indicative of the fasted state. Although it is mild, T3 levels were significantly reduced in mutant mice implicating decreased metabolic rate of these animals (Table 3-2). Since thyroid hormone is important in maintaining the basal level of metabolism and neonatal growth, I attempted to rescue the abnormal growth and survival of *ET-2* knockout mice by thyroid hormone replacement. I provided 3 week-old *ET-2* knockout mice with T3 (3.5ng/g body weight/day) by subcutaneous injection for 2 weeks. The concentration of T3 was found to return hypothyroid mice to the euthyroid state (Trost et al., 2000). Neither growth retardation nor early lethality was improved,

| | | *ET-2* WT | *ET-2* KO |
|---|---|---|---|
| Insulin (ng/ml) | Fed | 0.433±0.0665 | 0.457±0.0562 |
| | Fasted | 0.186±0.0370 | 0.147±0.0405 |
| Glucagon (pg/ml) | Fed | 183.0±29.02 | 913.6±242.5 ** |
| | Fasted | 334.8±83.01 | 295.5±25.40 |
| TSH (ng/ml) | | 67.67±7.260 | 231.3±49.26 ** |
| T3 (ng/ml) | | 0.7843±0.02562 | 0.5350±0.07486 * |
| T4 (μg/dl) | | 3.127±0.2273 | 3.329±0.3001 |

**Table 3-2 Hormone levels of constitutive *ET-2* knockout and wild type control mice.** Insulin and glucagon were measured with blood taken from casual (fed) and fasted conditions (n=5 mice per group). Thyroid hormones were assayed with blood from only normal condition (n=7 mice per group). Six weeks of aged wild type and ET-2 knock mice survived on the warm environment (Chapter 4) were used in this experiment. Error bars indicate ± SEM. *$p$<0.05, **$p$<0.01

however, by T3 supplementation (Figure 3-3). The same experiment conducted with P5 and P10 mice confirmed the unresponsiveness of *ET-2* knockout mice to T3 (data not shown).

The results of normal milk consumption and blood chemistry indicate that constitutive *ET-2* deficient mice suffered from apparent internal starvation. To verify this, I first examined the expression of genes known to be induced by starvation (Figure 3-4A). As expected, mRNA expression of *phosphoenolpyruvate carboxykinase (PEPCK)* and *pyruvate dehydrogenase kinase isozyme 4 (PDK4)*, key gluconeogenic enzymes, was

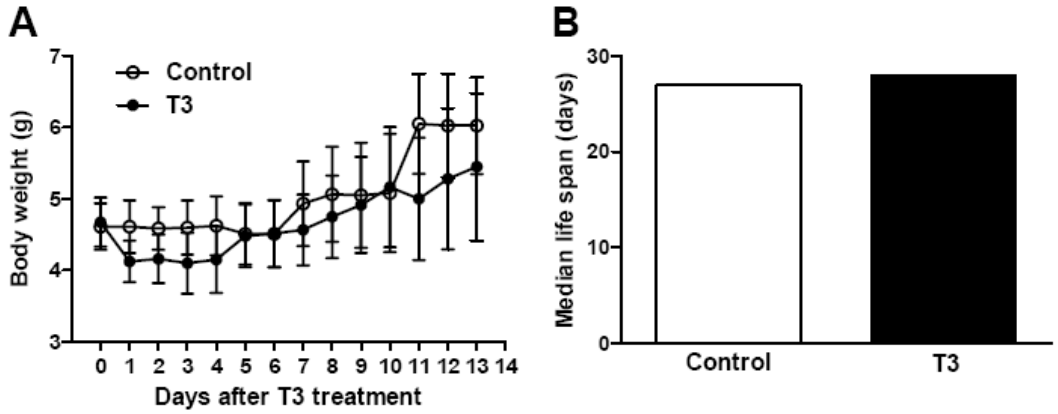


**Figure 3-3 No detectable effect of T3 supplement on growth regulation and survival of constitutive *ET-2* knockout mice.** (A) Body weight of constitutive *ET-2* knockout mice treated with T3 at 3 weeks of age (n=10 mice per group). (B) Median life span of constitutive *ET-2* knockout mice and wild type controls (n=10 mice per group) treated with T3. Error bars indicate ± SEM.

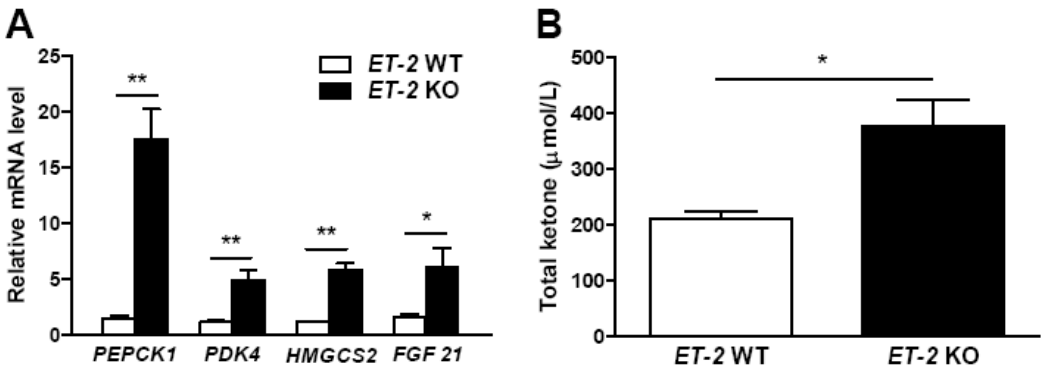


**Figure 3-4 Increased expression of starvation-induced genes and serum ketone levels.** (A) Quantitative RT-PCR analysis of starvation-induced genes in liver (n=4 mice per group). Values were normalized by *18s rRNA* expression. (B) Serum ketone levels of constitutive *ET-2* knockout mice and wild type controls (n=5 mice per group). Error bars indicate ± SEM. **p*<0.05, ***p*<0.01

up-regulated in the liver of *ET-2* null mice. Expression of *hydroxymethylglutaryl-CoA synthase 2 (HMGCS2)*, which catalyzes a key step in ketone-body synthesis (Figure 3-

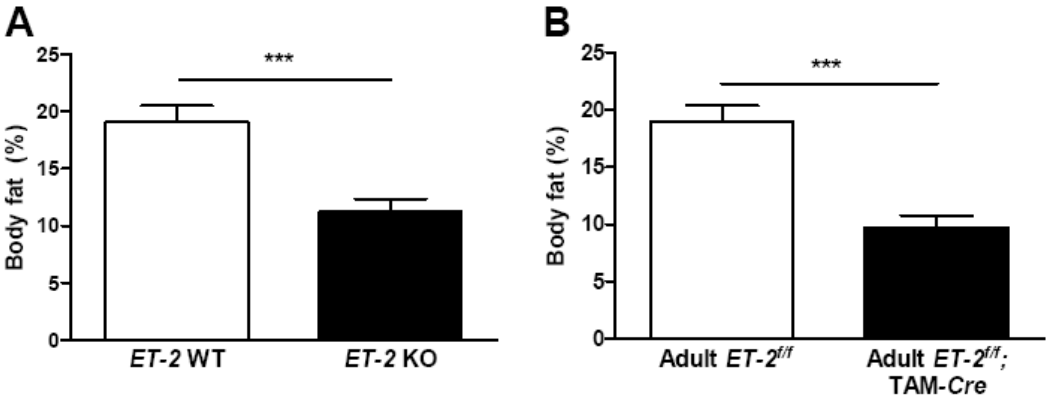


**Figure 3-5 Decreased body fat mass of *ET-2* knockout mice.** NMR analysis of fat content of (A) constitutive *ET-2* knockout (n=10 mice per group) and (B) adult *ET-2$^{flox/flox}$;* TAM-*Cre* (n=9 mice per group), and their wild type control mice. Error bars indicate ± SEM. ***$p$<0.001

4A), and the concentration of serum total ketone bodies were also elevated in *ET-2* knockout mice compared to wild type controls (Figure 3-4B). Furthermore, expression of *fibroblast growth factor 21 (FGF21)* which was recently discovered as a key regulator of the body's adaptation to fasting (Inagaki et al., 2007) was significantly induced in the liver of *ET-2* knockout mice (Figure 3-4A). Next, I determined body composition with NMR. Compared to wild type mice, which exhibited a 20% of body weight as fat mass, *ET-2* mutant mice exhibited only 12 % fat mass (Figure 3-5A). Ordinarily under the fasted and starved state, animals will reduce physical activity to conserve energy (Inagaki et al., 2007). As expected, the *ET-2* deficient mice have drastically reduced locomotor activity (Figure 3-6A).

Neonate and adult *ET-2$^{flox/flox}$*; TAM-*Cre* mice also exhibited significantly lower blood glucose levels than wild type controls (Figure 3-2B). As seen in constitutive *ET-2* knockout mice, inactivation of *ET-2* in the adult led to decreased body fat mass (Figure 3-

5B) as well as decreased physical movement (Figure 3-6B). These data suggest that deficiency of *ET-2* contributes to an internally starved state in mice and this may be the critical underlying mechanism of the growth retardation and early lethality of *ET-2* null mice.

**Intestinal ET-2 is not essential for the growth regulation and survival of mice**

The overall starvation phenotype of *ET-2* deficient mice, the expression profile of *ET-2* mRNA and local activity of endothelins strongly support a hypothesis by which the small intestine would be the responsible tissue for this ET-2-related phenotype. To comprehensively test this hypothesis, I first examined the cell types expressing *ET-2* and its receptors in the small intestine. *In situ* hybridization in the ileum revealed that *ET-2* mRNA is specifically expressed in the villous and crypt epithelium (Figure 3-7A and B). In contrast, the $ET_A$ and $ET_B$ receptor mRNAs are located in the lamina propria under the epithelium (Figure 3-7C and D). This expression pattern strengthen, again supports the hypothesis that ET-2 may exert a particular signaling mechanism in the (patho)physiology of the small intestine by mediating the interaction between epithelial and mesenchymal cells.

To first determine if a morphological abnormality was caused by ET-2 absence, I examined intestinal histology in the *ET-2* deficient mice. However, there were no apparent histological defects in the small intestine and colon of mutant mice (Figure 3-8) and the epithelium of the small intestine contained a normal number of Paneth cells, goblet cells, and various enteroendocrine cell populations (data not shown). In the epithelium, *ET-2* is highly expressed in the crypt and the expression is gradually

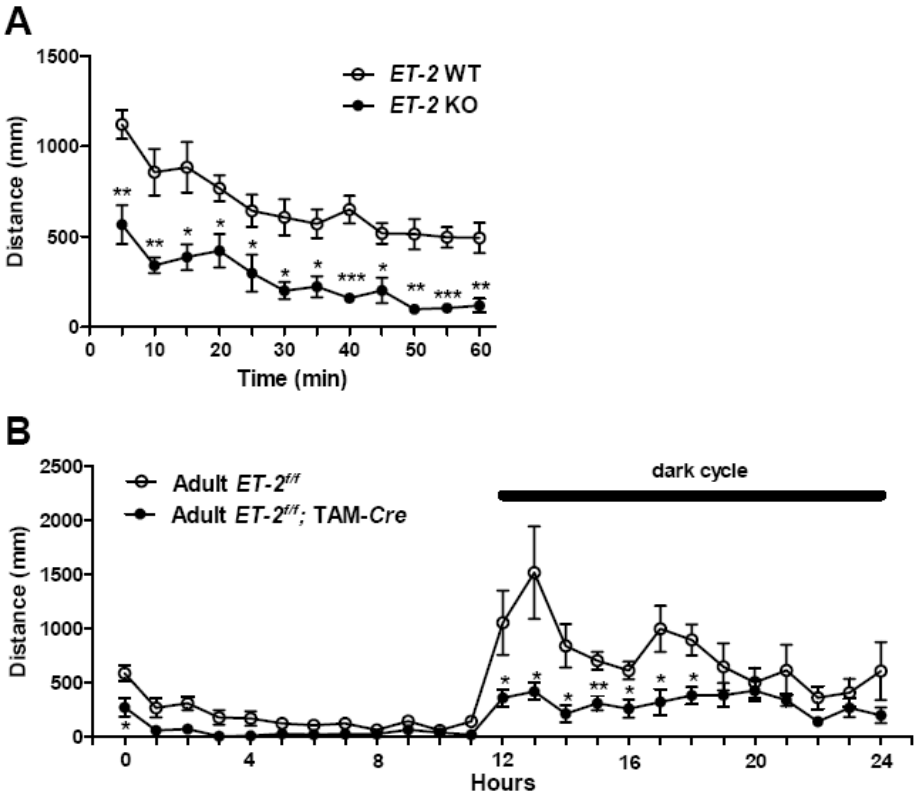


**Figure 3-6 Reduced locomotor activity of *ET-2* knockout mice.** Total moving distance was measured in (A) 3 week-old constitutive *ET-2* knockout mice during 1 hour (n=5 mice per each group) and (B) 12 week-old adult *ET-2*$^{flox/flox}$*;* TAM-*Cre* (n=8 mice per group) during casual condition. Error bars indicate ± SEM. **p*<0.05, ***p*<0.01, ****p*<0.001

decreased toward the villous tip (Figure 3-7A). This expression pattern suggests that ET-2 might regulate the rate of cell division and/or migration to maintain appropriate renewal of intestinal epithelial cells. To examine this possibility, epithelial cells during S phase were labeled with 5'-bromo-2' deoxyurdine (BrdU) and examined for the number and migration of cells. As presented in Figure 3-9, *ET-2* deficient mice have a decrease in the number of cells in S phase at 2 hours after BrdU incubation. The migration rate of labeled

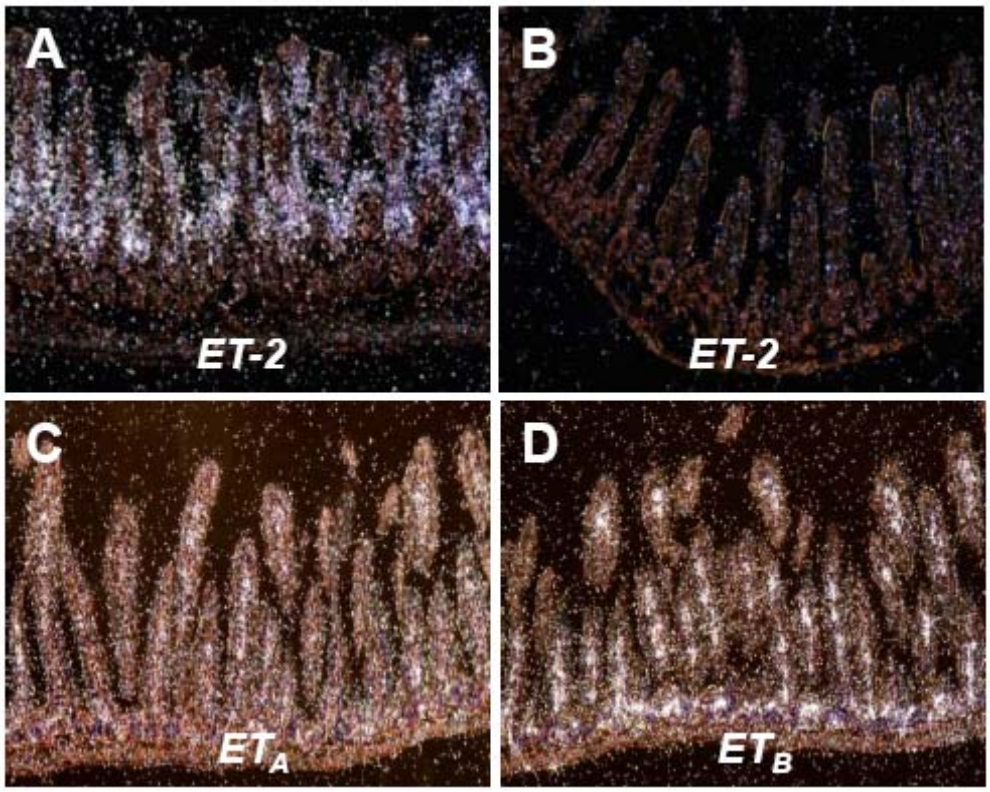


**Figure 3-7 Localization of *ET-2*, $ET_A$ and $ET_B$ mRNA in ileum of small intestine.** *In situ* hybridization was conducted with anti-sense probes of each gene to wild type (A, C and D) and *ET-2* knockout mice (B). Representative photographs are shown by dark field images. Magnification: x20

cells along the intestinal villous was also reduced in the mutant mice at 48 hours post BrdU incorporation. To confirm the decreased number of mitotic cells observed in *ET-2* deficient mice, I stained each part of the intestine with Ki 67 and the proliferating cell nuclear antigen (PCNA), and counted positive cells in each crypt. It was evident that there is decreased proliferation rate of intestinal epithelial cells in *ET-2* knockout mice (data not shown).

To investigate whether the defective homeostasis of epithelial cells in *ET-2* knockout mice results in abnormal villous architecture, I measured the villous length and

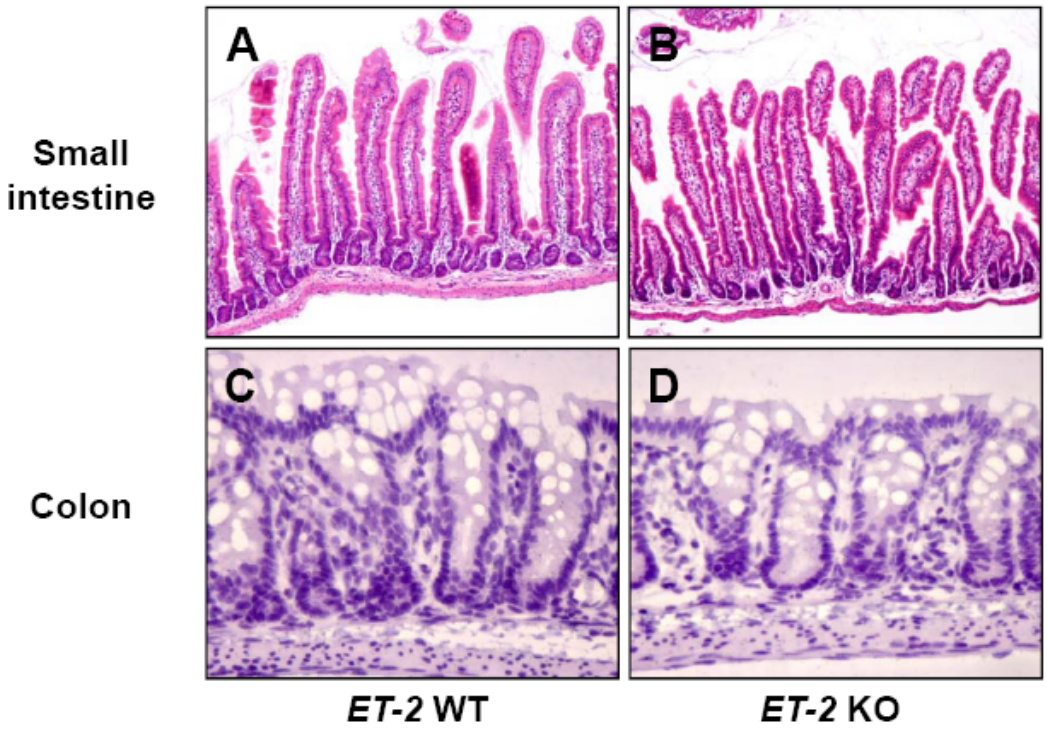


**Figure 3-8 No noticeable morphological changes in intestine of *ET-2* deficient mice.** H&E staining was conducted with intestine from wild type (A and C) and constitutive *ET-2* knockout (B and D) mice. Each group was matched with age. Magnification: x10 for small intestine and x40 for colon

number in each part of the intestine. Although it is moderate, villous length of *ET-2* knockout mice was significantly shorter than that of wild type controls in the duodenum and jejunum (Figure 3-10). Nevertheless, there was no gross deficiency in villous number (data not shown). Evaluation of the morphology and number of microvillous with electron microscopy failed to exhibit any apparent changes (data not shown). Despite the normal architecture, defects in renewal of progenitors by ET-2 deficiency might result in intestinal dysfunction leading to malabsorption and/or malnutrition, which could cause the internally starved state of the mutant animals. To address this possibility, I first

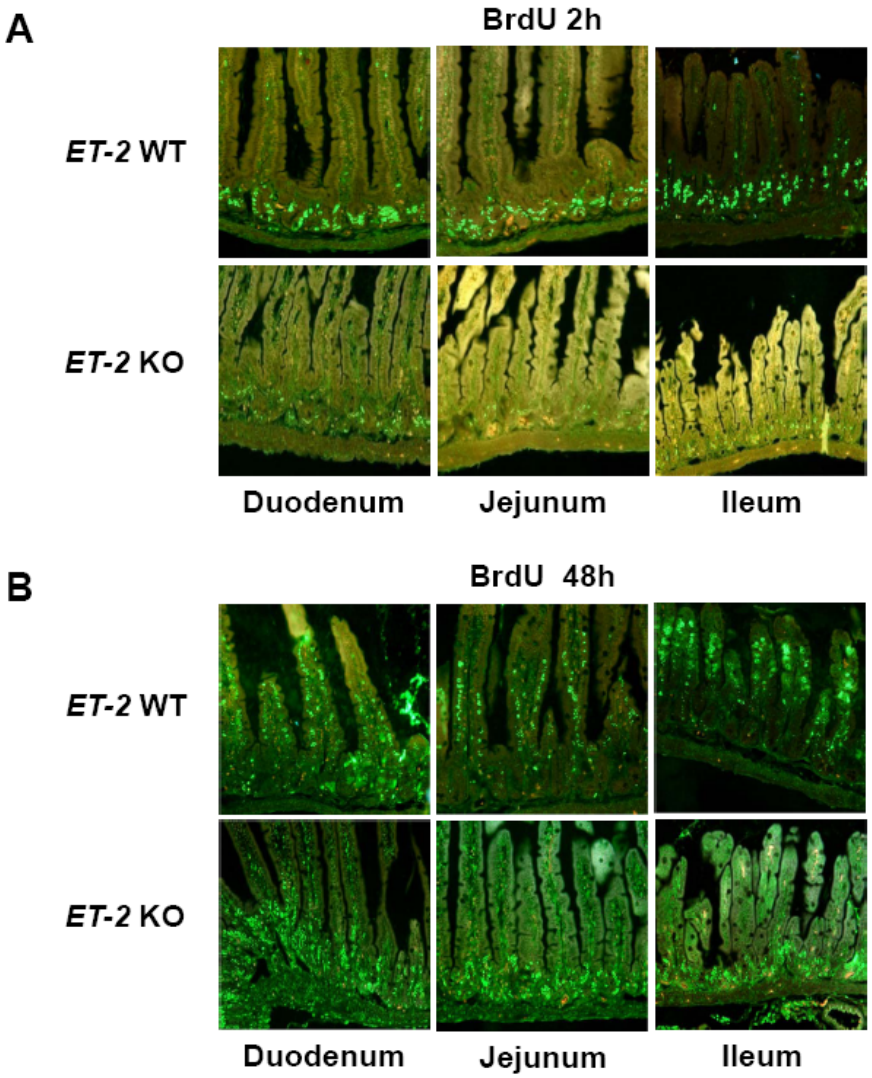


**Figure 3-9 Decreased self-renewal of intestinal epithelium in *ET-2* deficient mice.** *In vivo* BrdU labeling was conducted by giving a single intraperitoneal injection to *ET-2* deficient mice and age matched wild type controls. Each part of intestine was harvested after 2 (A) and 48 hours (B) later. Magnification: x20

compared intestinal absorption of fat, which is the most abundant energy source during the pre-weaning period (Girard et al., 1992) in wild type and constitutive knockout mice. The amount of [$^3$H] triolein present in the small intestine and its contents after an oral

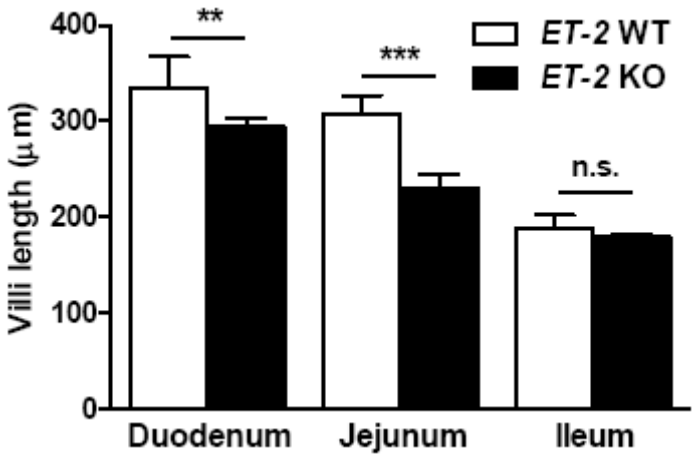


**Figure 3-10 Short villous length in *ET-2* knockout mice.** Each part of intestine was taken from the designated genotypes and sections were stained with H&E. The height of representative villi was measured with the AxioVision program 4.5 (n=3 mice per group and 9 villous per each mice). Error bars indicate ± SEM. ***p*<0.01, ****p*<0.001, n.s.: non-significant

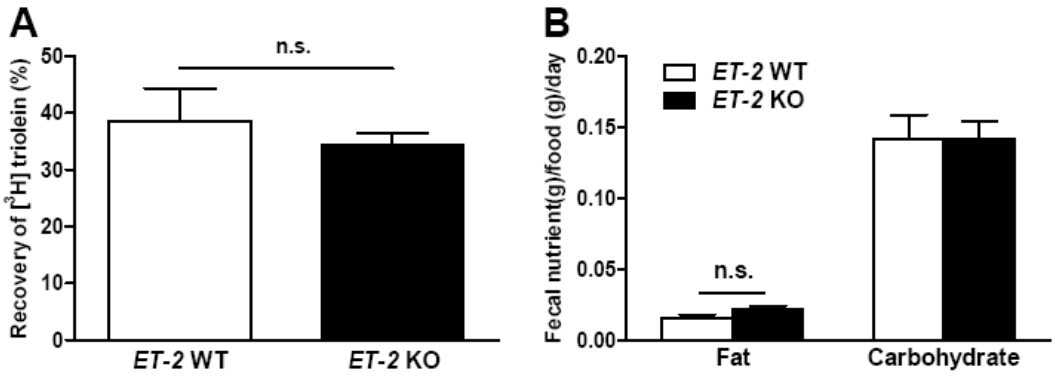


**Figure 3-11 Normal fat absorption of *ET-2* deficient mice.** Radioactivity of [$^3$H] triolein from small intestine and its content (A), and amount of recovered nutrients from fecal matter (B) of constitutive *ET-2* knockout mice and wild type controls (n=5 mice per group). Error bars indicate ± SEM. n.s., non-significant

gavage was similar in both mouse lines (Figure 3-11A). In addition, the proportion of fat and carbohydrate in feces of these mice did not exhibit any apparent difference between genotypes (Figure 3-11B). Finally, as measured by quantitative PCR, mRNA levels of

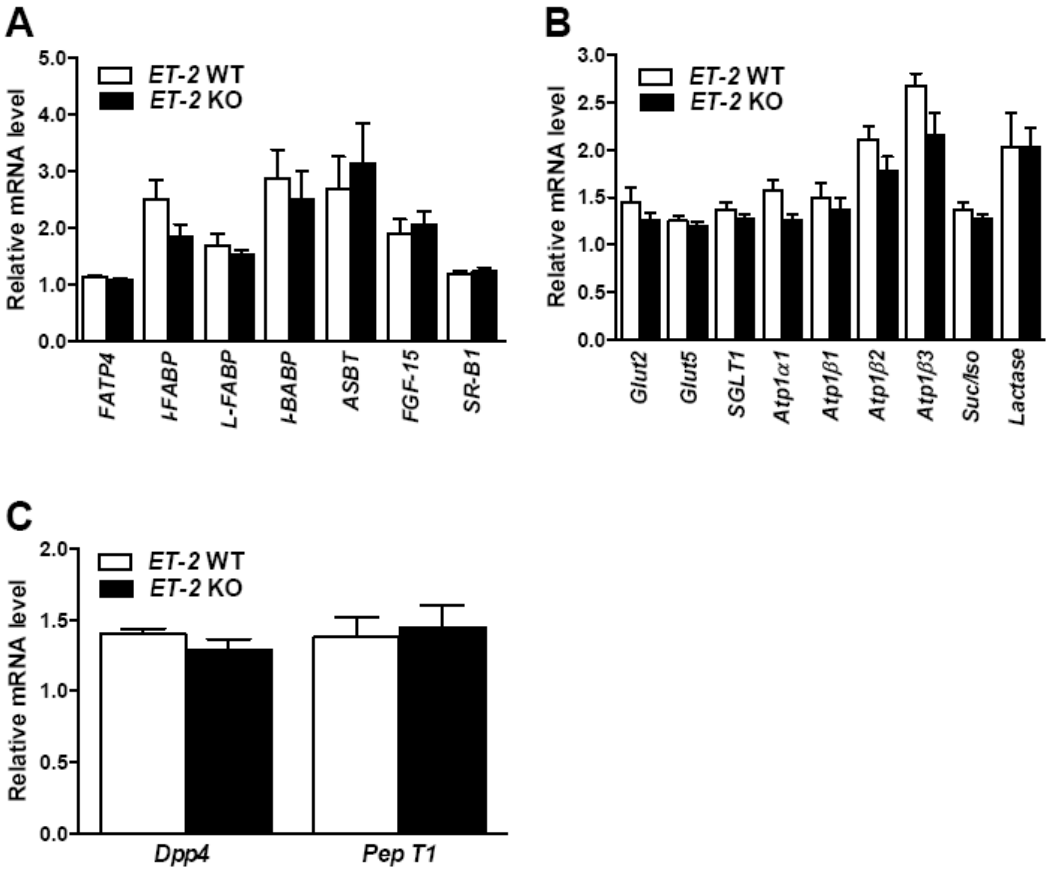


**Figure 3-12 No significant change in the expression of genes responsible for nutrient uptake or digestion in the intestine.** Quantitative RT-PCR was performed using mRNA extracted from intestine of indicated genotypes to examine genes are involved in the management of fat **(**A), carbohydrate (B), and protein (C) (n=8 mice per group). Error bars indicate ± SEM.

genes responsible for digestion and absorption of fat, carbohydrate, and protein were not significantly altered in *ET-2* deficient mice compared to wild type controls (Figure 3-12). Once nutrients are absorbed from the intestinal lumen by enterocytes, they then leave the cell and diffuse into the blood capillary (monosaccharides and amino acids) and lymphatic vessels (lipids) inside the villous, which brings them into the bloodstream. In order to determine deformities of the intestinal vascular system, morphological and

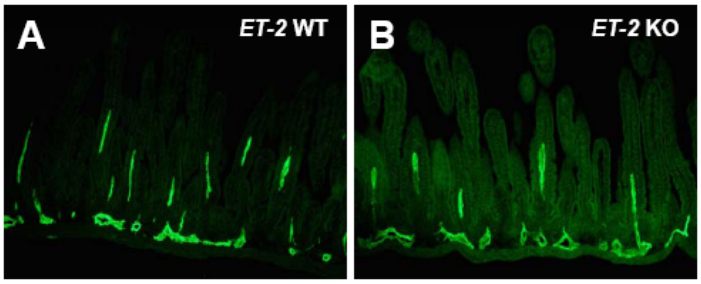


**Figure 3-13 No noticeable deformity of small intestinal lymphatics in *ET-2* deficient mice.** Immunostaining for Lyve-1 was performed in the small intestine of wild type and *ET-2* knockout mice at 10 day-old. Magnification: x20

molecular analyses were conducted. As shown by immunostaining, both blood (data not shown) and lymphatic (Figure 3-13) vasculature were indistinguishable between genotypes. This is confirmed by no obvious change in the mRNA level of genes known to be involved in the vasculature development (data not shown). In summary, constitutive ET-2 null mice show normal intestinal architectures, no changes in nutrient absorption, and decreased cell proliferation. These findings are against a role for ET-2 in intestine to affect energy homeostasis and growth.

To directly address the role of enterocytic ET-2, I generated intestine epithelial-specific *ET-2* knockout mice by crossing mice carrying a *villin-Cre* transgene (Madison et al., 2002) with *ET-2*$^{flox}$ mice (Figure 2-4A). Intestinal epithelium-specific recombination of the *loxP* sites was verified by PCR (Figure 3-14A) and loss of *ET-2* mRNA expression was confirmed by quantitative PCR in different parts of the intestine (Figure 3-14B). No change in ET-2 levels was observed in other organs, and as previously reported (Madison et al., 2002), the villin promoter is inactive in the stomach thus, expression of stomach *ET-2* remained intact (Figure 3-14B). *ET-2*$^{flox/flox}$; *villin-Cre* mice were born healthy and, unlike constitutive and inducible *ET-2* knockout mice, no

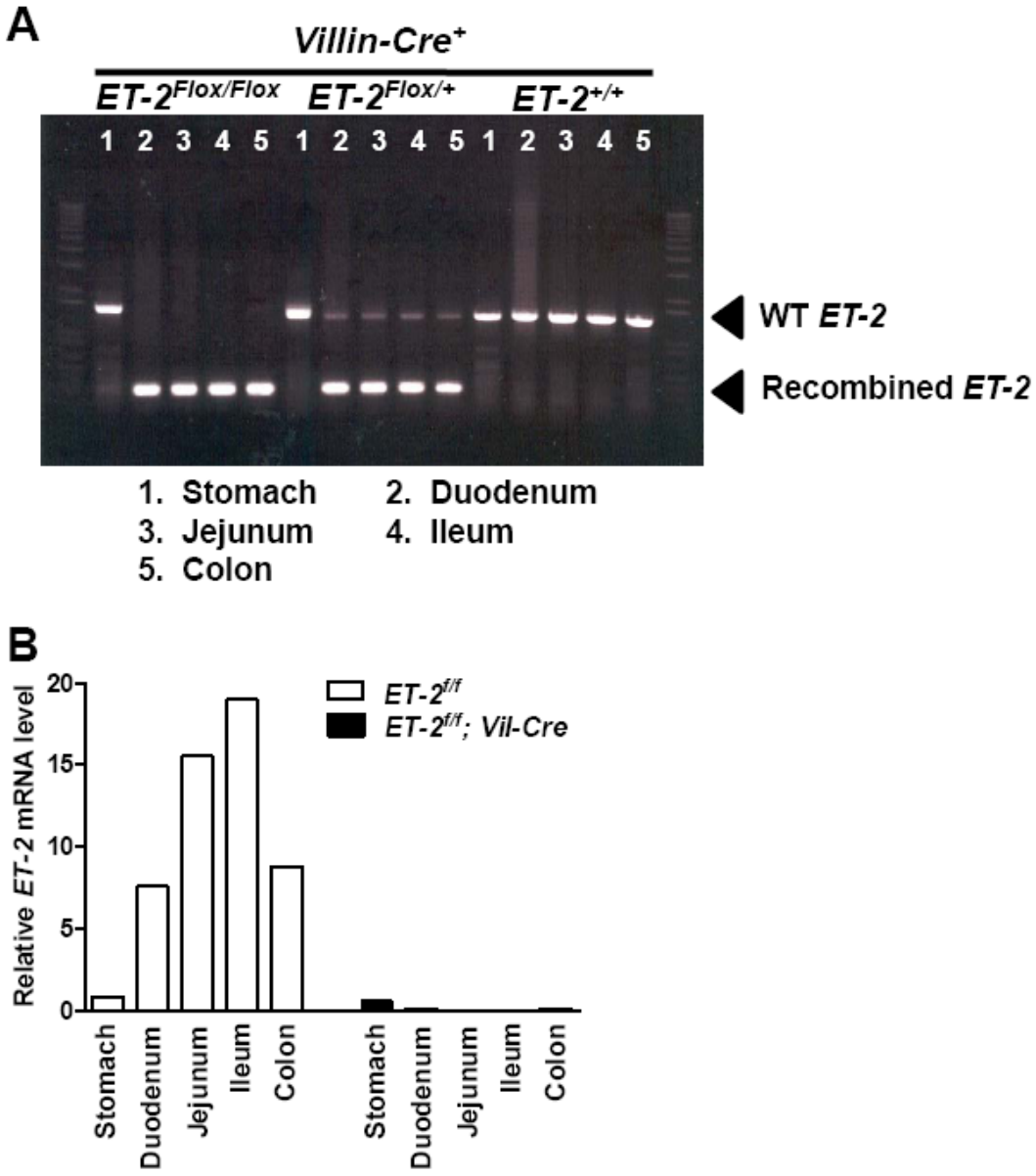


**Figure 3-14 Conditional deletion of *ET-2* in mouse intestinal epithelium.** (A) A representative picture of PCR products of genomic DNA. DNA was extracted from stomach and each part of intestine of indicated genotypes. (B) Quantitative RT-PCR of intestine-specific *ET-2* deletion by *villin* promoter-driven *Cre* recombinase.

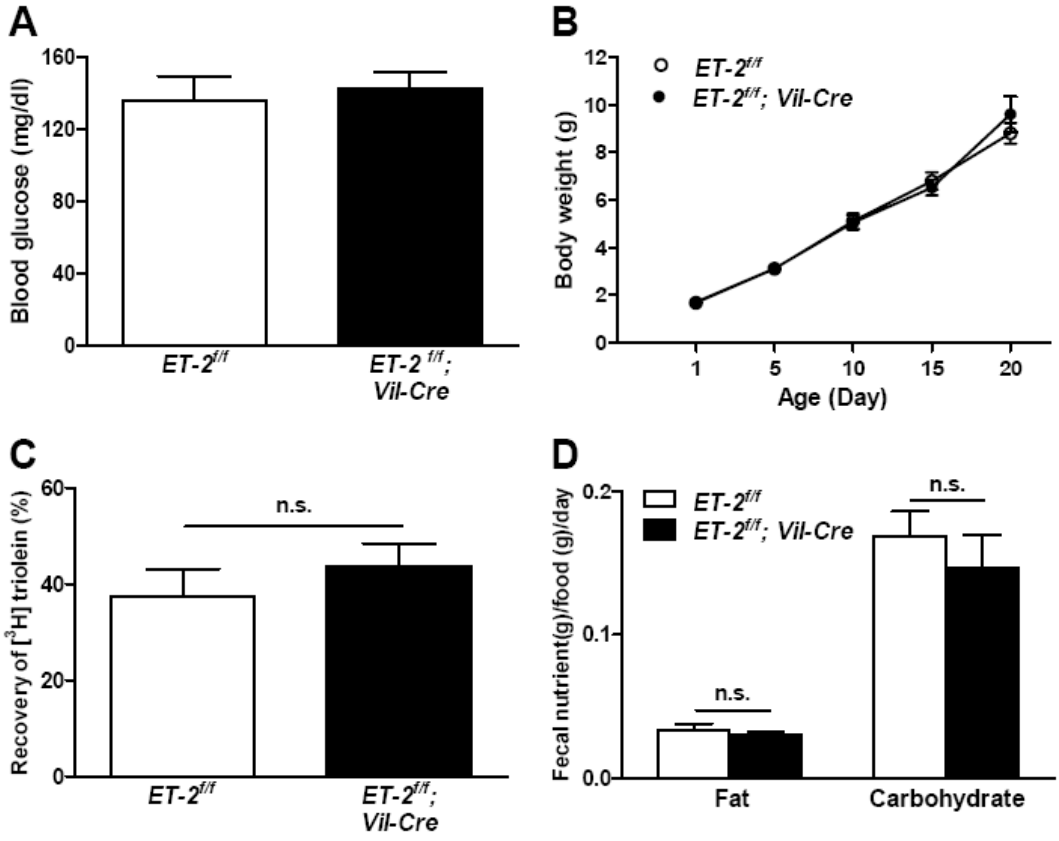


**Figure 3-15 No detectable abnormalities in energy-related processes of intestinal epithelium-specific *ET-2* deficient mice.** (A) Blood glucose levels of *ET-2*$^{flox/flox}$ and *ET-2*$^{flox/flox}$*; Vil-Cre* mice (n=10 mice per group). (B) Body weight of *ET-2*$^{flox/flox}$ and *ET-2*$^{flox/flox}$*; Vil-Cre* mice (n=21 mice per group) and wild type controls (n=23 mice per group). (C) Radioactivity of [$^3$H] triolein from small intestine and its content (n=5 mice per group) (D) Amount of recovered nutrients from fecal matter of *ET-2*$^{flox/flox}$ and *ET-2*$^{flox/flox}$*; Vil-Cre* mice (n=5 mice per group). Error bars indicate ± SEM. n.s., non-significant

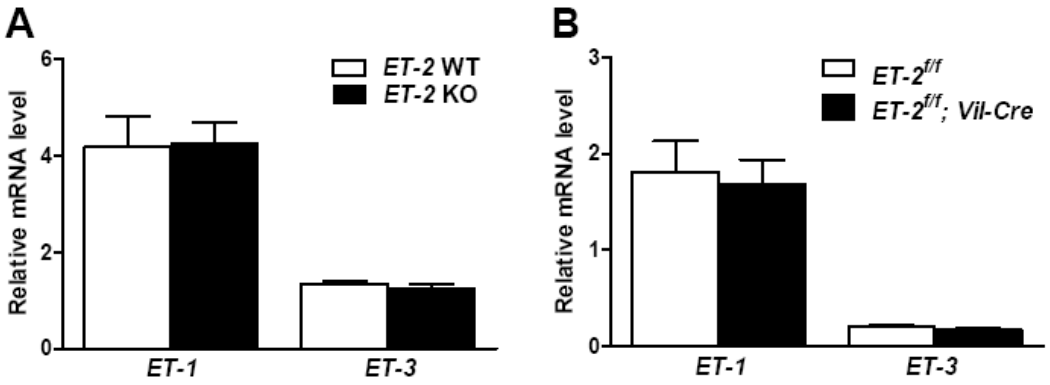


**Figure 3-16 No compensatory increase of intestinal *ET-1* and *ET-3* mRNA level by *ET-2* deficiency.** Quantitative RT-PCR was performed using mRNAs extracted from the small intestine of constitutive *ET-2* knockout (A) and *ET-2*$^{flox/flox}$*; Vil-Cre* (B), and their wild type control mice (n=4 mice per group). Values were normalized by *18s rRNA* expression. Error bars indicate ± SEM.

apparent growth or survival phenotypes were observed. They exhibited a normal growth rate (Figure3-15A), and exhibited normal blood glucose levels (Figure 3-15B). Moreover, as shown in *ET-2* knockout mice, neither lipid absorption nor excretion of lipids and carbohydrates in feces significantly changed in *ET-2*$^{flox/flox}$; *villin-Cre* mice (Figure 3-15C and D).

The finding that expression of *ET-1* and *ET-3* mRNA was unchanged in the small intestine of constitutive *ET-2* knockout and *ET-2*$^{flox/flox}$; *villin-Cre* mice (Figure 3-16) excludes the possibility that ET-1 and ET-3 might have compensates for ET-2 loss in our mutant mice. Therefore, contrary to previous speculation as well as my hypothesis that ET-2 may play important role in pathophysiology of the intestine, these data reveal that the intestine is not an essential site of ET-2 action under normal physiological conditions.

**Other potential candidate tissues for ET-2 action**

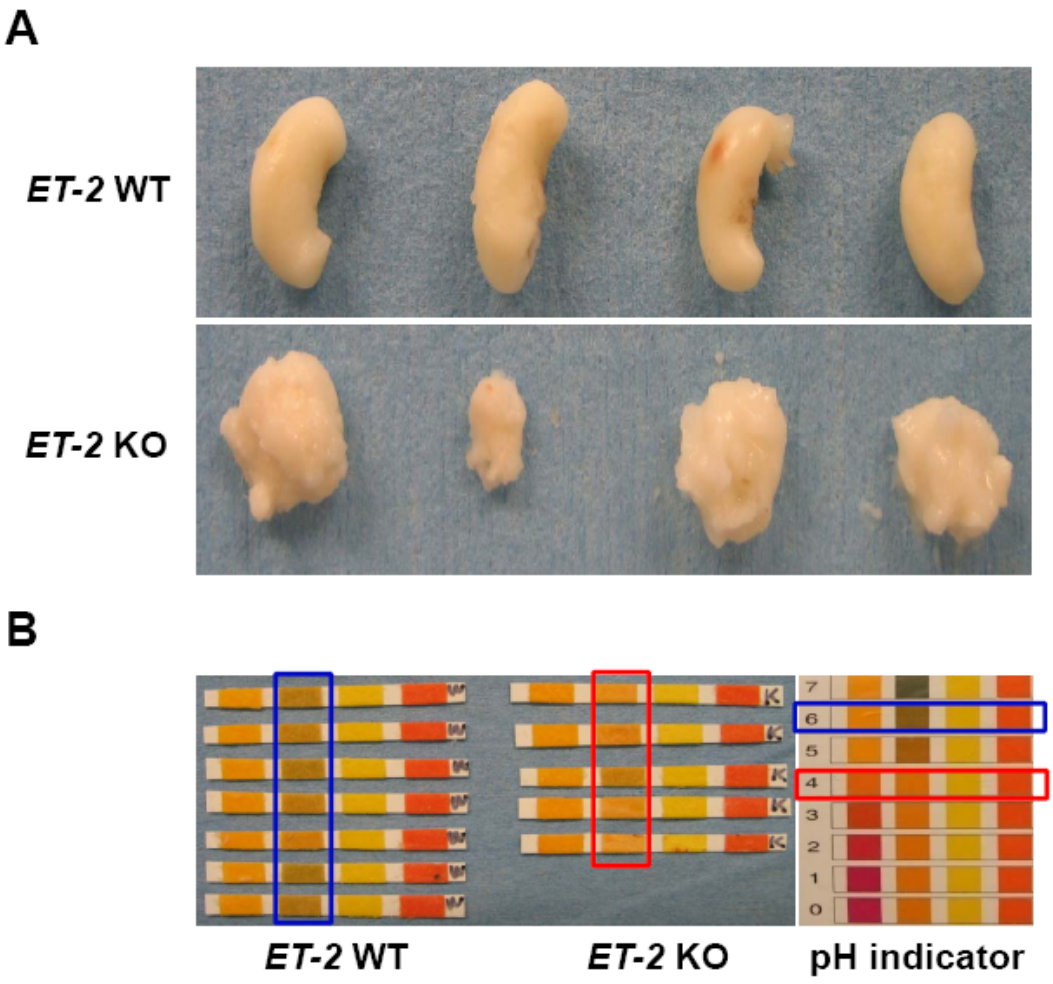


**Figure 3-17 Examination of stomach content.** (A) Abnormal coagulation of milk from stomach of constitutive *ET-2* knockout mice. (B) Acidic pH of stomach content from constitutive *ET-2* knockout (red rectangle) and wild type control (blue rectangle) mice.

Since stomach *ET-2* mRNA expression is intact (Figure 3-14B) and no significant abnormality was displayed in *ET-2*$^{flox/flox}$; *villin-Cre* mice (Figure 3-15), the stomach may be another candidate tissue of ET-2 function. While the milk content of stomachs is similar in both genotypes, the nature of the stomach chyme differs in the *ET-2* knockout displaying excessive air and a more fluid chyme. This raised a possibility that pH and

enzyme secretion by cells of the stomach may be affected by *ET-2* deficiency (Figure 3-17A). pH of stomach contents from *ET-2* knockout mice was more acidic (pH≈3-4) than that of wild type controls (pH≈5-6) perhaps contributing to enhanced protein denaturation (Figure 3-17B). Therefore, I first examined mRNA levels for key proteins regulating acidification, digestion of proteins, or coagulation of milk in the stomach. The expression was not significantly different between stomach samples of wild type and *ET-2* deficient mice (Figure 3-18A). To determine if abnormal growth rate is caused by the aberrant digestion and/or absorption of nutrients due to an altered stomach pH, I provided the mice with sodium bicarbonate in their drinking water to neutralize stomach pH. However, no improvement in body weight (Figure 3-18B) or life span of *ET-2* deficient mice (Figure 3-18C) was observed.

Among the numerous ET-2 expressing tissues, albeit low levels, *ET-2* expression was detected in whole pancreas (Figure 2-1A). Because insulin secretion is normally regulated in *ET-2* deficient mice (Table 3-2), I analyzed expression of exocrine pancreatic enzymes to determine the critical contribution of ET-2 deficiency in pancreatic function. mRNA level of genes involved in the digestion and absorption of fat, carbohydrate, and protein was not significantly changed in *ET-2* knockout mice compared to wild type controls, however (Figure 3-19).

Lastly, I attempted to overcome malabsorption and/or malnutrition of the mutant mice by high fat and semisynthetic diet containing easily digested and absorbed nutrients. Neither high-fat nor semisynthetic diets appeared to prolong survival (Figure 3-20A and B) or increase body weight (data not shown) of the *ET-2* knockout mice.

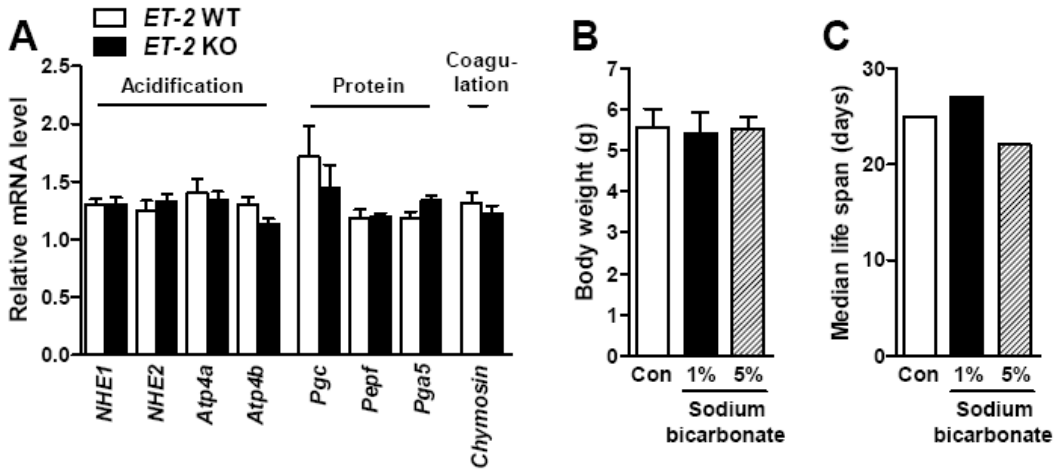


**Figure 3-18 Normal stomach function of *ET-2* knockout mice.** (A) No significant change in the expression of genes responsible for acidification, digestion, and coagulation of milk in stomach. Quantitative RT-PCR was performed using mRNAs extracted from stomach of indicated genotypes. Values were normalized by *18s rRNA* expression. (B and C) No effect of antacid diet on body weight and life span of *ET-2* knockout mice. Error bars indicate ± SEM.

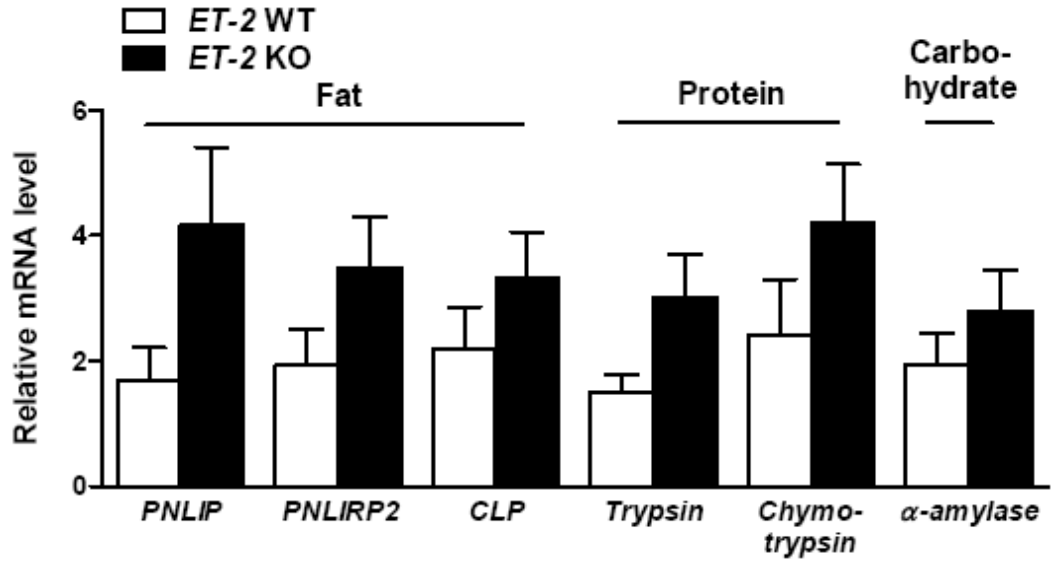


**Figure 3-19 No significant change in the expression of exocrine pancreatic enzymes.** Quantitative RT-PCR was performed using mRNAs extracted from pancreas of indicated genotypes. Values were normalized by *18s rRNA* expression.

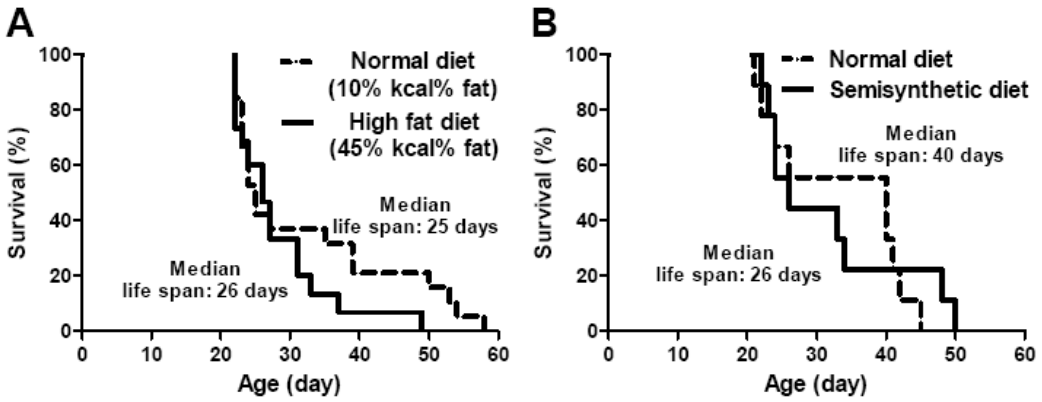


**Figure 3-20 No obvious effect of rescuing attempt by dietary supplement.** 3 week-old wild type and constitutive *ET-2* knockout mice were given high fat diet (A) or TPN diet (B) and assayed the survival ratio. $p$=0.2164 (A) and $p$=0.8084 (B) by log-rank test

## Discussion

The results of these studies demonstrated that ET-2 plays an important role in the regulation of energy homeostasis. Given the overall phenotype and expression pattern of ET-2, I initially hypothesized that growth retardation and early lethality of *ET-2* deficient mice results from internal starvation due to intestinal dysfunction. My molecular, physiological and genetic analyses show, however, that intestinal ET-2 is not fully accountable for the defect in the regulation of energy homeostasis.

The result that the intestine is not a site of ET-2 function in the regulation of growth was astounding and led me to examine other tissues. Relatively high expression of *ET-2* is detected in the stomach and dysregulation of stomach content pH is suspected. However, I cannot find other abnormalities - such as morphological changes or altered expression of genes for acidification and nutrient digestion - in *ET-2* deficient mice. Exocrine pancreatic insufficiency is an inability to properly digest food due to a lack of digestive enzymes made by the pancreas and this leads to maldigestion and

malabsorption of nutrients. Moreover, procolipase-deficient mice show decreased postnatal survival and growth retardation even in the absence of steatorrhea (D'Agostino et al., 2002). My examination shows that expression levels of pancreatic enzymes such as lipases, proteases, and amylases are similar between genotypes. Although I found that mRNA levels of genes related to nutrient regulation is expressed in normal quantities in the mutant mice, it might also be instructive to determine, using immunoblot analysis, whether the proteins are indeed expressed normally in these mice, as well as to perform *in vitro* studies to examine if those digestive enzymes are capable of functioning appropriately. It is also entirely possible that some other tissue expressing *ET-2* at low levels in a very small subset of cells might explain the growth retardation and juvenile lethality. Interestingly, pituitary, thyroid and adrenal gland express *ET-2* and *ET* receptors (Davenport et al., 1996; Tsushima et al., 1994). Moreover, ET-2 increases the secretion rate of aldosterone by zona glomerulosa cells (Hinson et al., 1991) and I found that T3 hormone level, although mild, is decreased in *ET-2* deficient mice. Further experiments to test this idea need to be performed. Histological and hormonal analysis might give us additional information regarding an entirely new possibility that ET-2 appears to regulate the secretion of essential hormones.

Because the intestine does not appear to be the target tissue for ET-2 in a normal physiological condition, the significance of the defect in the mitotic renewal of progenitor cells is not clear in relation to the growth retardation and juvenile lethality. It might be a secondary effect of starvation because food deprivation has been found to inhibit intestinal cell proliferation and migration (Gomes and Alvares, 1998; Palanch and Alvares, 1998).

## Materials and methods

### Serum and plasma study

Blood for analysis was collected through retrobulbar plexus or either by cardiac puncture or by decapitation. For serum, blood was transferred to Vacutainer® SST™ Tubes (BD) and centrifuged (1500 x g for 15 min at 4°C), and serum was stored at -20°C until analysis. For plasma, blood was transferred to Vacutainer® K2 EDTA Tubes (BD) and centrifuged (1000 x g for 15 min at 4°C), and plasma was frozen in liquid nitrogen and stored at -80°C, or analyzed immediately by Dallas Children's Medical Center, Pathology Laboratory.

### Blood glucose measurement

Blood was taken from tail vein and glucose levels were assayed using a Glucometer Elite XL (Bayer).

### Body composition analysis

Total body fat mass was analyzed by NMR using Minispec mq spectrometer (Bruker).

### Milk consumption

Milk was taken from the stomach of the wild type and mutant mice and weighed.

### Locomotor activity

For constitutive *ET-2* knockout mice, movement of mice was videotaped and the distance of movement analyzed by TopScan Lite (Clever Sys. Inc.). For adult *ET-2*$^{flox/flox}$*;* TAM-

*Cre* mice, locomotor activity was determined from infrared beam breaks within an open field apparatus, subdivided into 8 inch×8 inch activity chambers by Plexiglas dividers (VersaMax Animal Activity Monitor, AccuScan Instruments, Inc., Columbus, OH, USA), and modified to allow *ad libitum* access to food and water. Litter covered the floor of the activity chambers throughout. Individual mice were placed in a clean activity chamber at the midpoint of the light phase and were monitored continuously for the subsequent 24 h. Raw beam break data were collected on-line via computer and subsequently analyzed to calculate locomotor activity as total distance traveled.

### *In situ* hybridization

A 0.45 kb segment of mouse ET-2 was PCR amplified using 5′-TTTGAATTCAGGCTCCTGCTGCTGTGT-3′ and 5′-TTTCTCGAGGCATGTTCATTTGTCCTC-3′ as primers and cloned into pBluescript II SK (+/-). Sense and antisense riboprobes were generated with T3 and T7 polymerases, respectively, using the Maxiscript kit (Ambion) in the presence of $^{35}$S-CTP and -UTP (Amersham). Paraffin-embedded sections were prepared from the tissues of wild type control and *ET-2* deficient mice. Following prehybridization, sections were hybridized at 70 $^{o}$C with sense and antisense riboprobes. Following overnight incubation, unhybridized probe was removed with stringent washes and treatment with RNase A. Slides were subsequently coated with K.5 nuclear emulsion, exposed at 4 $^{o}$C for 4-5 weeks, developed, counterstained with hematoxylin, and examined using bright and dark field optics.

***In vivo* 5'-bromo-2' deoxyurdine staining**

Wild type or ET-2 deficient mice were given an intraperitoneal injection with 500mg/kg body weight of 5'-bromo-2'-deoxyuridine (Roche Diagnostics). 2hr and 48hr after injection, the entire gastrointestinal tract was removed immediately after sacrifice. The small intestine and colon were separated from each other and flushed with PBS. The small intestine was divided into equal thirds (designated duodenum, jejunum, and ileum) and fixed in 4 % paraformaldehyde overnight. Tissues were embedded in paraffin and sectioned at 5μm intervals. Briefly, deparaffinized sections were incubated in 2N HCl for 60 minutes to denature DNA and immersed in 0.1 M borate buffer. The sections were permeabilized in PBST (0.3% Triton X-100 in PBS), blocked with 3% normal horse serum in PBS, incubated with a monoclonal mouse BrdU antibodies (1:25, Roche Diagnostics) overnight at 4$^{o}$C, and treated with 1:200 dilution of biotinylated horse anti-mouse antibodies (Vector Laboratories) for 30 minutes. Samples were developed with 1:200 dilution of Alexa 488 (Invitrogen) for 5 minutes, and images acquired using a Nikon Distal Camera DXM 1200F.

**Histochemistry and immunohistochemistry**

For H&E staining, tissues were harvested, fixed in 4 % paraformaldehyde for paraffin embedding and sectioned at 5μm intervals. Sections were stained with hematoxylin and eosin using standard procedures. For immunofluorescence, briefly, fixed tissue was cryoprotected in 10% sucrose in PBS (3h at 4$^{o}$C), immersed in 20% sucrose/10% glycerol in PBS (overnight at 4$^{o}$C), and then frozen in OCT TissueTek compound (VWR Scientific) before preparing 8 μm thick cryosections. A rabbit polyclonal antibody to

mouse LYVE1 (Abcam) and biotinylated goat anti-rabbit IgG (Vector Laboratories) was diluted 1:1000 and 1:200 in PBS, respectively. Alexa 488-streptoavidin antibody (Invitrogen) was used to visualize antigen-antibody complexes.

**Measurements of intestinal villous length**

Images were taken at low-magnification (x10). Representative villi were selected and lengths measured using the AxioVision program 4.5. These analyses were performed by two independent investigators. A total of 10 intestinal villi were evaluated per mice and total 3 mice were analyzed.

**Nutrient absorption and excretion**

Dietary fat absorption was examined by measuring remaining radioactivity after oral gavage of [$^{3}$H] triolein (PerkinElmer) as described (Oishi et al., 2006). For fecal nutrient analyses, stools were collected over 12 hours from individually housed mice. Lipid content was determined gravimetrically as described (Ameen and Powell, 1985; Folch et al., 1957; Schwarz et al., 1996). Fecal carbohydrate content was determined by a spectrophotometric method as described (Ameen and Powell, 1985).

**Rescue experiments by dietary supplement**

For antacid treatment, sodium bicarbonate was dissolved in water and provided to mice at 3 weeks of age *ET-2* null mice. High fat diet (45% kcal% fat) and control diet (10% kcal% fat) were purchased from Research Diets. Vivonex® Pediatric diet (Novartis) was used as semisynthetic diet.

**Statistical Analysis**

Values depict the mean ± SEM. Statistical significance was evaluated using two-tailed unpaired student's *t* tests (GraphPad Prism 5) and considered significantly different $p<0.05$.

# Chapter 4

# Endothelin-2 in Thermoregulation

## Introduction

The endothelin (ET) system is abundantly present in the brain. *ET-1*, *ET-3*, $ET_A$ and $ET_B$ are expressed by vascular, neuronal, and glial cells of the cerebral cortex, striatum, amygdala, hippocampus, paraventricular and supraoptic nuclei of the hypothalamus, subfornical organ, median eminence, raphe nuclei, and pituitary gland (Giaid et al., 1991a; Lee et al., 1990; Takahashi et al., 1991). *ECE-2* mRNA was predominantly expressed in the central nervous system, including the cerebrum, cerebellum, and pituitary gland (Emoto and Yanagisawa, 1995) as well as the thalamus, hypothalamus, amygdala, dentate gyrus, and CA3 (Yanagisawa et al., 2000). Presence of ET-2 was recently examined in the central nervous system and pituitary gland. In both mouse and rat, *ET-2* gene expression is relatively high in the pituitary gland. Moderate expression is observed in the medulla oblongata, cerebral cortex, septum, striatum, hypothalamus, and midbrain. The hippocampus, thalamus, and cerebellum show a low level of expression (Masuo et al., 2003).

The expression of ET system components in these distinct areas of the brain suggests a function in the nervous system. The critical role of the ET pathway in the regulation of central blood pressure was reported: Intraventricular injection of ET-1 results in transient increases in arterial blood pressure. Blockage by the $ET_A$ antagonist, BQ 123, but not by the $ET_B$ antagonist, BQ 788, suggests that the ET-1/$ET_A$ pathway is

involved in the regulation of blood pressure (Kuwaki et al., 1997; Mosqueda-Garcia et al., 1995). The critical role of ETs in respiratory control was demonstrated by direct injection of ET-1. Whereas the delivery into the ventrolateral medulla causes complete cessation of respiratory activity, intracisternal injection induces apnea (Dreshaj et al., 1995). *ET-1* heterozygous mice have lower arterial oxygen concentrations and higher arterial carbon dioxide concentrations but maintain a normal respiratory rate and volume. In a hypercapnic or hypoxic environment, these mice have attenuated increases of respiratory volume and rate (Kuwaki et al., 1996). The ET system is also implicated in modulation of behavior. Intraventricular injection of ET-1 in rats results in behavioral changes, including barrel rolling, body tilting, nystagmus, facial clonus, forelimb clonus, and tail extension despite normal cerebral blood flow (Chew et al., 1995). Injection of ET-1 into the periaqueductal gray matter reduces pain response to the hot plate paradigm in a dose-dependent manner (D'Amico et al., 1996). Other studies implicate involvement of ET in the control of fluid intake. ET-3 administration suppresses water intake in animals that are water deprived or treated with angiotensin II but it does not have direct effect on drinking behavior in mice under standard laboratory conditions (Samson et al., 1991; Zhu and Herbert, 1996).

A potential role of ET in thermoregulation is also suggested. ET-1 causes fever after intracerebroventricular (ICV) injection into rats. An $ET_B$ receptor antagonist attenuated fevers by systemically administered pyrogens such as LPS and IL-1β, as well as ICV of IL-1β or TNFα (Fabricio et al., 2005; Fabricio et al., 1998). ICV injection of ET-3 decreases the core temperature of rats (Zhu and Herbert, 1996). Previously, a central ET-1/$ET_B$ pathway was reported to participate in the development of LPS-induced

fever (Fabricio et al., 1998). Interestingly, ICV injection of ET-1causes an increase in body temperature (Fabricio et al., 2005). Despite the extensive studies of the ET system components of the brain, little is known regarding the physiological role of ET-2 in the brain.

## Results

### Defective thermoregulation of *ET-2* deficient mice

Constitutive *ET-2* deficient mice exhibited mild hypothermia which might be the secondary consequence of internal starvation (Figure 4-1A; group-housed). When the *ET-2* deficient mice were separated for 3 hours from the dam and siblings, which may have served as a heat source, core body temperature of the *ET-2* knockout mice drastically declined at room temperature and the extent of this decrease became more pronounced with age (Figure 4-1A; isolated). *ET-2* knockout and wild type control mice were challenged with a cold environment to examine whether ET-2 is important for heat generation and conservation. Unlike wild type control mice which maintained body temperature within 2.2$^{o}$C, the core body temperature of *ET-2* knockout mice dropped by nearly 30% to approximately 22 $^{o}$C within 4 hours of exposure to 4$^{o}$C (Figure 4-1B). Because all of the knockout mice showed slow breathing and unconsciousness, this experiment was terminated, and mice were moved to a warm environment to recover. Expression of *cold-inducible RNA-binding protein (CIRBP)* is known to be induced by lowering body temperature from 37$^{o}$C to 32$^{o}$C (Nishiyama et al., 1997). Hence, I investigated whether *CIRBP* is differentially expressed between genotypes. As supportive evidence of hypothermia in *ET-2* deficient mice, *CIRBP* mRNA level was clearly

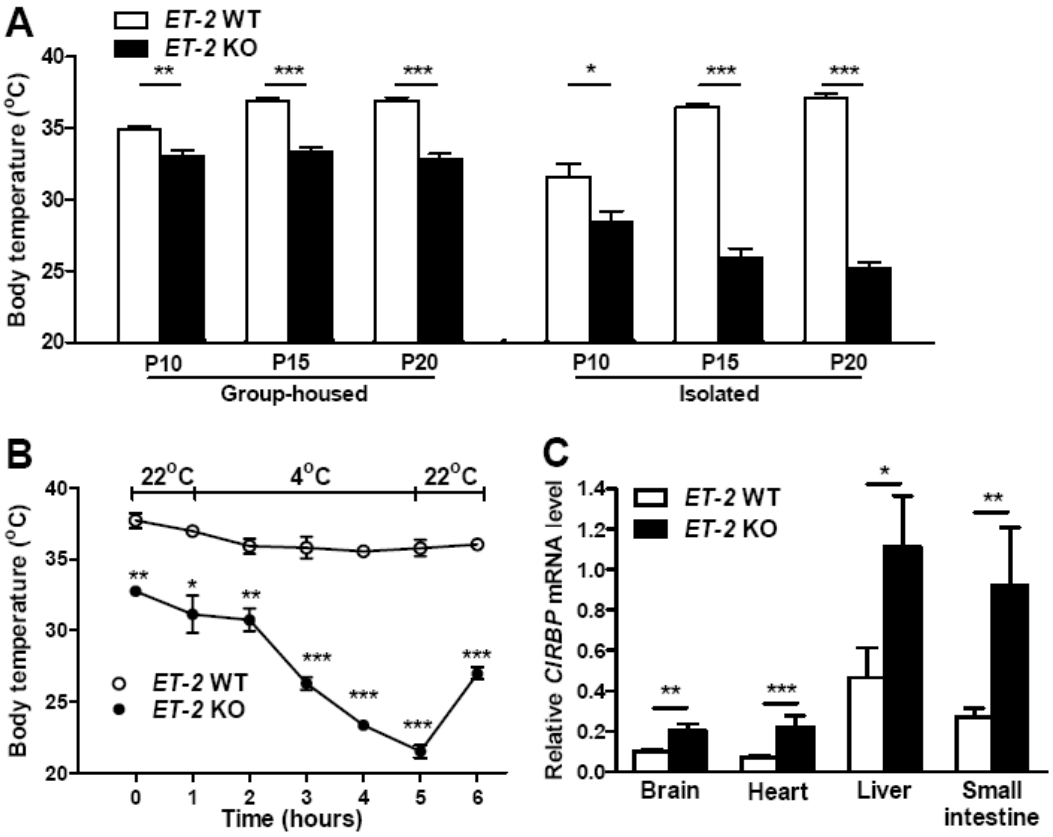


**Figure 4-1 Profound hypothermia of constitutive *ET-2* knockout mice in both ambient and cold environments.** (A) Core body temperature of constitutive *ET-2* knockout mice at group-housed and isolated condition (n=10 mice per group). (B) Core body temperature of constitutive *ET-2* knockout mice and wild type controls on cold environment (n=6 mice per group). (C) Quantitative RT-PCR of *CIRBP* mRNA level in individual tissues from constitutive *ET-2* knockout mice and wild type controls (n=4 mice per group). Error bars indicate ± SEM. **p*<0.05, ***p*<0.01, ****p*<0.001

induced in all the examined tissues of mutant mice on ambient temperature (Figure 4-1C). *Type 2 iodothyronine deiodinase (DIO2)* is activated during cold stress to increase triiodothyroine (T3) concentration in brown adipose tissue (Silva and Larsen, 1983). The level of *uncoupling protein 1 (UCP-1)*, the key thermogenic regulator in brown adipose

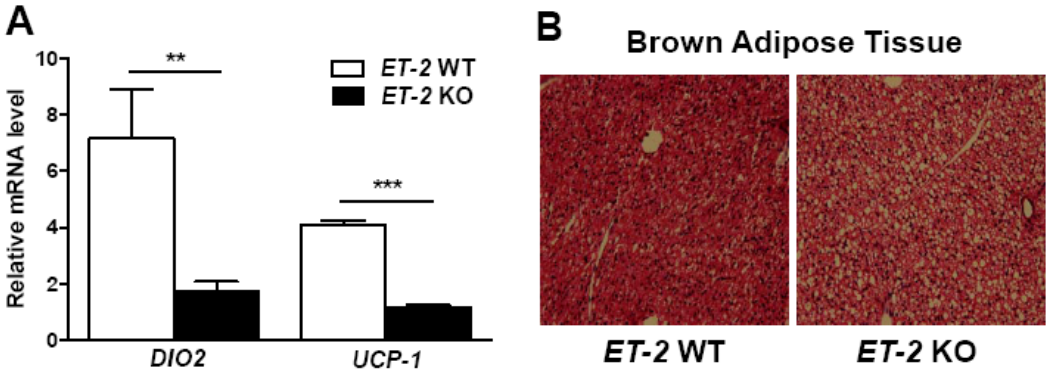


**Figure 4-2 Defective thermoregulation of *ET-2* knockout mice.** (A) Quantitative RT-PCR of *DIO2* and *UCP-1* mRNA level in brown adipose tissues from constitutive ET-2 null mice and wild type controls (n=4 mice per group) at ambient temperature. Error bars indicate ± SEM. $^{**}p<0.01$, $^{***}p<0.001$ (B) Representative histological sections (H&E staining) of brown adipose tissues from constitutive *ET-2* knockout mice and wild type controls. Magnification: x10

tissue, is regulated by T3 (Guerra et al., 1996). Therefore, I examined the expression of *DIO2* and *UCP-1* to determine whether *ET-2* deficiency affects these genes and leads to the defects of thermogenesis. As expected, *DIO2* and *UCP-1* mRNA levels were significantly reduced in brown adipose tissue of *ET-2* deficient mice (Figure 4-2A). Histological analysis of brown adipose tissue from *ET-2* deficient mice revealed abnormalities including reduced nuclei number and marked accumulation of large lipid vacuoles (Figure 4-2B). Low body temperature induces behavioral responses such as huddling in a curled posture and seeking a warmer place. Stationary curled posture was notably seen in constitutive *ET-2* deficient mice. Consistent with this observation, when wild type and *ET-2* deficient mice were placed into an apparatus with 2 available thermal zone (22 $^{o}$C vs.33 $^{o}$C), there was an apparent difference in the amount of time spent in each zone. Unlike the cold-zone preference of wild type mice, *ET-2* knockout mice clearly sought a warmer location (Figure 4-3).

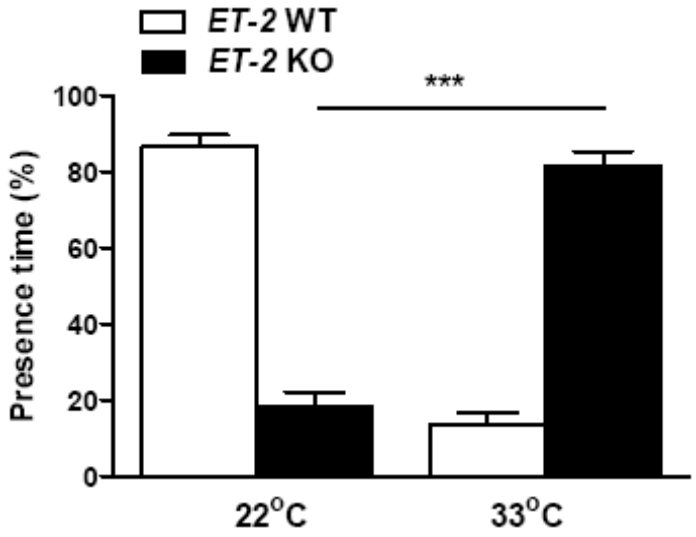


**Figure 4-3 Warm environment preference of *ET-2* knockout mice.** Experiment was performed by placing wild type control (n=14) and constitutive *ET-2* knockout mice (n=21) onto a plate harboring two different temperature settings (22 °C and 33°C). Mice were observed for 1 hr, and the percent time spent at each temperature was recorded. Error bars indicate ± SEM. ****p*<0.001

The results showing defective thermoregulation and preference for a warmed locale of *ET-2* deficient mice led me to hypothesize that placing *ET-2* deficient mice at higher ambient temperatures might delay their premature death. In order to test this question, 3 week-old *ET-2* deficient mice were housed in cages at room temperature, cages placed on a 33°C heating plate for added warmth. As expected, *ET-2* deficient mice housed at the higher temperature lived significantly longer (Figure 4-4) – in fact, median life span was extended from 4 weeks to 9 weeks. Due to the notable rescuing effect of external heat, I further analyzed physiological characteristics of "rescued" *ET-2* deficient mice provided with the higher temperature environment. Although constitutive *ET-2* deficient mice were still mildly hypothermic even under these warm conditions (Figure 4-

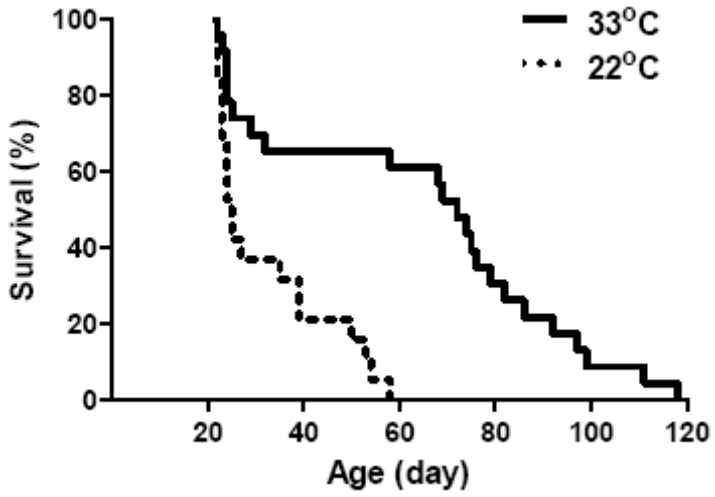


**Figure 4-4 Extended life span of *ET-2* deficient mice by warm environment.** Survival ratio was compared between one group of *ET-2* deficient mice (n=20) housed in ambient temperature (22°C) and the other (n=21) at warmer temperature (33°C). Median survival times were 25 days and 72 days, respectively, and significantly different by log-rank test ($p$<0.0001).

5A), their core body temperature was higher than that of the mice housed at normal ambient temperature (Figure 4-5B). Food intake of *ET-2* deficient mice in the warm environment was significantly elevated compared to the mice in the normal environment (Figure 4-5C). However, body weight and blood glucose were not improved in *ET-2* deficient mice raised in the warm environment (Figure 4-5D). These data suggest that defective thermoregulation may partially contribute to the early lethality of *ET-2* deficient mice. Although supplying external heat makes the mice active and consume more food, the mutant mice still exhibit defects in energy homeostasis.

As displayed in constitutive *ET-2* deficient mice, neonate and adult *ET-2*$^{flox/flox}$; TAM-*Cre* mice were also mildly hypothermic (Figure 4-6A). To examine whether adult *ET-2* deficiency at adulthood is also important for heat generation or conservation, adult *ET-*

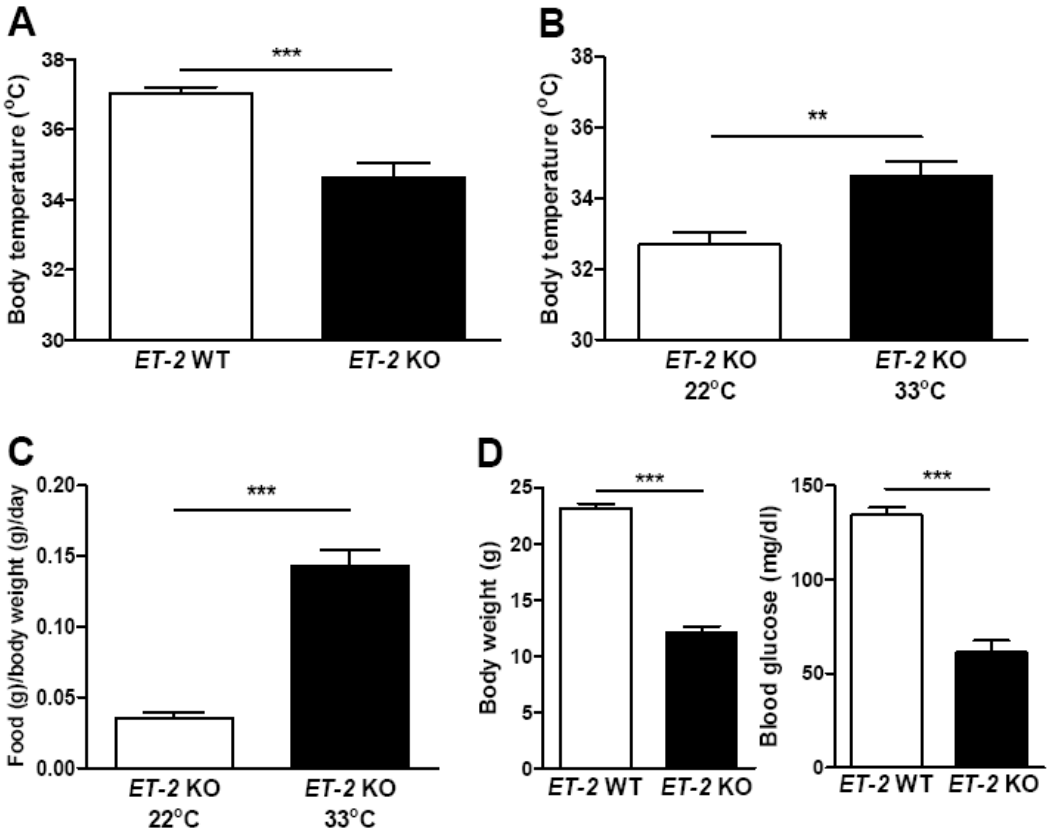


**Figure 4-5 Partially improved metabolism of constitutive *ET-2* deficient mice housed at warm condition.** (A) Core body temperature of constitutive *ET-2* deficient mice (n=12) and wild type controls (n=13) under warm environment. (B) Core body temperature of constitutive *ET-2* deficient mice housed at normal (22°C; n=11) and higher (33°C; n=12) ambient temperature. (C) Food intake of *ET-2* deficient mice at normal (22°C; n=6) and higher (33°C; n=7) ambient temperature. (D) Body weight and blood glucose level of *ET-2* deficient mice and wild type controls housed at higher ambient temperature (n=12 mice per group). Error bars indicate ± SEM. ***p*<0.01, ****p*<0.001

$2^{flox/flox}$ and *ET-*$2^{flox/flox}$; TAM-*Cre* mice were challenged with a cold environment. The core body temperature of *ET-*$2^{flox/flox}$ mice was maintained within 1.2°C over a 12 h period. However, as shown in constitutive *ET-2* deficient mice, core body temperature of

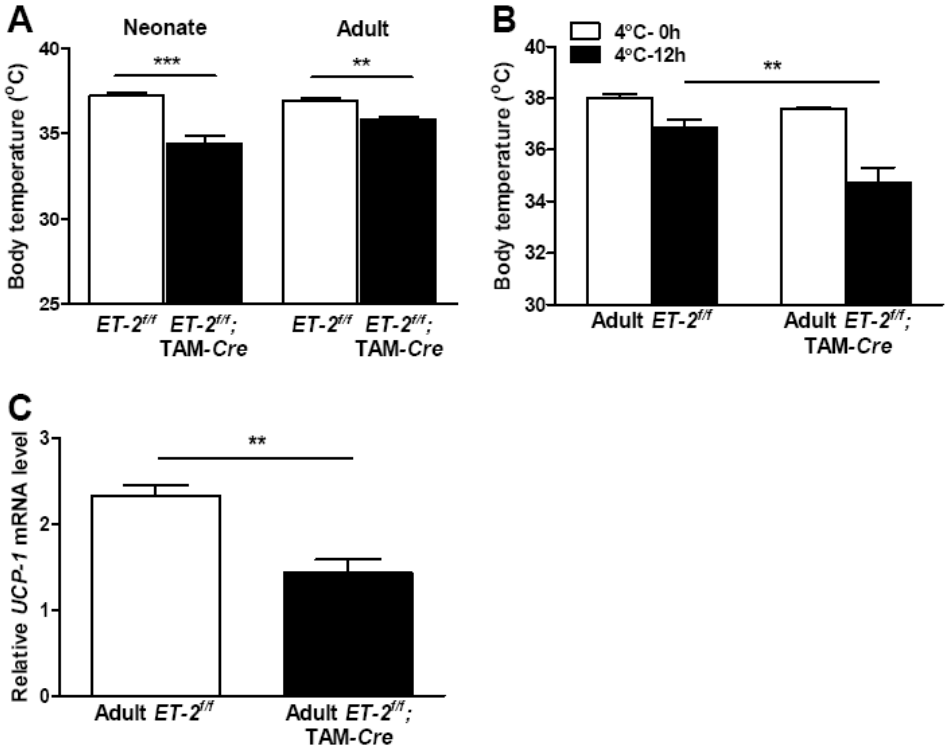


**Figure 4-6 Defective thermoregulation of systemically inducible *ET-2* knockout mice.** (A) Hypothermia of neonate (n=7, average body weight=6.63g) and adult (n=10, average body weight=22.1g) *ET-2*$^{flox/flox}$; TAM-*Cre* mice maintained at ambient temperature (22 °C). (B) Core body temperature of adult *ET-2*$^{flox/flox}$; TAM-*Cre* mice housed in a cold environment (n=10 mice per group). (C) Quantitative RT-PCR of *UCP-1* mRNA level in brown adipose tissues of cold-exposed adult *ET-2*$^{flox/flox}$; TAM-*Cre* and *ET-2*$^{flox/flox}$ mice (n=4 mice per group). Error bars indicate ± SEM. ***p*<0.01, ****p*<0.001

*ET-2*$^{flox/flox}$; TAM-*Cre* mice significantly dropped in 12 h of cold exposure (36.9 ± 0.3 °C vs. 34.7 ± 0.5 °C ; Figure 4-6B). This is not really as extreme as earlier studies on constitutive *ET-2* knockout mice (6 week-old rescued from warm environment, 10 g of body weight) which the body temperature went down to ~22 °C in 4hours) but could be contribute to larger mouse size (25 g of body weight) and decreased surface/volume ratio. *UCP-1* mRNA level in brown adipose tissue from cold-exposed adult *ET-2*$^{flox/flox}$; TAM-*Cre* was also down-regulated (Figure 4-6C).

**Uncertain role of ET-2 in central thermoregulation**

Reduced *DIO2* and *UCP-1* expression in the face of profound hypothermia (Figure 4-2) and the absence of *ET-2* in brown adipose tissues (Figure 2-1A) indicate the possibility of abnormal central thermoregulation by *ET-2* deficiency. As thermogenesis of brown adipose tissue is activated by the hypothalamus via the sympathetic nervous system (Gulati et al., 1997; Kumar et al., 1997; Silva and Larsen, 1983) and *ET-2* mRNA is present in thermoregulatory tissues such as brainstem, spinal cord, pituitary, adrenals and thyroid at low but detectable levels (Figure 4-7A). I explored the involvement of the ET-2 pathway in the regulation of body temperature, BQ 123 and BQ788 – selective $ET_A$ and $ET_B$ antagonists, respectively- were centrally injected and core body temperature was examined. Interestingly, BQ 123 reduced temperature within 5 min of administration and showed a peak at 30 min, while BQ 788 was totally ineffective (Figure 4-7B).

In order to directly examine the possibility that ET-2 regulates central thermoregulation, I generated neuron-specific *ET-2* knockout mice by crossing mice carrying *nestin-Cre* recombinase and *ET-2*$^{flox}$ transgenes (Figure 2-4A). Loss of *ET-2* mRNA expression in the brain was verified by quantitative RT-PCR (Figure 4-8A). Specific activity of *nestin* promoter was confirmed by intact expression of *ET-2* mRNA in the intestine. *ET-2*$^{flox/flox}$; *nestin-Cre* mice were born healthy. However, unlike constitutive *ET-2* deficient mice, the mutant mice displayed normal core body temperature (Figure 4-8C). Even in a cold environment, there was no apparent abnormality of thermoregulation in *ET-2*$^{flox/flox}$; *nestin-Cre* mice (Figure 4-8D). In addition, analysis of *ET-2* mRNA expression in the brain by *in situ* hybridization revealed that it is expressed at non thermoregulatory neurons such as 7N facial neurons, trigeminal

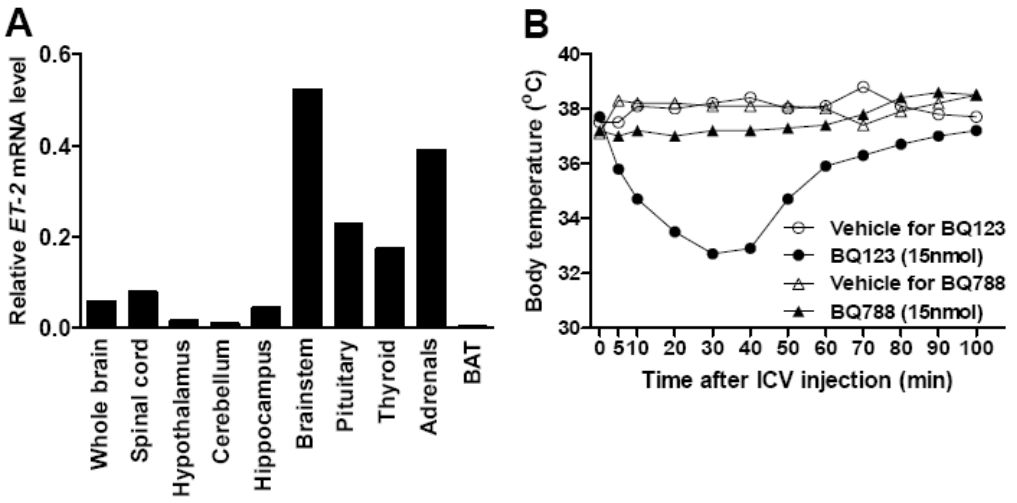


**Figure 4-7 Potential role of *ET-2* in central thermoregulation.** (A) Expression profile of *ET-2* mRNA in thermoregulatory tissues. Quantitative RT-PCR was performed with mRNA from individual tissues. Values were normalized by *18s rRNA* expression. (B) Effect of selective $ET_A$ antagonist (BQ 123) and $ET_B$ antagonist (BQ 788) on core body temperature.

motor neurons in the brain, and motor neurons in the spinal cord (Figure 4-9). These results suggest that although systemic loss of *ET-2* leads to defects in thermoregulation, this regulatory defect is not at the level of central nervous system.

When small animals, including mice, enter a hibernation-like state of torpor, body temperature is greatly reduced (Van Breukelen and Martin, 2002). Expression of *pancreatic lipases, pancreatic lipase-related protein 2 (PNIRP2)* and *colipase (CLP)* are induced outside the pancreas (including the liver) during torpor (Zhang et al., 2006). *FGF 21*, which promotes torpor (Inagaki et al., 2007), is up-regulated in *ET-2* deficient mice (Figure 3-4A).

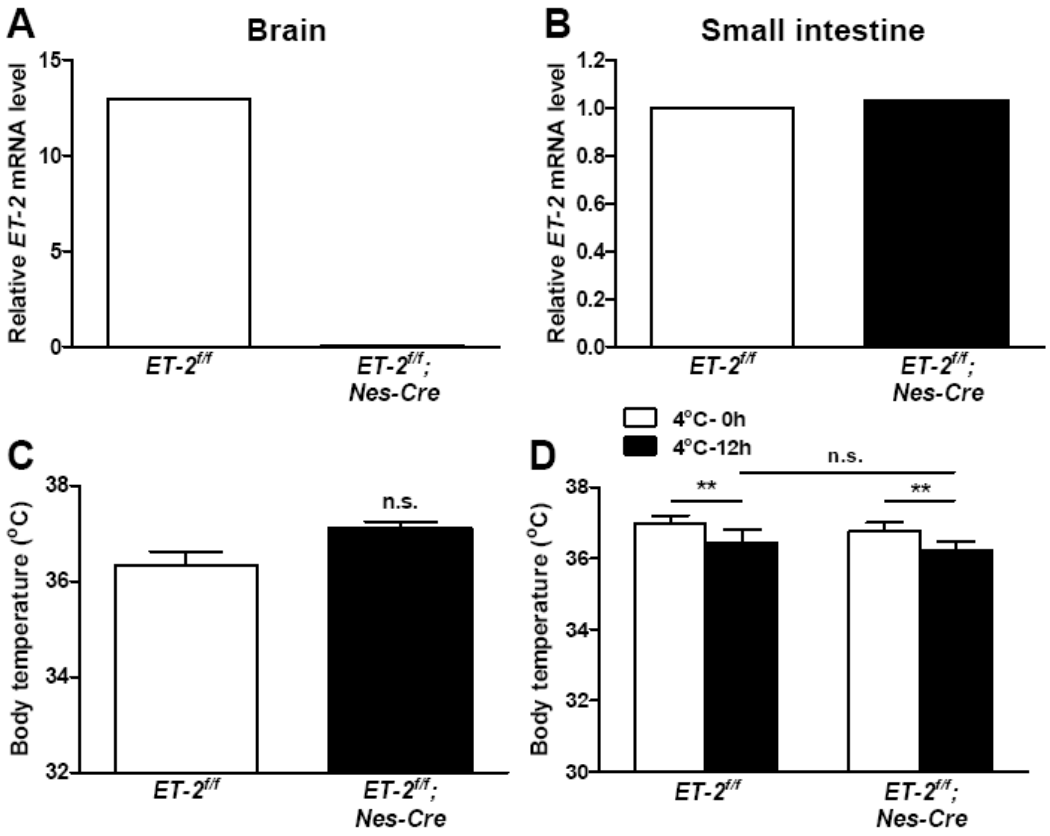


**Figure 4-8 No detectable abnormalities of neuron-specific *ET-2* null mice.**
(A) Quantitative RT-PCR of brain-specific *ET-2* deletion by *nestin* promoter-driven *Cre* recombinase. (B) Intact expression of ET-2 in intestine from *ET-2*$^{flox/flox}$; *nestin-Cre* mice. Values were normalized by *18s rRNA* expression. (C) Core body temperature of *ET-2*$^{flox/flox}$ and *ET-2*$^{flox/flox}$; *nestin-Cre* mice (n=10 mice per group) (D) Core body temperature of *ET-2*$^{flox/flox}$ and *ET-2*$^{flox/flox}$; *nestin-Cre* mice in cold environment (n=5 mice per group). Error bars indicate ± SEM. ***p*<0.01

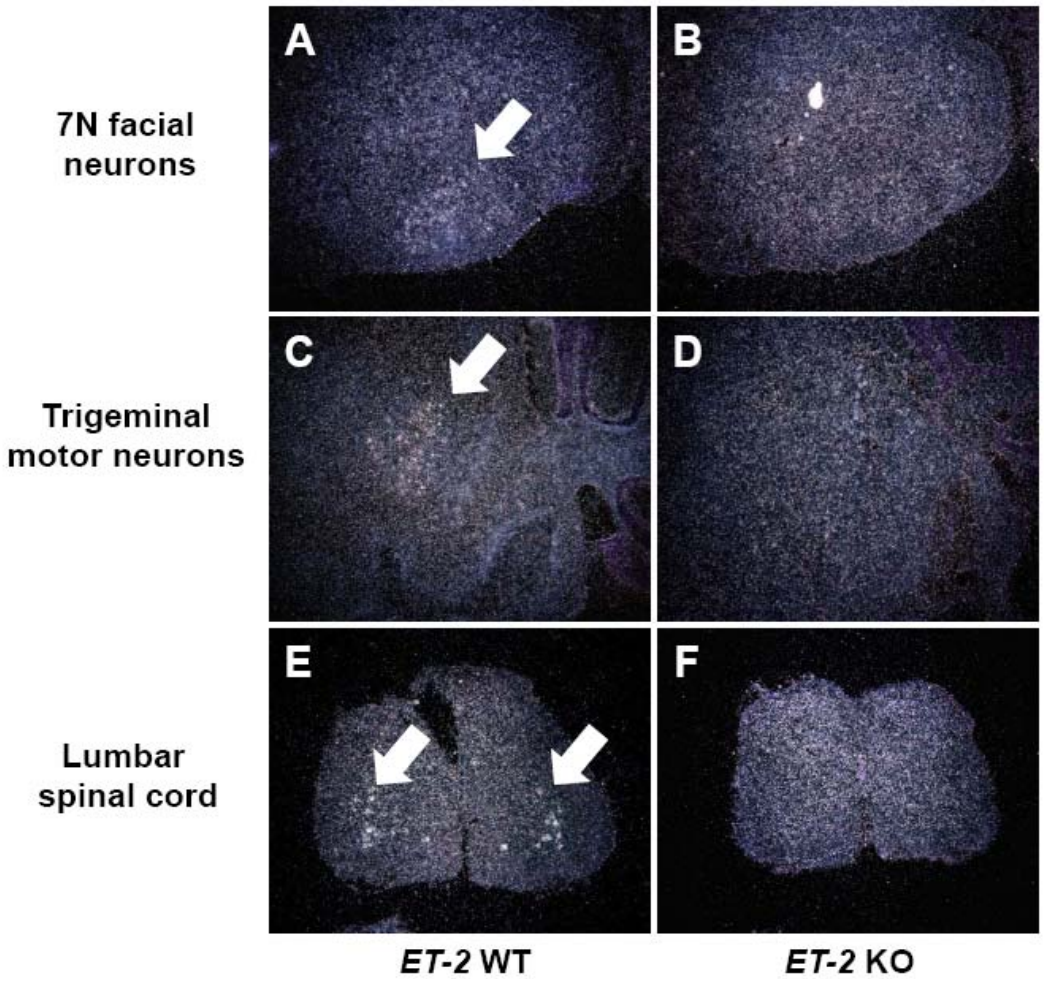


**Figure 4-9 Localization of *ET-2* mRNA in central nervous system.** *In situ* hybridization was conducted with anti-sense *ET-2* probe to wild type (A, C and E) and *ET-2* knockout mice (B, D and F). Representative photographs are shown by dark field images. Arrows indicate location of *ET-2* mRNA. Magnification: x20

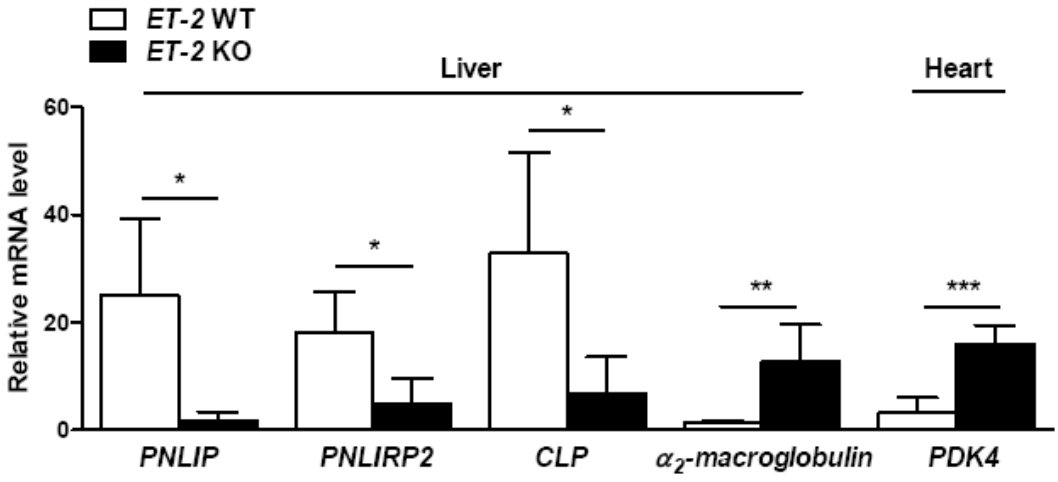


**Figure 4-10 Expression of torpor-induced genes.** Quantitative RT-PCR analysis was conducted with mRNA from liver and heart of constitutive *ET-2* knockout and wild type mice (n=4 mice per group). Values were normalized by *18s rRNA* expression. Error bars indicate ± SEM. **p*<0.05, ***p*<0.01, ****p*<0.001

To examine whether a decrease in body temperature in *ET-2* deficient mice is caused by entering a state of torpor, I explored the expression of the pancreatic lipase family and other torpor marker genes such as *$\alpha_2$-macroglobulin* in the liver and *PDK4* in the heart (Carey et al., 2003). Unlike increased mRNA levels of *$\alpha_2$-macroglobulin* and *PDK4*, expression of the pancreatic lipase family is paradoxically decreased (Figure 4-10).

## Discussion

It is clear that mice with constitutive or systemically-induced deletion of ET-2 exhibit defects in thermoregulation. This could be secondary to the internal starvation phenotype. However, as ET-2 is expressed in thermoregulatory tissues including the brainstem, spinal cord, pituitary, adrenals and thyroid, we examined a potential role of ET-2 in central thermoregulation. Core body temperature of isolated *ET-2* deficient mice

drastically goes down to around ambient temperature in a normal environment. These mice cannot maintain or increase their body temperature in the cold environment. Molecular and histological analysis of brown adipose tissues is consistent with the defect in thermogenesis as there is no apparent increase in lipolysis to generate heat. More importantly, external heat rescues the premature death of the mutant mice. However, neuron-specific *ET-2* knockout mice do not exhibit any abnormalities in the regulation of core body temperature. Although it is less sensitive than quantitative RT-PCR, *in situ* hybridization reveals *ET-2* gene expression only in non thermoregulatory neurons.

Therefore, it is more likely that hypothermia of *ET-2* deficient mice is a secondary consequence of starvation. Heat production is impaired due to depletion of energy sources. Glucose deprivation by 2-deoxy-D-glucose results in a hypometabolic state and accompanying hypothermia (Dark et al., 1994; Westman and Geiser, 2004). Core body temperature of torpid animals can be as deep as 20$^{o}$C, and can last from a few minutes up to approximately 14 hours (Geiser, 2004). Because of relatively large surface area-to-volume ratio, heat loss of the mutant mice might be proportionally higher than that of wild type mice. Although rearing at the higher ambient temperature prolongs the life span of *ET-2* deficient mice, other physiological parameters such as body weight and blood glucose are not improved. This suggests that the defect in energy homeostasis would be upstream of hypothermia.

Thermogenesis is regulated by agonists of the $\beta_3$-adrenergic receptors and PPAR$\gamma$, as well as by several hormones including leptin, ghrelin and glucocorticoids. Future experiments determining a change of body temperature by administrating agonists or antagonists for the receptors in mutant mice would give us additional information that

ET-2 may affect thermoregulation. The relation between starvation and thermoregulation will be understood more completely when the level of thermoregulatory hormones are analyzed in future studies.

My ET antagonism study clearly shows that $ET_A$ receptor is implicated in thermoregulation. Since the central thermoregulatory role of ET-2 is elusive, ET-1 might act on thermogenesis via the $ET_A$ receptor. Previous studies showing ICV injection of ET-1 increases body temperature while ET-3 decreases body temperature (Fabricio et al., 2005; Zhu and Herbert, 1996) support this hypothesis. However, it is possible that hypothermia might not be a defective regulation of the central nervous system so much as a result of bradycardia because ET system influences on the cardiovascular system. Therefore, it would be instructive to examine the heart rate of *ET-2* deficient mice to address this possibility.

## Materials and methods

### Core body temperature

Core body temperature was monitored using Thermalert TH-5 with rectal probes or flexible implantable probes (Physitemp) between 11:00 and 14:00.

### Cold challenges

The mouse cage was placed in a cold room set to $4^{o}C$ and core body temperature was measured every 1 hr.

### Temperature preference test

Cage was placed on two juxtaposed heating pads set at 22 $^{o}$C and 33 $^{o}$C. (Mediheat V500 Vstat; Peco Services Ltd). One of pads was heated at designated temperature. Mice were videotaped over 1 hr, and the location of the mice was recorded and analyzed every 5 min by TopScan Lite (Clever Sys. Inc.).

**ICV injection**

The $ET_A$ selective antagonist (BQ123; American Peptide) and $ET_B$ selective antagonist (BQ788; American Peptide) were diluted with water or 20% acetonitrile in water respectively before use and administrated through an implanted intracerebral cannula. For intracerebral cannula implantation, mice were anaesthetized with ketamine and xylazine (100mg/kg and 10mg/kg, respectively, i.p.). A cannula (Brain Infusion Kit III; Alzet) was implanted into the right lateral ventricle (0.3 mm posterior from the bregma, 0.9 mm lateral from the midline, and 2.4 mm from the surface of skull) using standard sterile stereotactic techniques.

**Survival study in warm environment**

Three-week-old mice were housed in the normal environment (22 $^{o}$C) or cage were placed on a heating pad (Gaymar) to set at 33$^{o}$C. Mice were daily observed to check for survival.

**Statistical analysis**

Values depict the mean ± SEM. Statistical significance was evaluated using two-tailed unpaired student's *t* tests (GraphPad Prism 5) and considered significantly different $p<0.05$.

# Chapter 5

# Endothelin-2 in Lung Morphology and Function

## Introduction

Endothelin-1 is highly expressed in the lung and is involved in a variety of pulmonary functions. Despite this abundance, there is no agreement on pulmonary ET-1 expression except in endothelial cells. Some reports describe ET-1 expression in the airway epithelial cells (Nakanishi et al., 1999; Rozengurt et al., 1990; Springall et al., 1991), whereas even in the same species, others reported confined expression to endocrine cells (Giaid et al., 1991b; Giaid et al., 1993; Seldeslagh and Lauweryns, 1993). This discrepancy also exists throughout developmental stages. In neonatal mice, ETs are reported to be present in pulmonary endocrine cells (Seldeslagh and Lauweryns, 1993) and most airway epithelial cells are positive for ET expression in young mice (Rozengurt et al., 1990). A recent time-course study revealed the presence of immunoactivity was found in epithelial cells of developing and adult mice. The expressing cells were identified as Clara cells and the signal was present in the apical region of these cells. In the adult, apart from epithelial cells, expression has also been observed in mouse vascular muscle and parenchymal cells (Guembe and Villaro, 2001). ET receptors are present in airway smooth muscle cells and on the pulmonary circulating vessels (Koseki et al., 1989). $ET_B$ receptors are also found on neuronal bodies and on neuronal processes of the intramural tracheal autonomous nervous system (Takimoto et al., 1993).

The apical localization of ET suggests the possibility of secretion towards the airway lumen. In this manner, ET could act through a paracrine mechanism on the airway smooth muscle where ET receptors have been detected (Koseki et al., 1989). In addition to the control of ventilation, other effects such as proliferation of pulmonary epithelial cells, smooth muscle cells, and fibroblasts have been described (Janakidevi et al., 1992; Peacock et al., 1992). Therefore, endothelins could act in the mouse lung as a growth factor during development, as suggested in other species (Giaid et al., 1991b). The ET system exerts a number of pathological functions in the lung. Patients with pulmonary hypertension have increased levels of *ET-1* mRNA and peptides in the endothelial cells of pulmonary arteries (Giaid et al., 1993). They also have higher plasma ET-1 levels, implying increased pulmonary ET-1 production combined with its decreased lung clearance (Stewart et al., 1991). The ET system also influences airway tone, which may have particular importance in the pathogenesis of interstitial lung diseases and asthma. The $ET_A$-selective antagonist BQ-123 attenuates the immediate and late phase of asthmatic response (Uchida et al., 1996). Additionally, patients with asthma have high levels of ET-1 in the bronchoalveolar lavage fluid (Sofia et al., 1993). Progressive pulmonary fibrosis and accumulation of inflammatory cells in mice overexpressing *ET-1* imply a role in pulmonary remodeling (Hocher et al., 2000). Enhanced expression of ET-1 in alveolar macrophages, bronchial epithelium, and alveolar epithelium in interstitial lung disease again suggests a role in pulmonary function (Takeda et al., 1997).

Among the endothelin isopeptides, the pathophysiological role of ET-1 has been extensively studied in the lung. Despite their similar specificity for receptors, little is known regarding the *in vivo* role of ET-2 in the lung. In this chapter, I will present data

suggesting that ET-2 plays an important role in lung morphology and functional maintenance.

## Results

I often observed constitutive *ET-2* deficient mice notably make wheezy sound from the age of one week. As previously reported (Uchide et al., 2002), I determined that *ET-2* mRNA is expressed at a low level in the lung (Figure 2-1A) and exhibited a transient increase at birth (Figure 5-1A). In order to indentify the *ET-2* expressing cell types in the lung, *in situ* hybridization was performed. Despite several attempts, this experiment failed to reveal any *ET-2* expression. I then conducted quantitative RT-PCR with isolated epithelial and mesenchymal cell populations of rat lung (E18.5) to indentify *ET-2* expression. Most of the ET-2 mRNA expression was detected in the epithelium (Figure 5-1B) and the purity of this epithelial fraction was confirmed by quantitative RT-PCR for specific genes known to be restricted to the epithelium (*cytokeratin-18*) and mesenchyme (*vimentin*) (Figure 5-1C). Very low levels of *vimentin* mRNA in the epithelial fraction reflect a minor contamination of fibroblasts.

Histological analysis of the lung in constitutive *ET-2* knockout and adult *ET-2*$^{flox/flox}$; TAM-*Cre* mice displayed abnormalities. Both strains of mutant mice exhibited air-space enlargement by a marked lack of secondary septation with substantial simplification of lung alveolar structure compared with those of wild type controls (Figure 5-2). To examine the physiological and functional relevance of these morphological abnormalities, I first measured blood gases of the *ET-2* deficient mice (Figure 5-3). Partial pressure of carbon dioxide ($pCO_2$) was apparently elevated in both

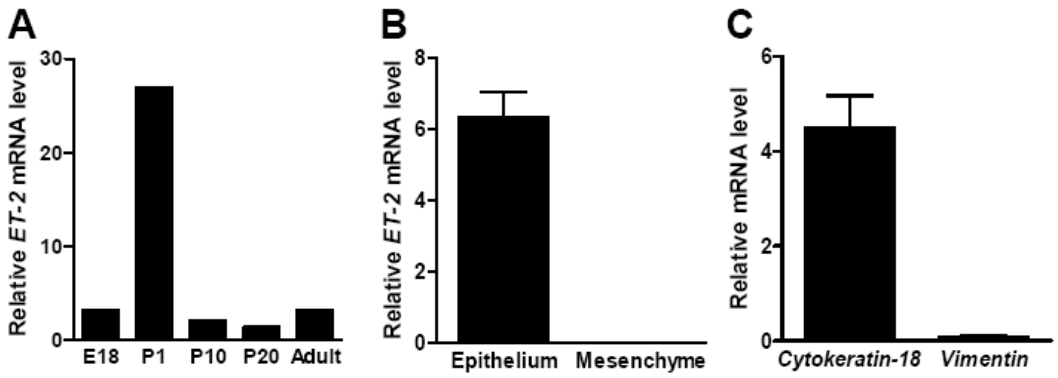


**Figure 5-1 Expression profile of *ET-2* in lung.** Quantitative RT-PCR was performed with mRNA from mouse lung at the designated ages (A) and separated epithelial cells and fibroblast of rat lung (B). Purity of epithelial cells was confirmed by the differential expression of indicated markers (C). Values were normalized by *18s rRNA* (A) or *GAPDH* (B and C) expression. Error bars indicate ± SEM.

constitutive *ET-2* deficient and adult *ET-2*$^{flox/flox}$; TAM-*Cre* mice (Figure 5-3A). As a result of hypercapnia, blood pH was more acidic and bicarbonate level was clearly elevated in both *ET-2* mutant mice (Figure 5-3B and C). The percent of oxygen saturation of arterial hemoglobin (SpO2) of *ET-2* deficient mice was markedly decreased revealing hypoxemia (Figure 5-4A). Consistent with the decrease of $SpO_2$, mRNA synthesis of *Epo (erythropoietin)* in the kidneys was induced (Figure 5-4B). Epo protein levels in serum also significantly increased in *ET-2* deficient mice (Figure 5-4C). This correlated to an increase of plasma hematocrit in mutant mice (Figure 5-4D). As a consequence of altered structure, the lung of *ET-2* null mice had larger total lung capacities compared to wild type controls (Figure 5-5). These results indicate that morphological abnormalities of *ET-2* deficiency develop into hypoxemic hypoxia in the mutant mice.

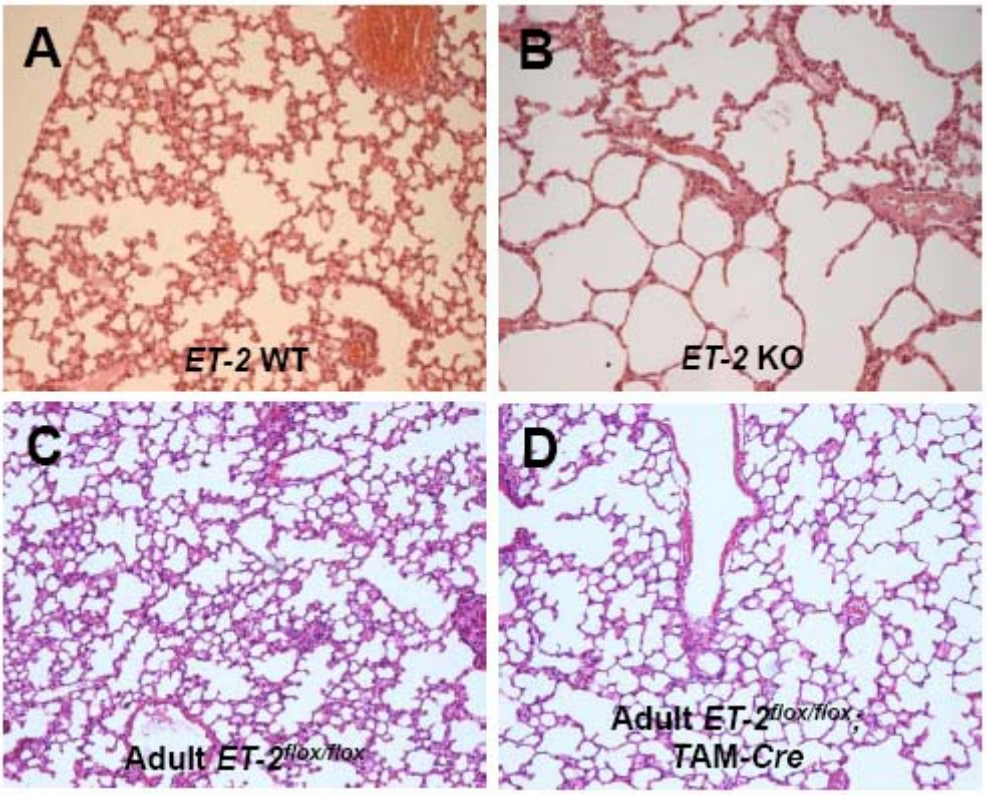


**Figure 5-2 Structural abnormalities of lung in *ET-2* deficient mice.** (A and B) H&E staining was conducted with the lung of wild type control and constitutive *ET-2* deficient mice at P10. (C and D) H&E staining was performed with the lung of adult *ET-2*$^{flox/flox}$ and *ET-2*$^{flox/flox}$; TAM-*Cre* mice at 8 weeks after tamoxifen administration. Magnification: x20

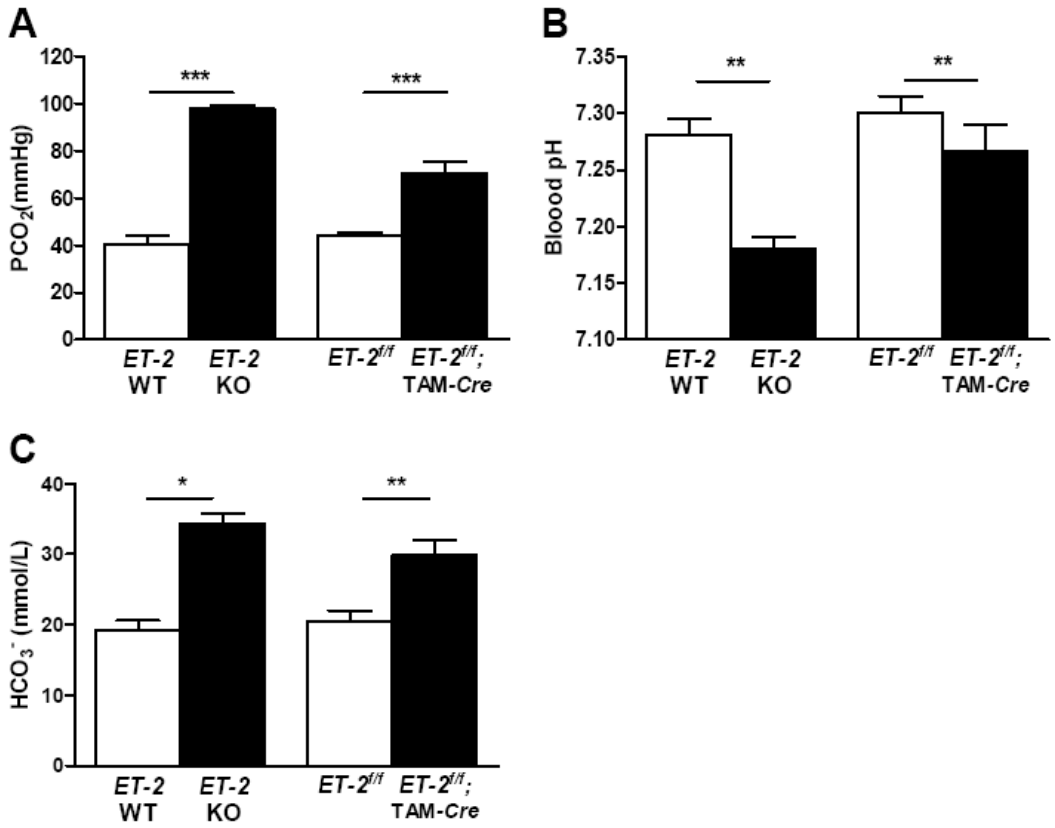


**Figure 5-3 Respiratory acidosis of *ET-2* mutant mice.** Levels of partial pressure of carbon dioxide (A), blood pH (B) and bicarbonate (C) were measured with the blood from constitutive *ET-2* null and adult *ET-2*$^{flox/flox}$; TAM-*Cre* mice and their control littermates (n=6 mice per group). Error bars indicate ± SEM. **p*<0.05, ***p*<0.01, ****p*<0.001

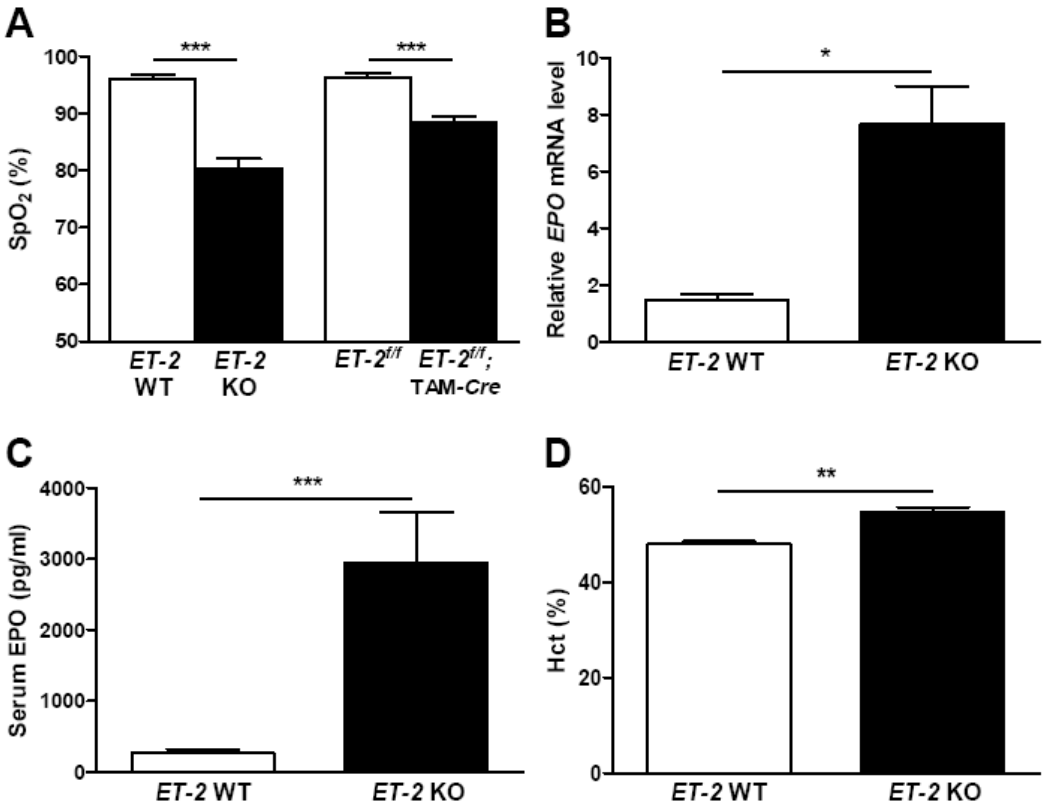


**Figure 5-4 Chronic hypoxemia of *ET-2* null mice.** (A) Comparison of saturated percent oxygen level (SpO2) of 6 week-old constitutive *ET-2* mice rescued by warm environment and adult $ET\text{-}2^{flox/flox}$; TAM-*Cre* mice 8 weeks after *ET-2* inactivation with their wild type controls (n=7 mice per group). Renal *Epo* mRNA level (B), serum Epo level (C) and blood hematocrit level (D) of *ET-2* null mice and wild type controls (n=5 per group). Error bars indicate ± SEM. **p*<0.05, ***p*<0.01, ****p*<0.001

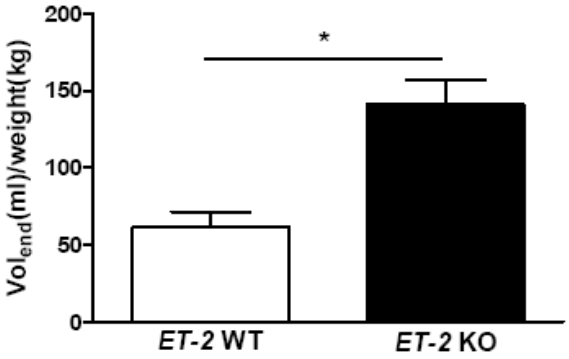


**Figure 5-5 Increased total lung capacity of *ET-2* null mice.** Lung compliance test was performed with *ET-2* null mice and wild type littermates at 3 weeks of age. Error bars indicate ± SEM. *$p$<0.05

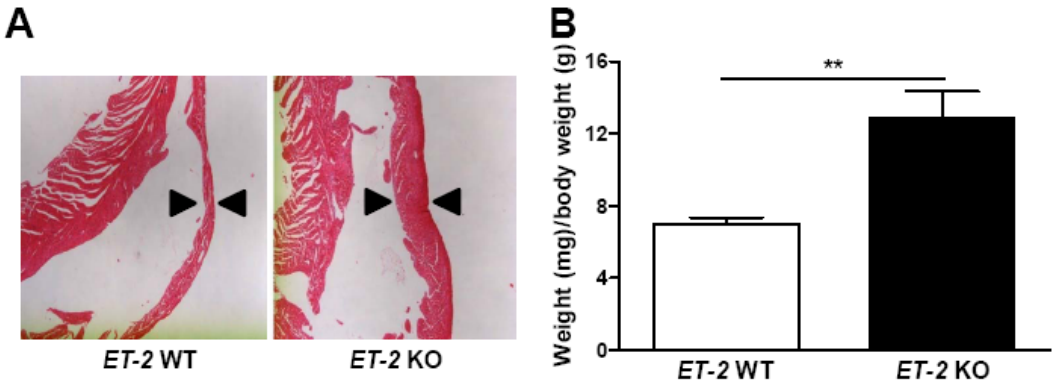


**Figure 5-6 Cardiac hypertrophy of *ET-2* null mice.** (A) Sections of right heart ventricle walls. Arrows indicate the difference in right ventricular wall thickness between *ET-2* null mice and wild type controls. (B) Heart-to-body weight ratio of *ET-2* null mice and wild type controls (n=5 mice per group). Error bars indicate ± SEM. **$p$<0.01

The heart of *ET-2* knockout mice revealed a hypertrophic right ventricle with a more than doubled myocardium thickness (Figure 5-6A). Overall heart-to-body weight ratio also increased in the mutant mice (Figure 5-6B). As previously described (Bostrom et al., 1996), cardiac hypertrophy would be a consequence of defective lung function.

## Discussion and future directions

Direct implications of a defective lung morphology and function by *ET-2* deficiency are elusive at this time. Since nutrition availability is an important determinant of normal lung development, it is highly possible that this abnormal lung phenotype might be a secondary consequence of internal starvation. Indeed, a number of studies have produced evidence that starvation leads to specific changes in the structure and function of the lung (Massaro et al., 2004; Sahebjami and Domino, 1992; Sahebjami and MacGee, 1985). The lung of rats fed a protein-deficient diet for several weeks exhibit similar appearance to the lung of humans with emphysema: elastic fibers appear short, irregular and fewer in number, electron microscopy shows an enlarged air-space, thin irregular and effaced alveolar walls, and an increased number and size of interalveolar pores. Lung compliance was increased and the elastin and protein content remained depleted. Anorexia nervosa of adolescents also leads to changes in lung structure and function, specifically emphysematous changes in the terminal air-spaces.

Generation and analysis of lung specific *ET-2* deficient mice will give us information relating to the possibility that a small amount of pulmonary *ET-2* is critical for the growth regulation and survival of mice. However, although it is clearly detected by quantitative RT-PCR, its expression is too low to be revealed as expressing a subset of cells by *in situ* hybridization in the lung. Instead, the majority of *ET-2* mRNA expression is found in a crude compartment of non-mesenchyme including a large population of epithelial cells and smaller numbers of endocrine and endothelial cells. Lung epithelium is comprised of several specific cell types. The alveolar epithelium is a heterogeneous monolayer consisting of squamous alveolar (type I) and great alveolar (type II) cells.

Respiratory bronchioles are lined by a simple cuboidal epithelium, consisting of ciliated cells and non-ciliated Clara cells. Thus, cell type-specific gene promoters combined with the Cre/loxP system have been available for each lung epithelial cell populations: *surfactant protein C (SP-C)* for type II cells, *Clara cell secretory protein (CCSP)* for Clara cells, and *FOXJ1* for ciliated cells (Bertin et al., 2005; Perl et al., 2002). It is therefore difficult to study the function of the *ET-2* gene lacking its expression in a cell type-specific manner. To overcome this limit, future studies to define the *ET-2* expressing cell types using a reporter mouse strain or using more elaborate methods to separate epithelial cell populations need to be performed first.

## Materials and methods

### Separation of epithelial and mesenchymal cells

Lungs from rat fetuses minced, then digested with trypsin, DNase, and collagenase and plated in cold Hanks' balanced salt solution without calcium or magnesium. After overnight incubation, the cell monolayer was briefly treated with trypsin. Gentle shaking separated epithelial cells from mesenchymal cells.

### Blood gas

Blood was drawn from the retro-orbital plexus into lithium-heparin coated capillary tubes (Instrumentation Laboratory) and analyzed with STAT profile® Critical Care Xpress (Nova Biomedical).

### Blood oxygen saturation

Real-time percent oxygen saturation of arterial hemoglobin was provided by MouseOxTM (STARR Life Sciences Corp.) according to the manufacturer's manual.

**Erythropoietin ELISA**

Erythropoietin protein levels in blood plasma were determined with the Mouse/Rat Erythropoietin Quantikine ELISA Kit (R&D Systems).

**Blood hematocrit**

Hematocrit was measured with blood drawn by retro-orbital bleeding into heparinized hematocrit tubes.

**Total lung capacity**

Total lung capacity was defined as the lung volume of full inflation as judged by visual inspection of the lung that fully occupied the chest cavity. The values were expressed as lung volumes at the final measured point divided by body weight.

**Statistical Analysis**

Values depict the mean ± SEM. Statistical significance was evaluated using two-tailed unpaired student's t tests (GraphPad Prism 5) and considered significantly different $p<0.05$.

## Acknowledgement

Part of this study was conducted in collaboration with Alexa Bramall (Figure 5-4C and Figure 5-5).

# Chapter 6

# Endothelin-2 in Inflammatory Bowel Disease

## Introduction

Inflammatory bowel disease (IBD) is a chronic inflammatory disorder of the intestine that is thought to result from defects in both the barrier function of the intestinal epithelium and the mucosal immune system. The major types of IBD are Crohn's disease (CD) and ulcerative colitis (UC). They are generally considered to be distinct entities defined by the occurrence location and the character of the inflammatory lesion. Although accumulating evidence suggests that genetic factors, bacteria, toxins, antibodies, nonsteroidal anti-inflammatory drugs, smoking, and food additives can lead to the progression of disease, the etiology is still unknown (Angerio et al., 2005; Podolsky, 2002).

A role ET-1 as an inflammatory agent in IBD has been suggested. The level of ET-1/2 peptide in the colonic mucosa was elevated in patients with CD and UC (Murch et al., 1992). In an animal model of IBD, 2,4,6-trinitrobenzene sulfonic acid (TNBS)-induced colitis in rat, it has been shown that two non-selective $ET_{A/B}$ receptor antagonists, bosentan and Ro 48-5695, markedly reduce the tissue injury, particularly if administered prior to the induction of colitis (Gulluoglu et al., 1999; Hogaboam et al., 1996; Padol et al., 2000). Activated leukocytes and several pro-inflammatory cytokines that play an essential role in IBD can substantially increase ET-1 production (Klemm et al., 1995; Sessa et al., 1991). The excessive release of ET-1 promotes vasoconstriction, ischemia,

necrosis, and inflammation. This pathological condition by ET-1 can lead to tissue damage and chronic inflammation associated with IBD (Angerio et al., 2005).

Despite this evidence, the involvement of endothelin in IBD is controversial. The initial study of increased tissue ET-1/2 content in human IBD has not been reproduced, and instead, reduced ET-1/2 levels in ulcerative colitis was reported (Rachmilewitz et al., 1992). The relative expression and role of individual endothelin within the human gastrointestinal tract and IBD have been examined; *ET-2* gene expression is more predominant than *ET-1* in the human colon, although the *ET-2* mRNA level is not significantly changed in human IBD. In the rat TNBS-induced colitis, the gene expression of *ET-1/2* was induced, but unlike in humans, *ET-1* is predominant over *ET-2* gene expression (McCartney et al., 2002).

Dextran sodium sulfate (DSS)-induced colitis is another experimental animal model of human IBD and mimics ulcerative colitis. Mice provided with drinking water containing DSS develop acute colitis accompanied by diarrhea, gross rectal bleeding, and weight loss within 6-10 days. After 5 administration cycles comprised of 5% DSS in drinking water for 7 days, followed by 10 days of regular water, mice developed chronic colitis showing signs of erosion and prominent regeneration of the colonic mucosa including dysplasia, shortening of the large intestine, and frequent formation of lymphoid follicles (Okayasu et al., 1990). The expression of *ET-2* during DSS-induced colitis in mouse was investigated (Takizawa et al., 2005). In contrast to human and rat, *ET-1* and *ET-2* gene expression is similar under normal conditions and colonic ET-2 is induced only during the late stage (day 3-7) of DSS treatment. Thus, it is suggested that increased ET-2 might be secreted from the basement membrane into the lamina propria during

DSS-induced colitis, and that it modulates mucosal immune defense (Takizawa et al., 2005).

Taken together, the role of endothelins in IBD is controversial and a clear role for ET-2 in the pathogenesis of IBD has not been conclusively established. As presented in the results of this chapter, *in situ* hybridization suggests the epithelial-mesenchymal interaction of colonic ET system. *ET-2*$^{flox/flox}$; *villin-Cre* mice are prone to acute DSS-induced colitis as revealed by increased mortality, morbidity, and colonic epithelial injury. Although the results are still in their early stages, it strongly suggests that ET-2 has a protective role in IBD.

## Results

Like its expression in small intestine, colonic *ET-2* is also specifically expressed in epithelial cells and $ET_A$ and $ET_B$ mRNA are localized underneath the lamina propria (Figure 6-1).

Since *ET-2*$^{flox/flox}$; *villin-Cre* mice do not exhibit any abnormalities under normal conditions, *ET-2* could play a role in the pathological condition of the colon by mediating the interaction between epithelial and mesenchymal cells. Therefore, I chose a model of intestinal injury and inflammation by using oral administration of DSS, a sulfated polysaccharide known to be directly toxic to colonic epithelium (Kitajima et al., 1999) to examine the role of colonic ET-2 in IBD. *ET-2*$^{flox/flox}$; *villin-Cre* mice showed severe mortality and morbidity upon administration of DSS (2.5%; wt/vol) in drinking water for

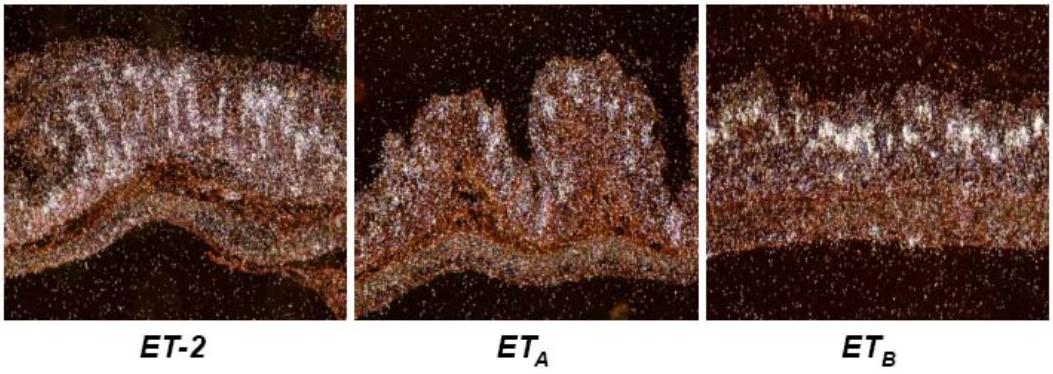


**Figure 6-1 Localization of *ET-2*, $ET_A$ and $ET_B$ mRNA in colon.** *In situ* hybridization was conducted with anti-sense probes of each gene to wild type mice. Representative photographs are shown by dark field images. Magnification: x20

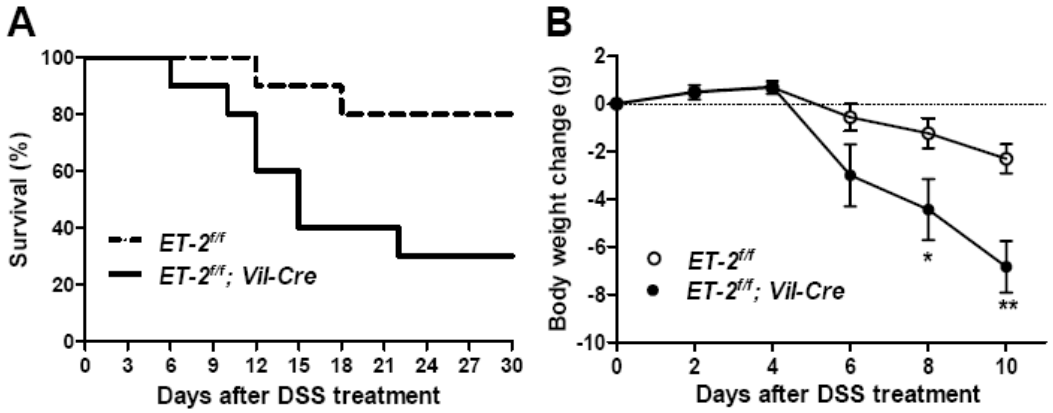


**Figure 6-2 Increased mortality and morbidity in *ET-2$^{flox/flox}$; villin-Cre* mice following DSS administration.** (A) Survival was monitored until day 30 after the start of DSS (n=10 mice per group). Survival ratio is significantly different by log-rank test ($p$<0.0226). (B) Weight change of mice was determined from weight of day 0 (n=10 mice per group). Error bars indicate ± SEM. Error bars indicate ± SEM. *$p$<0.05, **$p$<0.01

seven days (Figure 6-2A). In accordance with the observed difference in survival ratio, *ET-2$^{flox/flox}$*; *villin-Cre* mice showed much more severe weight loss compared to the controls (Figure 6-2B). Thus, the ET-2 signaling pathway appears to be critical for protection against DSS-induced mortality and morbidity. As seen from the comparison of

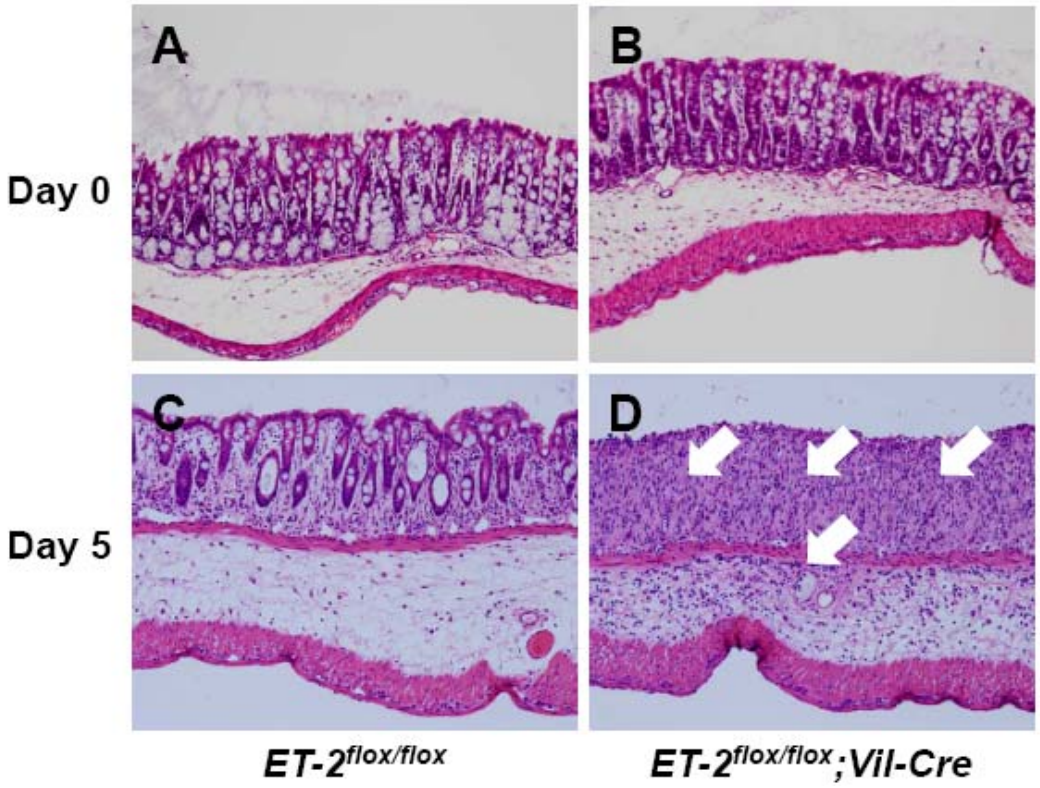


**Figure 6-3 Colonic epithelial damage in *ET-2*$^{flox/flox}$*; villin-Cre* following DSS administration.** Representative photographs are taken colons from *ET-2*$^{flox/flox}$ (A and C) and *ET-2*$^{flox/flox}$; *villin-Cre* (B and D) mice at day 0 and 5 of DSS administration. Magnification; x20

representative photographs taken on day 5 post-DSS treatment, *ET-2*$^{flox/flox}$; *villin-Cre* mice colons show severe and extensive denudation of the surface epithelium (erosions), mucodepletion of glands, and increased number of infiltrating leukocytes compared to wild type control mice (Figure 6-3).

Since expression of endothelins in IBD models is not consistent between species and IBD-inducing agents (McCartney et al., 2002; Murch et al., 1992), I examined these parameters in the DSS-treated colon (Figure 6-4). In contrast to TNBS-induced colitis in

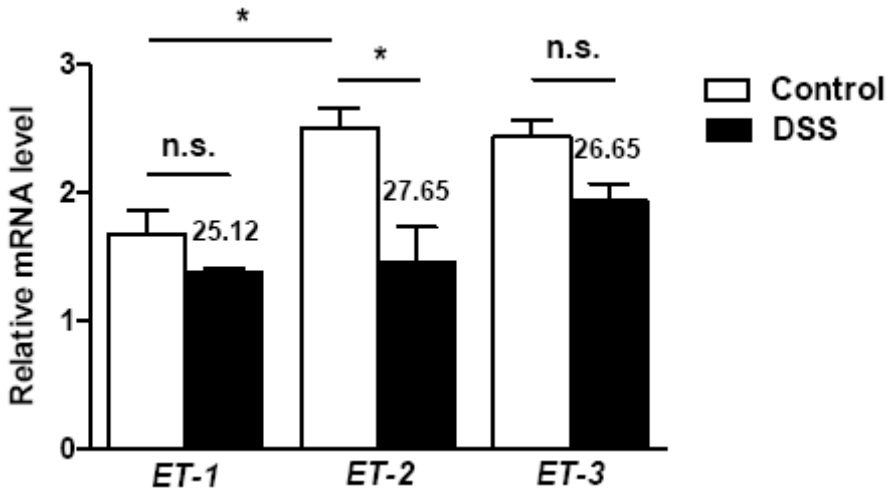


**Figure 6-4 Expression of endothelins in DSS-treated colon.** Quantitative RT-PCR analysis of colonic *ET* genes from wild type mice treated with the indicated agent. (n=4 mice per group). Numbers indicate the $C_T$ value. Values were normalized by *18s rRNA* expression. Error bars indicate ± SEM. *$p$<0.05

rat, *ET-1* and *ET-2* gene expression is not induced. Rather *ET-2* expression is significantly reduced. In the mouse colon, *ET-2* gene expression is predominant over *ET-1*.

## Discussion and future directions

In this chapter, I propose that ET-2 protects mice from DSS-induced epithelial injury and inflammation by using a mouse model with genetically inactivated ET-2 in intestinal epithelium. Contrary to previous reports indicating a pro-inflammatory role of endothelins in IBD (Angerio et al., 2005; Takizawa et al., 2005), the loss of ET-2 made mice more susceptible to DSS-induced IBD. Specially, Takizawa *et al.* showed that colonic *ET-2* increased upon the administration of DSS and suggested that increased ET-2 might be secreted from the basement of epithelial cells into the lamina propria.

However, they did immunohistochemistry using an anti-ET-2 antibody and showed the change of intensity which is an inadequate quantitative measure. Since ET-2 is immunologically indistinguishable from ET-1, such antibody based-techniques do not discriminate between ET-1 and ET-2 and therefore, their results are of questionable significance. I examined the change of *ET-2* mRNA expression by DSS-induced colitis and find that it is reduced, not increased, following DSS treatment. Further experiments are required to address this question, including the determination of *ET-2* mRNA levels in isolated epithelial and mesenchymal cells from DSS-treated mice.

The potential pathophysiological role of endothelins in IBD and the endothelin genes expression profiles in colonic mucosa are different among humans, rats, and mice: in humans and mice, ET-2 is more abundant than ET-1, whereas in rats more ET-2 is present than ET-1. Although studies involving ET receptor antagonists and reported changes in ET-1 expression suggest the involvement of the ET system in the pathogenesis of IBD in rats, it is uncertain whether these changes occur in humans. Furthermore, my study revealed a protective role of ET-2 in the murine IBD model. I speculate that the differences may arise from species differences or depend on unidentified physiological conditions. Although both TNBS and DSS are non specific agents, it may well be that mucosal damage in TNBS colitis represents an acute vascular injury rather than an ongoing immune-mediated inflammation. Therefore, the efficacy of ET receptor antagonists in the acute model of rat TNBS colitis might not be an indicator of pathological roles of endothelins in IBD.

Protection from intestinal injury is determined by many factors such as the balance of proliferation and differentiation along the crypt axis (Booth and Potten, 2001)

and the production of mediators involved in protecting epithelial cells from initial injury (Dignass, 2001). It is entirely possible that ET-2 might be involved in the regulation of the mucosal defense mechanism against aberrant immune response. Future studies should focus on evaluating the colonic epithelial homeostasis in *ET-2*$^{flox/flox}$; *villin-Cre* mice. It might be also instructive to examine the induction of several factors which are involved in cytoprotection, tissue repair, and angiogenesis.

## Materials and methods

### Induction of DSS colitis

Mice received 2.5% (wt/vol) DSS (Fluka Biochemica), *ad libitum*, in their drinking water for seven days, then switched to regular drinking water. The amount of DSS water was recorded and no differences in intake between strains were observed.

### Survival study

Mice were followed for 30 days post start of DSS-treatment. Mice were weighed every other day for the determination of weight change. Animals were monitored for rectal bleeding, diarrhea, and general signs of morbidity, including hunched posture and failure to groom.

### Statistical Analysis

Values depict the mean ± SEM. Statistical significance was evaluated using two-tailed unpaired student's *t* tests (GraphPad Prism 5) and considered significantly different $p<0.05$.

# Chapter 7

# A Comprehensive View of ET-2 Action

## Feasible Scenarios one, two and three

In this report, starvation, hypothermia, and lung dysfunction by *ET-2* deficiency are proposed as possible independent underlying mechanisms to the growth retardation and early lethality of postnatal mice. Since metabolic rate, body temperature and breathing regulation are physiologically interrelated, it is highly possible that one of the abnormalities alters the physiological regulation of the others. First, starvation might be the primary abnormality caused by the absence of ET-2 (Figure 7-scenario1). Under the stressful environment imposed by reduced food availability and a low ambient temperature, small mammals including mice can enter torpor to conserve energy by dropping their body temperature to near ambient temperature levels (Gavrilova et al., 1999). Since nutrition availability is an important determinant of normal lung development, chronic nutrient restriction affects structural and functional alteration in the lung (Das, 1984; Maritz et al., 2005). Lungs of rat starved soon after birth exhibit less alveolar development and enlarged air spaces consistent with the phenotype in *ET-2* deficient mice (Das, 1984). Starvation or calorie restriction in adult animals including humans can also lead to structural and functional changes in the lung (Massaro et al., 2004). These studies support the idea that hypothermia and lung dysfunction might be secondary effects of starvation due to ET-2 deficiency.

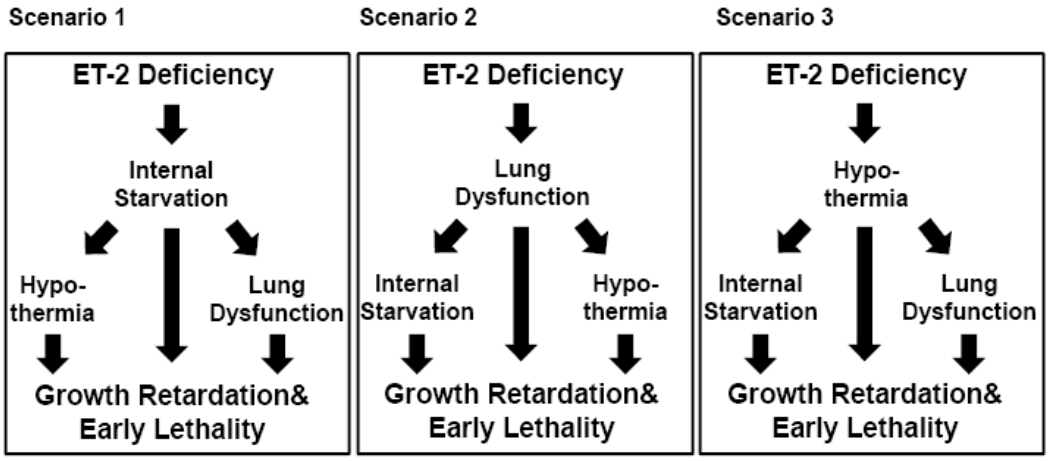


**Figure 7 Possible underlying mechanisms of *ET-2* deficiency.**

The other possible model is that lung dysfunction is the primary abnormality underlying the phenotype of *ET-2* deficient mice (Figure 7-Scenario 2). PDGF-A signaling is a critical event in lung alveolar myofibroblast development and alveogenesis. The core fucosylation (α1,6-fucosylation) of glycoproteins of TGF-β1 receptors is crucial for prevention of developmental and progressive/destructive emphysema. The null mice of *PDGF-A* and *α1,6-fucosyltransferase* displayed the air-space enlargement with the failure of alveolar septation in lung accompanying by postnatal growth retardation and early lethality (Bostrom et al., 1996; Wang et al., 2005). Malnutrition and weight loss are common problems in chronic obstructive pulmonary disease (COPD)(Wilson et al., 1990). Significant loss of body weight is also observed in mouse models exposed to hypoxia (Kozak et al., 2006). Many studies have reported that hypoxia evokes a regulated decrease in body temperature (i.e. anapyrexia) as a compensatory response to decreased oxygen consumption (Wood, 1991). Chronic hypercapnia can impair thermoregulation by increasing sweating and reducing shivering in humans (Schaefer et al., 1975). This

evidence supports the alternative hypothesis that an internally starved state and hypothermia might be the consequence of lung dysfunction.

Lastly, several indications suggest that profound hypothermia of *ET-2* null mice is not merely a byproduct of starvation and lung dysfunction, but might be an independent contributor to the phenotype (Figure 7- Scenario 3). My results showing that *ET-2* null mice reared in warm conditions lived longer than littermate null mice housed at room temperature (Figure 5F) strongly suggests that abnormal thermoregulation may play a critical role in the premature death of *ET-2* null mice. In a cold environment, *ET-2* null mice are unable to maintain body temperature. Although the expression of pancreatic lipases outside the pancreas is hallmark of torpor (Andrews et al., 1998; Zhang et al., 2006), paradoxically, it was rather decreased in liver of *ET-2* null mice suggesting hypothermia might not be the consequence of torpor (Figure 4-10). However, these results deserve cautious interpretation. ET-2 appears to be located in non thermoregulatory regions of the central nervous system. Moreover, genetic analysis shows that neuronal ET-2 does not affect central thermoregulation. This model needs to be explored further for an alternative explanation for the thermoregulatory role of ET-2.

## A home for ET-2

One obviously important question that is not addressed in this study is which ET receptor ET-2 is engaging. $ET_B$ knockout mice do not display the grow retardation or early lethality seen in *ET-2* deficient mice. $ET_A$ deficient mice die at birth with severe craniofacial malformations and cardiac defects. Therefore, it is most likely that ET-2 is either acting exclusively via $ET_A$ or redundantly via $ET_A$ and $ET_B$ to exert its effects.

*$ET_A^{flox/flox}$;* TAM-*Cre* mice can circumvent the developmental defects of $ET_A$ loss. Similar phenotypes between postnatal *$ET_A^{flox/flox}$;* TAM-*Cre* mice and *ET-2* deficient mice might be revealed. However, this also might produce other additional defects due to the absence of ET-1 signaling through $ET_A$. In addition, evaluation of *$ET_A^{flox/flox}$; $ET_B^{flox/flox}$* mice would be useful to address the possibility that both $ET_A$ and $ET_B$ would be physiological partners of ET-2. When we inactivate $ET_B$ by a tissue specific manner in the time and tissue specific $ET_A$ rescued background, the phenotype of *ET-2* deficient mice might be revealed. However, information relating to the site for essential ET-2 action should be obtained first. Despite the potential pitfalls and lack of information available, these experiments might give us further insight into the endothelin signaling pathways.

## Future direction

Low levels of *ET-2* expression are clearly detected in the lung. I observed that the expression level is markedly and transiently increased immediately after birth. This result is consistent with the previous report showing a sharp increase of *ET-2* expression in the lung within 3 to 6 hours after birth (Uchide et al., 2002) and strongly implies that the beginning of respiration induces an increase of *ET-2* expression. In retina, ET-2 is localized to photoreceptors and is significantly induced by the models of photoreceptor disease or injury (Rattner and Nathans, 2005). ET-2 is specifically and temporarily expressed in the granulose cells of the ovary immediately before ovulation as well (Ko et al., 2006). Given the expression in the lung, these results strongly suggest that physiological or pathological changes might stimulate the increase of *ET-2* expression within a very limited time period. Immunological similarity with ET-1 and temporal

expression pattern may hinder the identification of *ET-2* expressing sites and time points. Thus, the production of a reporter mouse strain driven by the ET-2 promoter would be an invaluable tool for visualizing unknown *ET-2* expressing tissues and cells, and for understanding ET-2 function.

# APPENDIX A

## Primer sequences

| Gene | | Sequence (5'⟶3') |
|---|---|---|
| *ET-2* | F | TCTGCCACCTGGACATCATC |
| | R | GAGCACTCACAACGCTTTGG |
| *18s rRNA* | F | ACCGCAGCTAGGAATAATGGA |
| | R | GCCTCAGTTCCGAAAACCA |
| *PEPCK1* | F | CACCATCACCTCCTGGAAGA |
| | R | GGGTGCAGAATCTCGAGTTG |
| *PDK4* | F | CAAAGACGGGAAACCCAAGCC |
| | R | CGCAGAGCATCTTTGCACAC |
| *HMGCS2* | F | CCGTATGGGCTTCTGTTCAG |
| | R | AGCTTTGTGCGTTCCATCAG |
| *FGF 21* | F | CCTCTAGGTTTCGCCAACAG |
| | R | AAGCTGCAGGCCTCAGGAT |
| *UCP-1* | F | AAGCTGTGCGATGTCCATGT |
| | R | AAGCCACAAACCCTTTGAAAA |
| *FATP4* | F | TTGCAAGTCCCATCAGCAACT |
| | R | GCATACAGAGGCAGCTCCTTTT |
| *I-FABP* | F | ACTGACAATCACACAGGATGGAA |
| | R | CCGAGCTCAAACACAACATCA |
| *L-FABP* | F | CCAGGAGAACTTTGAGCCATTC |
| | R | TGTCCTTCCCTTTCTGGATGA |
| *I-BABP* | F | CAAGGCTACCGTGAAGATGGA |
| | R | CCCACGACCTCCGAAGTCT |
| *ABST* | F | TGTCTGTCCCCCAAATGCA |
| | R | TGCATTGAAGTTGCTCTCAGGTA |
| *FGF 15* | F | GAGGACCAAAACGAACGAAATT |
| | R | ACGTCCTTGATGGCAATCG |
| *SR-B1* | F | TCCCCATGAACTGTTCTGTGAA |
| | R | TGCCCGATGCCCTTGA |
| *Glut2* | F | TTCATGTCGGTGGGACTTGT |
| | R | TCATGCTCACGTAACTCATCCA |
| *Glut5* | F | GGGCCGTCAATGTGTTCAT |
| | R | CCGACGAGGAGTAGGAATCG |
| *SGLT1* | F | GGCAGCTGTAATTTACACAGATAC |
| | R | GAAAGCAAACCCAGTCAGGATA |

| Gene | | Sequence (5'⟶3') |
|---|---|---|
| *Atp1a1* | F | GGGTTGGACGAGACAAGTATGAG |
| | R | TTGGCCTTTTTGCCCTTTT |
| *Atp1b1* | F | TTTCGAGGACTGTGGCAATG |
| | R | CTCCTCGTTCGTGATTGATGTC |
| *Atp1b2* | F | GAATGTTGAATGCCGCATCA |
| | R | CACGGCCAGCGAACTTG |
| *Atp1b3* | F | AGCCTGGCCGAGTGGAA |
| | R | GGTGCGCCCCAGAAACT |
| *Suc/Iso* | F | AACCTCGGCAAAACCTTTATAGTT |
| | R | TGCCTACATCTGGATAACAAGTGA |
| *Lactase* | F | TGTATGTCCTCTTCGCTCTTGTG |
| | R | GGAGCGCTTGCAGTAGTATTTGTA |
| *Dpp4* | F | GAAGACACCGTGGAAGGTTCT T |
| | R | TTGGCACGGTGATGATGGT |
| *Pep T1* | F | CCACGGCCATTTACCATACG |
| | R | TGCGATCAGAGCTCCAAGAA |
| *NHE1* | F | TGTGACTTCAGACCGCATATTG |
| | R | GCCGTTGCCGGGTTTT |
| *NHE2* | F | CCATCCAGACCGTAGACGTGTT |
| | R | AATCAGCACCCCGC AATT |
| *Atp4a* | F | CGGCGGACACCACAGAAG |
| | R | CAGCGCTCGCCATGTCT |
| *Atp4b* | F | TGCAGGAGAAGAAGTCATGCA |
| | R | GTCCGGGTTCCAACAGTAGTG |
| *Pgc* | F | TAGGAGCCCAGGAAGGAGAGT |
| | R | GTGAGGGTAGGCAGGCTACTG |
| *Pepf* | F | CGAAAGGATCGGTCACACAA |
| | R | GGGTCTGATGGGTCATCCAT |
| *Pga5* | F | CGAAAGGATCGGTCACACAA |
| | R | GGGTCTGATGGGTCATCCAT |
| *Chymosin* | F | CCCATCCAAGTCCATCACCTT |
| | R | GCCCTCCATTCTACCAGTACCA |

# BIBLIOGRAPHY

Ahn, D., Ge, Y., Stricklett, P.K., Gill, P., Taylor, D., Hughes, A.K., Yanagisawa, M., Miller, L., Nelson, R.D., and Kohan, D.E. (2004). Collecting duct-specific knockout of endothelin-1 causes hypertension and sodium retention. J Clin Invest *114*, 504-511.

Ambar, I., Kloog, Y., Schvartz, I., Hazum, E., and Sokolovsky, M. (1989). Competitive interaction between endothelin and sarafotoxin: Binding and phosphoinositides hydrolysis in rat atria and brain. Biochem Biophys Res Commun *158*, 195-201.

Ameen, V.Z., and Powell, G.K. (1985). A simple spectrophotometric method for quantitative fecal carbohydrate measurement. Clin Chim Acta *152*, 3-9.

Andrews, M.T., Squire, T.L., Bowen, C.M., and Rollins, M.B. (1998). Low-temperature carbon utilization is regulated by novel gene activity in the heart of a hibernating mammal. Proc Natl Acad Sci U S A *95*, 8392-8397.

Angerio, A.D., Bufalino, D., Bresnick, M., Bell, C., and Brill, S. (2005). Inflammatory bowel disease and endothelin-1: a review. Crit Care Nurs Q *28*, 208-213.

Arai, H., Hori, S., Aramori, I., Ohkubo, H., and Nakanishi, S. (1990). Cloning and expression of a cDNA encoding an endothelin receptor. Nature *348*, 730-732.

Barton, M., and Yanagisawa, M. (2008). Endothelin: 20 years from discovery to therapy. Can J Physiol Pharmacol *86*, 485-498.

Baynash, A.G., Hosoda, K., Giaid, A., Richardson, J.A., Emoto, N., Hammer, R.E., and Yanagisawa, M. (1994). Interaction of endothelin-3 with endothelin-B receptor is essential for development of epidermal melanocytes and enteric neurons. Cell *79*, 1277-1285.

Bertin, G., Poujeol, C., Rubera, I., Poujeol, P., and Tauc, M. (2005). In vivo Cre/loxP mediated recombination in mouse Clara cells. Transgenic Res *14*, 645-654.

Bloch, K.D., Eddy, R.L., Shows, T.B., and Quertermous, T. (1989). cDNA cloning and chromosomal assignment of the gene encoding endothelin 3. J Biol Chem *264*, 18156-18161.

Bloch, K.D., Hong, C.C., Eddy, R.L., Shows, T.B., and Quertermous, T. (1991). cDNA cloning and chromosomal assignment of the endothelin 2 gene: vasoactive intestinal contractor peptide is rat endothelin 2. Genomics *10*, 236-242.

Booth, D., and Potten, C.S. (2001). Protection against mucosal injury by growth factors and cytokines. J Natl Cancer Inst Monogr, 16-20.

Bostrom, H., Willetts, K., Pekny, M., Leveen, P., Lindahl, P., Hedstrand, H., Pekna, M., Hellstrom, M., Gebre-Medhin, S., Schalling, M., *et al.* (1996). PDGF-A signaling is a critical event in lung alveolar myofibroblast development and alveogenesis. Cell *85*, 863-873.

Carey, H.V., Andrews, M.T., and Martin, S.L. (2003). Mammalian hibernation: cellular and molecular responses to depressed metabolism and low temperature. Physiol Rev *83*, 1153-1181.

Chew, B.H., Weaver, D.F., and Gross, P.M. (1995). Dose-related potent brain stimulation by the neuropeptide endothelin-1 after intraventricular administration in conscious rats. Pharmacol Biochem Behav *51*, 37-47.

Clerk, A., and Sugden, P.H. (1997). Regulation of phospholipases C and D in rat ventricular myocytes: stimulation by endothelin-1, bradykinin and phenylephrine. J Mol Cell Cardiol *29*, 1593-1604.

Clouthier, D.E., Hosoda, K., Richardson, J.A., Williams, S.C., Yanagisawa, H., Kuwaki, T., Kumada, M., Hammer, R.E., and Yanagisawa, M. (1998). Cranial and cardiac neural crest defects in endothelin-A receptor-deficient mice. Development *125*, 813-824.

D'Agostino, D., Cordle, R.A., Kullman, J., Erlanson-Albertsson, C., Muglia, L.J., and Lowe, M.E. (2002). Decreased postnatal survival and altered body weight regulation in procolipase-deficient mice. J Biol Chem *277*, 7170-7177.

D'Amico, M., Berrino, L., Maione, S., Filippelli, A., de Novellis, V., and Rossi, F. (1996). Endothelin-1 in periaqueductal gray area of mice induces analgesia via glutamatergic receptors. Pain *65*, 205-209.

Dark, J., Miller, D.R., and Zucker, I. (1994). Reduced glucose availability induces torpor in Siberian hamsters. Am J Physiol *267*, R496-501.

Das, R.M. (1984). The effects of intermittent starvation on lung development in suckling rats. Am J Pathol *117*, 326-332.

Davenport, A.P., Hoskins, S.L., Kuc, R.E., and Plumpton, C. (1996). Differential distribution of endothelin peptides and receptors in human adrenal gland. Histochem J *28*, 779-789.

de la Monte, S.M., Quertermous, T., Hong, C.C., and Bloch, K.D. (1995). Regional and maturation-associated expression of endothelin 2 in rat gastrointestinal tract. J Histochem Cytochem *43*, 203-209.

De Mey, J.G., and Vanhoutte, P.M. (1981). Role of the intima in cholinergic and purinergic relaxation of isolated canine femoral arteries. J Physiol *316*, 347-355.

Deng, A.Y. (1997). Structure and organization of the rat endothelin-2 gene. Mamm Genome *8*, 157.

Dignass, A.U. (2001). Mechanisms and modulation of intestinal epithelial repair. Inflamm Bowel Dis *7*, 68-77.

Dreshaj, I.A., Miller, M.J., Ernsberger, P., Haxhiu-Poskurica, B., Martin, R.J., and Haxhiu, M.A. (1995). Central effects of endothelin on respiratory output during development. J Appl Physiol *79*, 420-427.

Emoto, N., and Yanagisawa, M. (1995). Endothelin-converting enzyme-2 is a membrane-bound, phosphoramidon-sensitive metalloprotease with acidic pH optimum. J Biol Chem *270*, 15262-15268.

Fabricio, A.S., Rae, G.A., D'Orleans-Juste, P., and Souza, G.E. (2005). Endothelin-1 as a central mediator of LPS-induced fever in rats. Brain Res *1066*, 92-100.

Fabricio, A.S., Silva, C.A., Rae, G.A., D'Orleans-Juste, P., and Souza, G.E. (1998). Essential role for endothelin ET(B) receptors in fever induced by LPS (E. coli) in rats. Br J Pharmacol *125*, 542-548.

Folch, J., Lees, M., and Sloane Stanley, G.H. (1957). A simple method for the isolation and purification of total lipides from animal tissues. J Biol Chem *226*, 497-509.

Furchgott, R.F., and Zawadzki, J.V. (1980). The obligatory role of endothelial cells in the relaxation of arterial smooth muscle by acetylcholine. Nature *288*, 373-376.

Gavrilova, O., Leon, L.R., Marcus-Samuels, B., Mason, M.M., Castle, A.L., Refetoff, S., Vinson, C., and Reitman, M.L. (1999). Torpor in mice is induced by both leptin-dependent and -independent mechanisms. Proc Natl Acad Sci U S A *96*, 14623-14628.

Ge, Y., Bagnall, A., Stricklett, P.K., Strait, K., Webb, D.J., Kotelevtsev, Y., and Kohan, D.E. (2006). Collecting duct-specific knockout of the endothelin B receptor causes hypertension and sodium retention. Am J Physiol Renal Physiol *291*, F1274-1280.

Ge, Y., Bagnall, A., Stricklett, P.K., Webb, D., Kotelevtsev, Y., and Kohan, D.E. (2008). Combined knockout of collecting duct endothelin A and B receptors causes hypertension and sodium retention. Am J Physiol Renal Physiol *295*, F1635-1640.

Ge, Y., Stricklett, P.K., Hughes, A.K., Yanagisawa, M., and Kohan, D.E. (2005). Collecting duct-specific knockout of the endothelin A receptor alters renal vasopressin responsiveness, but not sodium excretion or blood pressure. Am J Physiol Renal Physiol *289*, F692-698.

Geiser, F. (2004). Metabolic rate and body temperature reduction during hibernation and daily torpor. Annu Rev Physiol *66*, 239-274.

Giaid, A., Gibson, S.J., Herrero, M.T., Gentleman, S., Legon, S., Yanagisawa, M., Masaki, T., Ibrahim, N.B., Roberts, G.W., Rossi, M.L., *et al.* (1991a). Topographical localisation of endothelin mRNA and peptide immunoreactivity in neurones of the human brain. Histochemistry *95*, 303-314.

Giaid, A., Polak, J.M., Gaitonde, V., Hamid, Q.A., Moscoso, G., Legon, S., Uwanogho, D., Roncalli, M., Shinmi, O., Sawamura, T., *et al.* (1991b). Distribution of endothelin-like immunoreactivity and mRNA in the developing and adult human lung. Am J Respir Cell Mol Biol *4*, 50-58.

Giaid, A., Yanagisawa, M., Langleben, D., Michel, R.P., Levy, R., Shennib, H., Kimura, S., Masaki, T., Duguid, W.P., and Stewart, D.J. (1993). Expression of endothelin-1 in the lungs of patients with pulmonary hypertension. N Engl J Med *328*, 1732-1739.

Gillespie, M.N., Owasoyo, J.O., McMurtry, I.F., and O'Brien, R.F. (1986). Sustained coronary vasoconstriction provoked by a peptidergic substance released from endothelial cells in culture. J Pharmacol Exp Ther *236*, 339-343.

Girard, J., Ferre, P., Pegorier, J.P., and Duee, P.H. (1992). Adaptations of glucose and fatty acid metabolism during perinatal period and suckling-weaning transition. Physiol Rev *72*, 507-562.

Gomes, J.R., and Alvares, E.P. (1998). Cell proliferation and migration in the jejunum of suckling rats submitted to progressive fasting. Braz J Med Biol Res *31*, 281-288.

Grimshaw, M.J., Hagemann, T., Ayhan, A., Gillett, C.E., Binder, C., and Balkwill, F.R. (2004). A role for endothelin-2 and its receptors in breast tumor cell invasion. Cancer Res *64*, 2461-2468.

Grimshaw, M.J., Naylor, S., and Balkwill, F.R. (2002a). Endothelin-2 is a hypoxia-induced autocrine survival factor for breast tumor cells. Mol Cancer Ther *1*, 1273-1281.

Grimshaw, M.J., Wilson, J.L., and Balkwill, F.R. (2002b). Endothelin-2 is a macrophage chemoattractant: implications for macrophage distribution in tumors. Eur J Immunol *32*, 2393-2400.

Guembe, L., and Villaro, A.C. (2001). Immunohistochemical mapping of endothelin in the developing and adult mouse lung. J Histochem Cytochem *49*, 1301-1309.

Guerra, C., Roncero, C., Porras, A., Fernandez, M., and Benito, M. (1996). Triiodothyronine induces the transcription of the uncoupling protein gene and stabilizes its mRNA in fetal rat brown adipocyte primary cultures. J Biol Chem *271*, 2076-2081.

Gulati, A., Rebello, S., and Kumar, A. (1997). Role of sympathetic nervous system in cardiovascular effects of centrally administered endothelin-1 in rats. Am J Physiol *273*, H1177-1186.

Gulluoglu, B.M., Kurtel, H., Gulluoglu, M.G., Yegen, C., Aktan, A.O., Dizdaroglu, F., Yalin, R., and Yegen, B.C. (1999). Role of endothelins in trinitrobenzene sulfonic acid-induced colitis in rats. Digestion *60*, 484-492.

Hauck, A.L., Swanson, K.S., Kenis, P.J., Leckband, D.E., Gaskins, H.R., and Schook, L.B. (2005). Twists and turns in the development and maintenance of the mammalian small intestine epithelium. Birth Defects Res C Embryo Today *75*, 58-71.

Hayashi, S., and McMahon, A.P. (2002). Efficient recombination in diverse tissues by a tamoxifen-inducible form of Cre: a tool for temporally regulated gene activation/inactivation in the mouse. Dev Biol *244*, 305-318.

Hickey, K.A., Rubanyi, G., Paul, R.J., and Highsmith, R.F. (1985). Characterization of a coronary vasoconstrictor produced by cultured endothelial cells. Am J Physiol *248*, C550-556.

Hinson, J.P., Kapas, S., Teja, R., and Vinson, G.P. (1991). Effect of the endothelins on aldosterone secretion by rat zona glomerulosa cells in vitro. J Steroid Biochem Mol Biol *40*, 437-439.

Hocher, B., Schwarz, A., Fagan, K.A., Thone-Reineke, C., El-Hag, K., Kusserow, H., Elitok, S., Bauer, C., Neumayer, H.H., Rodman, D.M., *et al.* (2000). Pulmonary fibrosis and chronic lung inflammation in ET-1 transgenic mice. Am J Respir Cell Mol Biol *23*, 19-26.

Hogaboam, C.M., Muller, M.J., Collins, S.M., and Hunt, R.H. (1996). An orally active non-selective endothelin receptor antagonist, bosentan, markedly reduces injury in a rat model of colitis. Eur J Pharmacol *309*, 261-269.

Hosoda, K., Hammer, R.E., Richardson, J.A., Baynash, A.G., Cheung, J.C., Giaid, A., and Yanagisawa, M. (1994). Targeted and natural (piebald-lethal) mutations of endothelin-B receptor gene produce megacolon associated with spotted coat color in mice. Cell *79*, 1267-1276.

Inagaki, T., Dutchak, P., Zhao, G., Ding, X., Gautron, L., Parameswara, V., Li, Y., Goetz, R., Mohammadi, M., Esser, V., *et al.* (2007). Endocrine regulation of the fasting response by PPARalpha-mediated induction of fibroblast growth factor 21. Cell Metab *5*, 415-425.

Inoue, A., Yanagisawa, M., Kimura, S., Kasuya, Y., Miyauchi, T., Goto, K., and Masaki, T. (1989). The human endothelin family: three structurally and pharmacologically distinct isopeptides predicted by three separate genes. Proc Natl Acad Sci U S A *86*, 2863-2867.

Ishibashi, S., Brown, M.S., Goldstein, J.L., Gerard, R.D., Hammer, R.E., and Herz, J. (1993). Hypercholesterolemia in low density lipoprotein receptor knockout mice and its reversal by adenovirus-mediated gene delivery. J Clin Invest *92*, 883-893.

Janakidevi, K., Fisher, M.A., Del Vecchio, P.J., Tiruppathi, C., Figge, J., and Malik, A.B. (1992). Endothelin-1 stimulates DNA synthesis and proliferation of pulmonary artery smooth muscle cells. Am J Physiol *263*, C1295-1301.

Kawanabe, Y., and Nauli, S.M. (2005). Involvement of extracellular Ca2+ influx through voltage-independent Ca2+ channels in endothelin-1 function. Cell Signal *17*, 911-916.

Kedzierski, R.M., Grayburn, P.A., Kisanuki, Y.Y., Williams, C.S., Hammer, R.E., Richardson, J.A., Schneider, M.D., and Yanagisawa, M. (2003). Cardiomyocyte-specific endothelin A receptor knockout mice have normal cardiac function and an unaltered hypertrophic response to angiotensin II and isoproterenol. Mol Cell Biol *23*, 8226-8232.

Kedzierski, R.M., and Yanagisawa, M. (2001). Endothelin system: the double-edged sword in health and disease. Annu Rev Pharmacol Toxicol *41*, 851-876.

Kitajima, S., Takuma, S., and Morimoto, M. (1999). Changes in colonic mucosal permeability in mouse colitis induced with dextran sulfate sodium. Exp Anim *48*, 137-143.

Klemm, P., Warner, T.D., Hohlfeld, T., Corder, R., and Vane, J.R. (1995). Endothelin 1 mediates ex vivo coronary vasoconstriction caused by exogenous and endogenous cytokines. Proc Natl Acad Sci U S A *92*, 2691-2695.

Ko, C., Gieske, M.C., Al-Alem, L., Hahn, Y., Su, W., Gong, M.C., Iglarz, M., and Koo, Y. (2006). Endothelin-2 in ovarian follicle rupture. Endocrinology *147*, 1770-1779.

Koong, A.C., Denko, N.C., Hudson, K.M., Schindler, C., Swiersz, L., Koch, C., Evans, S., Ibrahim, H., Le, Q.T., Terris, D.J., *et al.* (2000). Candidate genes for the hypoxic tumor phenotype. Cancer Res *60*, 883-887.

Koseki, C., Imai, M., Hirata, Y., Yanagisawa, M., and Masaki, T. (1989). Autoradiographic distribution in rat tissues of binding sites for endothelin: a neuropeptide? Am J Physiol *256*, R858-866.

Kozak, W., Wrotek, S., and Walentynowicz, K. (2006). Hypoxia-induced sickness behaviour. J Physiol Pharmacol *57 Suppl 8*, 35-50.

Kumar, A., Morrison, S., and Gulati, A. (1997). Effect of ETA receptor antagonists on cardiovascular responses induced by centrally administered sarafotoxin 6b: role of sympathetic nervous system. Peptides *18*, 855-864.

Kurihara, Y., Kurihara, H., Suzuki, H., Kodama, T., Maemura, K., Nagai, R., Oda, H., Kuwaki, T., Cao, W.H., Kamada, N., *et al.* (1994). Elevated blood pressure and craniofacial abnormalities in mice deficient in endothelin-1. Nature *368*, 703-710.

Kuwaki, T., Cao, W.H., Kurihara, Y., Kurihara, H., Ling, G.Y., Onodera, M., Ju, K.H., Yazaki, Y., and Kumada, M. (1996). Impaired ventilatory responses to hypoxia and hypercapnia in mutant mice deficient in endothelin-1. Am J Physiol *270*, R1279-1286.

Kuwaki, T., Kurihara, H., Cao, W.H., Kurihara, Y., Unekawa, M., Yazaki, Y., and Kumada, M. (1997). Physiological role of brain endothelin in the central autonomic control: from neuron to knockout mouse. Prog Neurobiol *51*, 545-579.

Lee, M.E., de la Monte, S.M., Ng, S.C., Bloch, K.D., and Quertermous, T. (1990). Expression of the potent vasoconstrictor endothelin in the human central nervous system. J Clin Invest *86*, 141-147.

Liefeldt, L., Bocker, W., Schonfelder, G., Zintz, M., and Paul, M. (1995). Regulation of the endothelin system in transgenic rats expressing the human endothelin-2 gene. J Cardiovasc Pharmacol *26 Suppl 3*, S32-33.

Liefeldt, L., Schonfelder, G., Bocker, W., Hocher, B., Talsness, C.E., Rettig, R., and Paul, M. (1999). Transgenic rats expressing the human ET-2 gene: a model for the study of endothelin actions in vivo. J Mol Med *77*, 565-574.

Madison, B.B., Dunbar, L., Qiao, X.T., Braunstein, K., Braunstein, E., and Gumucio, D.L. (2002). Cis elements of the villin gene control expression in restricted domains of the vertical (crypt) and horizontal (duodenum, cecum) axes of the intestine. J Biol Chem *277*, 33275-33283.

Maritz, G.S., Morley, C.J., and Harding, R. (2005). Early developmental origins of impaired lung structure and function. Early Hum Dev *81*, 763-771.

Massaro, D., Massaro, G.D., Baras, A., Hoffman, E.P., and Clerch, L.B. (2004). Calorie-related rapid onset of alveolar loss, regeneration, and changes in mouse lung gene expression. Am J Physiol Lung Cell Mol Physiol *286*, L896-906.

Masuo, Y., Ishikawa, Y., Kozakai, T., Uchide, T., Komatsu, Y., and Saida, K. (2003). Vasoactive intestinal contractor/endothelin-2 gene expression in the murine central nervous system. Biochem Biophys Res Commun *300*, 661-668.

McCartney, S.A., Ballinger, A.B., Vojnovic, I., Farthing, M.J., and Warner, T.D. (2002). Endothelin in human inflammatory bowel disease: comparison to rat trinitrobenzenesulphonic acid-induced colitis. Life Sci *71*, 1893-1904.

Moncada, S., Gryglewski, R., Bunting, S., and Vane, J.R. (1976). An enzyme isolated from arteries transforms prostaglandin endoperoxides to an unstable substance that inhibits platelet aggregation. Nature *263*, 663-665.

Mosqueda-Garcia, R., Yates, K., O'Leary, J., and Inagami, T. (1995). Cardiovascular and respiratory effects of endothelin in the ventrolateral medulla of the normotensive rat. Hypertension *26*, 263-271.

Murch, S.H., Braegger, C.P., Sessa, W.C., and MacDonald, T.T. (1992). High endothelin-1 immunoreactivity in Crohn's disease and ulcerative colitis. Lancet *339*, 381-385.

Nakanishi, K., Tajima, F., Nakata, Y., Osada, H., Tachibana, S., Kawai, T., Torikata, C., Suga, T., Takishima, K., Aurues, T., *et al.* (1999). Expression of endothelin-1 in rats developing hypobaric hypoxia-induced pulmonary hypertension. Lab Invest *79*, 1347-1357.

Nishiyama, H., Itoh, K., Kaneko, Y., Kishishita, M., Yoshida, O., and Fujita, J. (1997). A glycine-rich RNA-binding protein mediating cold-inducible suppression of mammalian cell growth. J Cell Biol *137*, 899-908.

O'Gorman, S., Dagenais, N.A., Qian, M., and Marchuk, Y. (1997). Protamine-Cre recombinase transgenes efficiently recombine target sequences in the male germ line of mice, but not in embryonic stem cells. Proc Natl Acad Sci U S A *94*, 14602-14607.

Oishi, K., Atsumi, G., Sugiyama, S., Kodomari, I., Kasamatsu, M., Machida, K., and Ishida, N. (2006). Disrupted fat absorption attenuates obesity induced by a high-fat diet in Clock mutant mice. FEBS Lett *580*, 127-130.

Okayasu, I., Hatakeyama, S., Yamada, M., Ohkusa, T., Inagaki, Y., and Nakaya, R. (1990). A novel method in the induction of reliable experimental acute and chronic ulcerative colitis in mice. Gastroenterology *98*, 694-702.

Padol, I., Huang, J.Q., Hogaboam, C.M., and Hunt, R.H. (2000). Therapeutic effects of the endothelin receptor antagonist Ro 48-5695 in the TNBS/DNBS rat model of colitis. Eur J Gastroenterol Hepatol *12*, 257-265.

Palanch, A.C., and Alvares, E.P. (1998). Feeding manipulation elicits different proliferative responses in the gastrointestinal tract of suckling and weanling rats. Braz J Med Biol Res *31*, 565-572.

Palmer, R.M., Ferrige, A.G., and Moncada, S. (1987). Nitric oxide release accounts for the biological activity of endothelium-derived relaxing factor. Nature *327*, 524-526.

Peacock, A.J., Dawes, K.E., Shock, A., Gray, A.J., Reeves, J.T., and Laurent, G.J. (1992). Endothelin-1 and endothelin-3 induce chemotaxis and replication of pulmonary artery fibroblasts. Am J Respir Cell Mol Biol *7*, 492-499.

Perl, A.K., Tichelaar, J.W., and Whitsett, J.A. (2002). Conditional gene expression in the respiratory epithelium of the mouse. Transgenic Res *11*, 21-29.

Podolsky, D.K. (2002). Inflammatory bowel disease. N Engl J Med *347*, 417-429.

Pollock, D.M., Keith, T.L., and Highsmith, R.F. (1995). Endothelin receptors and calcium signaling. FASEB J *9*, 1196-1204.

Rachmilewitz, D., Eliakim, R., Ackerman, Z., and Karmeli, F. (1992). Colonic endothelin-1 immunoreactivity in active ulcerative colitis. Lancet *339*, 1062.

Rattner, A., and Nathans, J. (2005). The genomic response to retinal disease and injury: evidence for endothelin signaling from photoreceptors to glia. J Neurosci *25*, 4540-4549.

Rosahl, T.W., Geppert, M., Spillane, D., Herz, J., Hammer, R.E., Malenka, R.C., and Sudhof, T.C. (1993). Short-term synaptic plasticity is altered in mice lacking synapsin I. Cell *75*, 661-670.

Rozengurt, N., Springall, D.R., and Polak, J.M. (1990). Localization of endothelin-like immunoreactivity in airway epithelium of rats and mice. J Pathol *160*, 5-8.

Rubanyi, G.M., and Polokoff, M.A. (1994). Endothelins: molecular biology, biochemistry, pharmacology, physiology, and pathophysiology. Pharmacol Rev *46*, 325-415.

Sahebjami, H., and Domino, M. (1992). Effects of repeated cycles of starvation and refeeding on lungs of growing rats. J Appl Physiol *73*, 2349-2354.

Sahebjami, H., and MacGee, J. (1985). Effects of starvation on lung mechanics and biochemistry in young and old rats. J Appl Physiol *58*, 778-784.

Saida, K., Hashimoto, M., Mitsui, Y., Ishida, N., and Uchide, T. (2000). The prepro vasoactive intestinal contractor (VIC)/endothelin-2 gene (EDN2): structure, evolution, production, and embryonic expression. Genomics *64*, 51-61.

Saida, K., Mitsui, Y., and Ishida, N. (1989). A novel peptide, vasoactive intestinal contractor, of a new (endothelin) peptide family. Molecular cloning, expression, and biological activity. J Biol Chem *264*, 14613-14616.

Sakurai, T., Yanagisawa, M., Inoue, A., Ryan, U.S., Kimura, S., Mitsui, Y., Goto, K., and Masaki, T. (1991). cDNA cloning, sequence analysis and tissue distribution of rat preproendothelin-1 mRNA. Biochem Biophys Res Commun *175*, 44-47.

Sakurai, T., Yanagisawa, M., Takuwa, Y., Miyazaki, H., Kimura, S., Goto, K., and Masaki, T. (1990). Cloning of a cDNA encoding a non-isopeptide-selective subtype of the endothelin receptor. Nature *348*, 732-735.

Samson, W.K., Skala, K., Huang, F.L., Gluntz, S., Alexander, B., and Gomez-Sanchez, C.E. (1991). Central nervous system action of endothelin-3 to inhibit water drinking in the rat. Brain Res *539*, 347-351.

Schaefer, K.E., Messier, A.A., Morgan, C., and Baker, G.T., 3rd (1975). Effect of chronic hypercapnia on body temperature regulation. J Appl Physiol *38*, 900-906.

Schwarz, M., Lund, E.G., Setchell, K.D., Kayden, H.J., Zerwekh, J.E., Bjorkhem, I., Herz, J., and Russell, D.W. (1996). Disruption of cholesterol 7alpha-hydroxylase gene in mice. II. Bile acid deficiency is overcome by induction of oxysterol 7alpha-hydroxylase. J Biol Chem *271*, 18024-18031.

Seldeslagh, K.A., and Lauweryns, J.M. (1993). Endothelin in normal lung tissue of newborn mammals: immunocytochemical distribution and co-localization with serotonin and calcitonin gene-related peptide. J Histochem Cytochem *41*, 1495-1502.

Sessa, W.C., Kaw, S., Hecker, M., and Vane, J.R. (1991). The biosynthesis of endothelin-1 by human polymorphonuclear leukocytes. Biochem Biophys Res Commun *174*, 613-618.

Sharma, P., Lu, F., Rut, A., and Brown, M.J. (1998). Structure of human endothelin-2 gene and demonstration of common expression in human right atrial tissue. Biochem Biophys Res Commun *245*, 709-712.

Shiba, R., Sakurai, T., Yamada, G., Morimoto, H., Saito, A., Masaki, T., and Goto, K. (1992). Cloning and expression of rat preproendothelin-3 cDNA. Biochem Biophys Res Commun *186*, 588-594.

Shohet, R.V., Kisanuki, Y.Y., Zhao, X.S., Siddiquee, Z., Franco, F., and Yanagisawa, M. (2004). Mice with cardiomyocyte-specific disruption of the endothelin-1 gene are resistant to hyperthyroid cardiac hypertrophy. Proc Natl Acad Sci U S A *101*, 2088-2093.

Silva, J.E., and Larsen, P.R. (1983). Adrenergic activation of triiodothyronine production in brown adipose tissue. Nature *305*, 712-713.

Sofia, M., Mormile, M., Faraone, S., Alifano, M., Zofra, S., Romano, L., and Carratu, L. (1993). Increased endothelin-like immunoreactive material on bronchoalveolar lavage fluid from patients with bronchial asthma and patients with interstitial lung disease. Respiration *60*, 89-95.

Springall, D.R., Howarth, P.H., Counihan, H., Djukanovic, R., Holgate, S.T., and Polak, J.M. (1991). Endothelin immunoreactivity of airway epithelium in asthmatic patients. Lancet *337*, 697-701.

Stappenbeck, T.S., Wong, M.H., Saam, J.R., Mysorekar, I.U., and Gordon, J.I. (1998). Notes from some crypt watchers: regulation of renewal in the mouse intestinal epithelium. Curr Opin Cell Biol *10*, 702-709.

Stewart, D.J., Levy, R.D., Cernacek, P., and Langleben, D. (1991). Increased plasma endothelin-1 in pulmonary hypertension: marker or mediator of disease? Ann Intern Med *114*, 464-469.

Takahashi, K., Ghatei, M.A., Jones, P.M., Murphy, J.K., Lam, H.C., O'Halloran, D.J., and Bloom, S.R. (1991). Endothelin in human brain and pituitary gland: comparison with rat. J Cardiovasc Pharmacol *17 Suppl 7*, S101-103.

Takeda, S., Sawa, Y., Minami, M., Kaneda, Y., Fujii, Y., Shirakura, R., Yanagisawa, M., and Matsuda, H. (1997). Experimental bronchiolitis obliterans induced by in vivo HVJ-liposome-mediated endothelin-1 gene transfer. Ann Thorac Surg *63*, 1562-1567.

Takimoto, M., Inui, T., Okada, T., and Urade, Y. (1993). Contraction of smooth muscle by activation of endothelin receptors on autonomic neurons. FEBS Lett *324*, 277-282.

Takizawa, S., Uchide, T., Adur, J., Kozakai, T., Kotake-Nara, E., Quan, J., and Saida, K. (2005). Differential expression of endothelin-2 along the mouse intestinal tract. J Mol Endocrinol *35*, 201-209.

Thomson, A.B., Keelan, M., Thiesen, A., Clandinin, M.T., Ropeleski, M., and Wild, G.E. (2001). Small bowel review: normal physiology part 1. Dig Dis Sci *46*, 2567-2587.

Trost, S.U., Swanson, E., Gloss, B., Wang-Iverson, D.B., Zhang, H., Volodarsky, T., Grover, G.J., Baxter, J.D., Chiellini, G., Scanlan, T.S., *et al.* (2000). The thyroid hormone receptor-beta-selective agonist GC-1 differentially affects plasma lipids and cardiac activity. Endocrinology *141*, 3057-3064.

Tsushima, T., Arai, M., Isozaki, O., Nozoe, Y., Shizume, K., Murakami, H., Emoto, N., Miyakawa, M., and Demura, H. (1994). Interaction of endothelin-1 with porcine thyroid cells in culture: a possible autocrine factor regulating iodine metabolism. J Endocrinol *142*, 463-470.

Uchida, Y., Jun, T., Ninomiya, H., Ohse, H., Hasegawa, S., Nomura, A., Sakamoto, T., Sardessai, M.S., and Hirata, F. (1996). Involvement of endothelins in immediate and late asthmatic responses of guinea pigs. J Pharmacol Exp Ther *277*, 1622-1629.

Uchide, T., Fujimori, Y., Sasaki, T., Temma, K., Adur, J., Masuo, Y., Kozakai, T., Lee, Y.S., and Saida, K. (2002). Expression of endothelin-1 and vasoactive intestinal contractor genes in mouse organs during the perinatal period. Clin Sci (Lond) *103 Suppl 48*, 167S-170S.

Uchide, T., Masuda, H., Mitsui, Y., and Saida, K. (1999). Gene expression of vasoactive intestinal contractor/endothelin-2 in ovary, uterus and embryo: comprehensive gene expression profiles of the endothelin ligand-receptor system revealed by semi-quantitative reverse transcription-polymerase chain reaction analysis in adult mouse tissues and during late embryonic development. J Mol Endocrinol *22*, 161-171.

Van Breukelen, F., and Martin, S.L. (2002). Invited review: molecular adaptations in mammalian hibernators: unique adaptations or generalized responses? J Appl Physiol *92*, 2640-2647.

Walters, J.R. (2005). Recent findings in the cell and molecular biology of the small intestine. Curr Opin Gastroenterol *21*, 135-140.

Wang, X., Inoue, S., Gu, J., Miyoshi, E., Noda, K., Li, W., Mizuno-Horikawa, Y., Nakano, M., Asahi, M., Takahashi, M.*, et al.* (2005). Dysregulation of TGF-beta1 receptor activation leads to abnormal lung development and emphysema-like phenotype in core fucose-deficient mice. Proc Natl Acad Sci U S A *102*, 15791-15796.

Westman, W., and Geiser, F. (2004). The effect of metabolic fuel availability on thermoregulation and torpor in a marsupial hibernator. J Comp Physiol [B] *174*, 49-57.

Wilson, D.O., Donahoe, M., Rogers, R.M., and Pennock, B.E. (1990). Metabolic rate and weight loss in chronic obstructive lung disease. JPEN J Parenter Enteral Nutr *14*, 7-11.

Wood, S.C. (1991). Interactions between hypoxia and hypothermia. Annu Rev Physiol *53*, 71-85.

Xu, D., Emoto, N., Giaid, A., Slaughter, C., Kaw, S., deWit, D., and Yanagisawa, M. (1994). ECE-1: a membrane-bound metalloprotease that catalyzes the proteolytic activation of big endothelin-1. Cell *78*, 473-485.

Yamboliev, I.A., Hruby, A., and Gerthoffer, W.T. (1998). Endothelin-1 activates MAP kinases and c-Jun in pulmonary artery smooth muscle. Pulm Pharmacol Ther *11*, 205-208.

Yanagisawa, H., Hammer, R.E., Richardson, J.A., Emoto, N., Williams, S.C., Takeda, S., Clouthier, D.E., and Yanagisawa, M. (2000). Disruption of ECE-1 and ECE-2 reveals a role for endothelin-converting enzyme-2 in murine cardiac development. J Clin Invest *105*, 1373-1382.

Yanagisawa, M. (1994). The endothelin system. A new target for therapeutic intervention. Circulation *89*, 1320-1322.

Yanagisawa, M., Kurihara, H., Kimura, S., Tomobe, Y., Kobayashi, M., Mitsui, Y., Yazaki, Y., Goto, K., and Masaki, T. (1988). A novel potent vasoconstrictor peptide produced by vascular endothelial cells. Nature *332*, 411-415.

Zhang, J., Kaasik, K., Blackburn, M.R., and Lee, C.C. (2006). Constant darkness is a circadian metabolic signal in mammals. Nature *439*, 340-343.

Zhu, B., and Herbert, J. (1996). Behavioural, autonomic and endocrine responses associated with C-fos expression in the forebrain and brainstem after intracerebroventricular infusions of endothelins. Neuroscience *71*, 1049-1062.

Zigdon-Arad, T., Bdolah, A., Kochva, E., and Wollberg, Z. (1992). Activity of sarafotoxin/endothelin peptides in the heart and brain of lower vertebrates. Toxicon *30*, 439-448.

Zuidervaart, W., van der Velden, P.A., Hurks, M.H., van Nieuwpoort, F.A., Out-Luiting, C.J., Singh, A.D., Frants, R.R., Jager, M.J., and Gruis, N.A. (2003). Gene expression profiling identifies tumour markers potentially playing a role in uveal melanoma development. Br J Cancer *89*, 1914-1919.